ABSTRACT

Title of Thesis:	DEVELOPMENT OF PLANNING AND EVALUATION MODELS FOR SUPERSTREETS
	Liu Xu, Master of Science, 2016
Thesis Directed By:	Gang-Len Chang, Professor, Department of Civil & Environmental Engineering

Despite the extensive implementation of Superstreets on congested arterials, reliable methodologies for such designs remain unavailable. The purpose of this research is to fill the information gap by offering reliable tools to assist traffic professionals in the design of Superstreets with and without signal control. The entire tool developed in this thesis consists of three models. The first model is used to determine the minimum U-turn offset length for an Un-signalized Superstreet, given the arterial headway distribution of the traffic flows and the distribution of critical gaps among drivers. The second model is designed to estimate the queue size and its variation on each critical link in a signalized Superstreet, based on the given signal plan and the range of observed volumes. Recognizing that the operational performance of a Superstreet cannot be achieved without an effective signal plan, the third model is developed to produce a signal optimization method that can generate progression offsets for heavy arterial flows moving into and out of such an intersection design.

DEVELOPMENT OF PLANNING AND EVALUATION MODELS FOR SUPERSTREETS

by

LIU XU

Thesis submitted to the Faculty of the Graduate School of the
University of Maryland, College Park, in partial fulfillment
of the requirements for the degree of
Master of Science
2016

Advisory Committee:
Professor Gang-Len Chang, Chair
Professor Ali Haghani
Professor Cirillo Cinzia

© Copyright by
Liu Xu
2016

ACKNOWLEDGEMENTS

I would like to express the deepest appreciation to my committee chair Professor Gang-Len Chang, who has shown the attitude and the substance of a genius: he continually and persuasively conveyed a spirit of adventure in regard to research and scholarship, and an excitement in regard to teaching. Without his supervision and constant help this thesis would not have been possible.

My Special thanks go to the members of my thesis examination committee, Dr. Ali Haghani and Dr. Cirillo Cinzia, for their constructive comments and suggestions on this work.

I would also like to express my great appreciation to Dr. Xianfeng Yang, who kindly supported and guided me during my development of this thesis. Without his continuous inspiration and supervision, I could not make this thesis possible. Also, very special thanks go to my colleagues in the Traffic Safety and Operations Lab, Yao Cheng, Sung Yoon Park, Yang (Carl) Lu, Hyeonmi Kim, Anna Petrone and Dr. Chien-Lun Lan for the kind support they have offered to me. This thesis is supported by the Maryland State Highway Administration with warm thanks to our colleagues Minseok Kim and Saed Rahwanji who provided information and expertise that greatly assisted the research and for their kindness for sharing their pearls of wisdom with me during the course of this research.

Finally, I am also immensely grateful to my fiancé, Xinlei Zhang, my mother, Gaoai Li and my father, Jian Xu for all the unconditional support they have given.

TABLE OF CONTENTS

LIST OF TABLES

LIST OF FIGURES

Chapter 1: Introduction

1.1 Research Background

A Superstreet, as shown in Figure 1-1, is also known as a Restricted Crossing U-turn (RCUT) intersection, a J-turn intersection, and a synchronized street intersection. A Superstreet differs from a conventional intersection by eliminating the left-turn and through movements from the cross street approaches. To accommodate these movements, this type of design requires drivers to turn right onto the main road, and then make a U-turn maneuver at the downstream one-way median opening. At its main street approaches, the left-turn flows are typically accommodated in the same way as those at conventional intersections. Depending on the traffic demand patterns, a Superstreet can have either three or four legs. In the case of a four-legged Superstreet, there are two U-turn crossovers, and both the left-turn and through movements from the minor street are not allowed to exercise directly at the intersection.

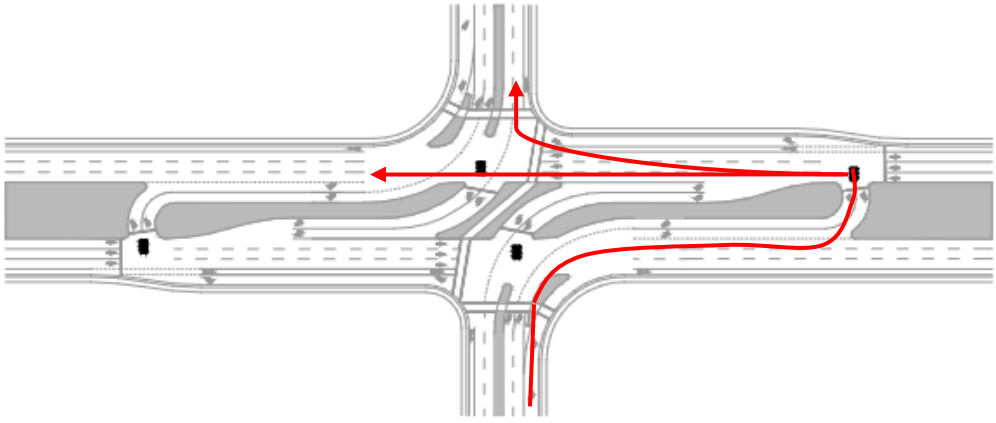

Figure 1-1 Schematic of Superstreet with illustration of minor road rerouting.

This type of unconventional intersection design was developed in the United States (Kramer, 1987) and then implemented in several states, including Maryland, North Carolina, and Texas . Focusing on congestion in suburban areas, Kremer proposed the Superstreet design along with a set of self-defined principles for an ideal suburban arterial to overcome congestion. The key objective behind this type of design is to form large, uninterrupted progression bands for both directions along the arterial. Based on this feature, this typical treatment is more applicable to arterial segments with heavy through and left-turn volumes in urban and suburban areas, especially at arterial intersections with low traffic from the side streets.

An Un-signalized Superstreet (usually under stop yield control) can allow a rural high-speed corridor to function similarly to a freeway corridor in the case where funding for interchanges and overpasses may not be available. In the case that the traffic demand keeps increasing over time, an Un-signalized Superstreet can be converted to a signal controlled intersection to ensure its safety performance. A Superstreet with proper signal control can also provide favorable progression along urban or suburban corridors. Signals in a Superstreet typically require only two phases, which can minimize the loss time at its intersections. Efficient progression can be provided in both directions with different speeds and offsets. By allocating a large portion of cycle length to accommodate heavy arterial through and left-turning volumes, it can reduce the travel time and delay for arterial movements, and also, if properly designed, potentially reduce the overall intersection delays.

If properly implemented, a Superstreet can also yield safety benefits. As illustrated in Figure 1-2, compared with a conventional intersection, it successfully reduces the conflicting points from 32 to 14. A number of studies in the literature have also confirmed its safety performance (Hummer, 2001, 2007, 2008, 2009, 2010, 2012; Kim, 2007; Edara, 2007).

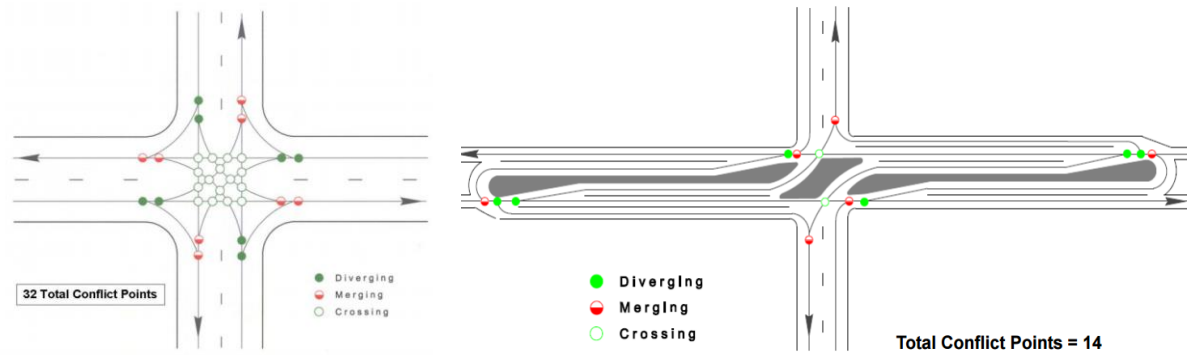

(a) Conventional Intersection (b) 4-leg Superstreet

Figure 1-2. Comparison Conflict Points between a Typical Conventional Intersection and a Superstreet

Notably, these research efforts have made remarkable contributions to promote the development and implementation of Superstreets. However, much remains to be done on the design and evaluation of such a design. In fact, over the past decades, only limited studies (Olarte, 2011) have attempted to address the issue of properly designing and operating a Superstreet. Despite the increasing popularity of implementing Superstreets as a countermeasure to alleviate safety and operational issues, many critical concerns such as queue blockage, the offset distance, and the signal progression need to be thoroughly investigated. For example, Figure 1-3 shows the following three possible blockage scenarios that may occur in a typical

Superstreet: 1) insufficient left-turn bay to accommodate the intended left-turn volumes, thus causing spillback to partially block the through traffic; 2) the overflowed queues from the through lane groups block the entry of the left-turn bay, and thus completely block the left-turn movement; and 3) the queuing vehicles reach the downstream link and block the upstream traffic. Hence, how to evaluate the geometric features of a Superstreet design becomes a critical issue. Unfortunately, the available literature and design standards fall short for conducting such an evaluation. Although a newly published report (FHWA, 2014) has indicated the desirable range of distance from the main intersection to crossovers, its information is not yet sufficient to assess the sufficiency of both link and bay lengths.

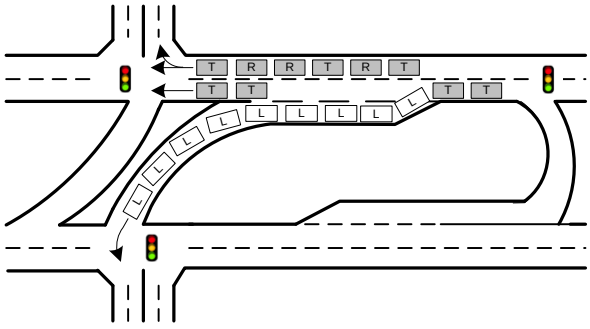

1) Left-turn lane group partially blocks the right-through lane group

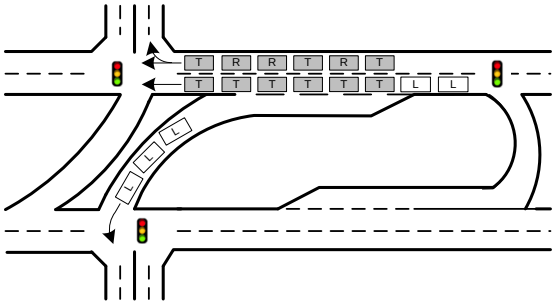

2) Right-through lane group completely blocks the left-turn lane group

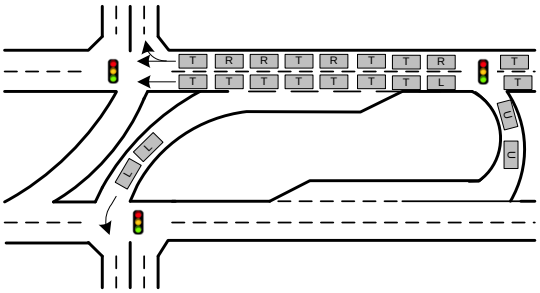

3) Through lane group completely blocks the upstream lane groups

Figure 1-3. Potential blockage scenarios in a typical Superstreet

Recognizing the aforementioned needs in the promotion of a Superstreet, this study has proposed a set of planning models to address the following vital issues:

- How to assess the geometric features of an Un-signalized Superstreet, based on its prevailing traffic conditions;
- What would be the criteria for determining the need of installing signals for a Superstreet;
- How to assess whether the bay length among a signalized Superstreet is sufficient to prevent any spillback from happening?
- How to design a proper signal timing plan, considering its unique geometric layouts; and
- How to minimize the delay experienced by the minor road drivers due to the detour operations in a Superstreet.

1.2 Research Objectives

The primary focus of the thesis is on developing a systematic tool to assist traffic engineers in both planning and evaluating a Superstreet. More specifically, the entire research includes the following tasks:

- Identify the critical links that dominate the performance of an un-signalized Superstreet, and determine the minimum required link length to meet safety needs. To do so, the proposed model will consider the complex spatial interrelations among link length, traffic flow variation and drivers' gap acceptance behavior;

- Develop the criteria for converting an un-signalized Superstreet into a signalized one in order to accommodate the observed traffic demand;
- Estimate the required length of each critical link that may be one primary contributor to the overall intersection delay, and to accommodate heavy volumes and their variations. Essential activities for this task include a reliable estimate of the required link length, based on the range of potential queue variation, and their complex interaction in a signalized Superstreet;
- Formulate an optimal signal design strategy to achieve efficient progression along the arterial in both directions while minimizing the delay experienced by minor road drivers.

1.3 Thesis Organization

The thesis consists of six chapters and their logic relations are illustrated in Figure 1-4.

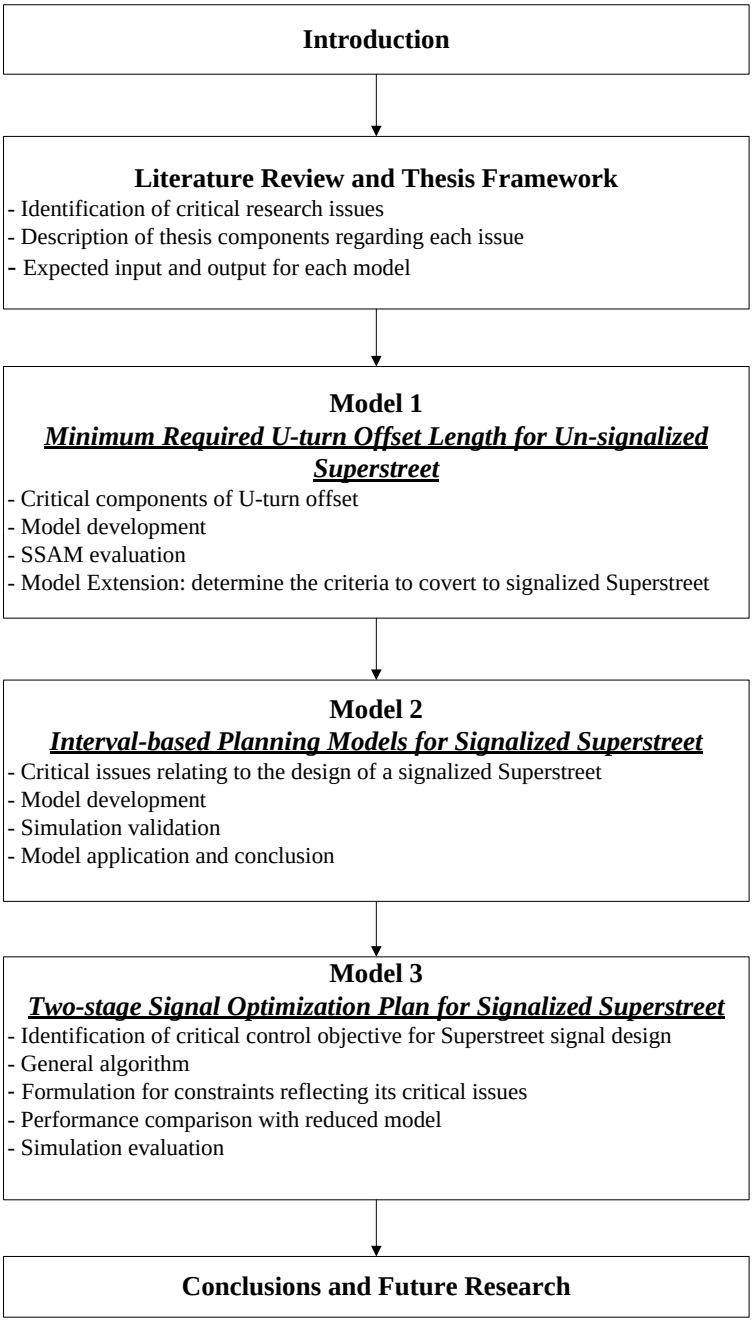

Figure 1-4 Thesis Organization

The remaining chapters are organized as follows:

- **Chapter 2** offers an in-depth literature review of the existing studies on Superstreets with regard to both their safety and operational needs. Based on the limitations of those existing studies, this chapter will summarize

key research issues and present a set of models to address them, including their key functional features, expected inputs and outputs, as well as their potential application.

- **Chapter 3** presents a model to compute the minimum U-turn offset length in an un-signalized Superstreet. The developed model is capable of capturing the complex nature of human behavior and traffic flow fluctuations. To ensure the model's reliability, this study has applied an assessment model for evaluation and has conducted extensive simulations to assess its applicability. The developed model can also serve as a tool to decide whether a signal is needed in a Superstreet.
- **Chapter 4** presents a planning method that allows users to reliably estimate the queue size and its variation on each critical link in a Superstreet, based on the given signal plan and the observed range of volumes. Based on the results of simulation experiments, this chapter has further identified the interrelations between intersection delay and link traffic queues. The estimated queue intervals in comparison with the proposed link length offer a basis for design engineers to evaluate whether any queue spillover and lane blockage may occur on any critical links and to determine whether the preliminary geometric design needs to be revised, or whether the signal coordination between a Superstreet's sub-intersections should be redesigned. Results of extensive experiments confirm the reliability and applicability of the proposed model in evaluating the geometric features of a Superstreet.

- **Chapter 5** illustrates the formulations and solution algorithm for the two-stage signal optimization model for a Superstreet. Based on the well-recognized MAXBAND algorithm, this study presents a set of innovative formulations to reflect the unique geometric features of such a design at Stage 1, and then applies a multi-objective model to minimize the delays experienced by minor road drivers. The evaluation results of the developed model along with extensive simulation experiments are also reported in this chapter.
- **Chapter 6** highlights the primary contributions of this thesis and indicates the directions for future research.

Chapter 2: Literature Review and Research Framework

2.1 Introduction

This chapter consists of two parts: an in-depth literature review and the proposed research framework.

The first part focuses on reviewing the existing studies of Superstreets' geometric design, safety performance, and operational features. In the category of Superstreet development, the review has covered the existing reports and publications related to the design and implement of Superstreets, especially the challenges encountered by traffic professionals. On the subject of safety performance, the core aspect of the review is to compare the safety performance of Superstreets with the conventional design, including the identification of possible contributing factors. The final category of the review is on the operational performance of Superstreets, compared with conventional designs under similar demand levels.

Based on these existing studies, several critical design issues that have not been adequately addressed are identified in the second part. Realizing that without proper design guidelines may render some safety and operational issues on the increasingly popular Superstreet implementation, this study will propose a set of models to address those key issues, including the procedures to compute the offset, the guidelines to assess the turning bay length for operational efficiency, and a signal

planning model to coordinate the traffic flows between vehicles from the side streets and the main road.

2.2 Development of Superstreet

A Superstreet, proposed by Kramer (1987), is an innovative intersection design that intends to mitigate right-angle crashes by reducing its total conflict points. This typical design is to reroute the left-turn and through movements from the cross street approaches to the directional crossover. Kramer's design logic is to provide wide and continuous progression bands along the arterial at a desirable speed in both directions. Independent from Kramer's research, the Maryland State Highway Administration (FHWA, 2014) has explored such a design concept to address the concerns caused by the growing traffic volume on rural highways. In view of the fact that signalization can reduce the mobility and require additional design efforts, it is suggested that an Un-signalized Superstreet (also called a Maryland J-turn) could be a viable option to circumvent such needs. The first Un-signalized Superstreet was installed in Maryland on US-15 near the Pennsylvania border. Focusing on mitigating the conflicts between left-turning movements from the minor road and the main arterial vehicles at the un-signalized Superstreet, North Carolina (FHWA, 2014), after decades of practice, has successfully installed a series of such designs that are reported to work effectively.

Recognizing its potential to yield a relatively safe and efficient environment, the traffic community in recent years has increasingly adopted Superstreets in many states, including Alabama, Louisiana, Minnesota, Missouri, Maryland, North Carolina, Ohio, and Texas . Some critical issues and related studies associated with the Superstreet design are reviewed in sequence below.

2.3 Operational Performance of Superstreet

Over the past decades, some pioneer researchers have devoted significant efforts on unconventional intersections, including Superstreets. For example, Hummer (1998) focused on studying the treatment of heavy left-turn flows on arterials. On both median U-turns and Superstreets, most studies conclude that the main strength of the Superstreet design lies in that the through movements can experience much less delay by eliminating the direct left-turn and through vehicles from the minor approaches. Consequently, delays for through and left-turn vehicles from the minor roads will be increased.

Reid and Hummer (1998, 2000) compared travel time efficiency between Superstreets and median U-turns, based on CORSIM simulation results. Using the peak hour traffic data from one median U-turn intersection in Detroit in simulation experiments, they concluded that a Superstreet was inferior to a median U-turn design in terms of total travel time, mean stops per vehicle, and mean speed. Their report states that

Superstreets are not designed to handle high cross-street volumes, because their primary function is to serve the main arterial traffic flows.

Hummer (2001) further conducted simulation-based travel time comparisons between Superstreets and conventional intersections under different volume levels. Based on the extensive simulation results, he pointed out that a Superstreet can outperform a conventional intersection when the volumes for left-turns and through movements from the minor streets are at the low-medium level. In addition to travel time comparisons, Hummer (2007) further explored the method to determine the capacity of Superstreets by adjusting the critical lane volume used in HCM. Note that his recommended procedure served as an effective tool for planners and traffic engineers to determine the feasibility of a Superstreet design. The impact of such a design on the delay or travel times, however, has not been adequately addressed.

Realizing the lack of reliable information on operational efficiency, Haley et al. (2011) compared the performance of a signalized Superstreet with a conventional intersection under various conditions with data from several existing intersections. Their operational analyses involved the use of calibrated and validated VISSIM models for three existing signalized Superstreets in North Carolina; two are isolated intersections and one is a five-intersection corridor. Results from those three calibrated simulation models were compared with equivalent conventional intersections at various volume levels, using travel time as their primary measure of effectiveness. Their analysis results justify the operational advantages of the Superstreet design.

Also with simulation experiments, Kim et al. (2007) reported apparent operational and safety benefits offered by Superstreets under high volume conditions. Similar to the aforementioned studies, they also conducted simulation-based comparisons between Superstreets and conventional intersections. Aside from the operation analysis, they performed a safety assessment using a surrogate safety assessment module developed by the U.S. Department of Transportation. With respect to safety, their results show that Superstreets can outperform the conventional intersections under a high volume level.

Furthermore, Haley et al. (2011) analyzed the performance of Superstreets by comparing them with equivalent conventional intersections, based on the calibrated simulation results. They reported that it would be effective to adopt a Superstreet design when the arterial's left-turn volume per lane is greater than 80 percent of the volume on the minor roads during the same signal phase.

More recently, as part of the efforts to promote popular unconventional intersection designs, the Federal Highway Administration (FHWA, 2010; FHWA, 2014) has offered a series of guides to help transportation professionals to evaluate and implement such designs. Although this report summarizes the state of knowledge and practices in detail, it still pointed out that there is a need to refine existing practices and to develop reliable methodologies for both design and evaluation.

2.4 Safety Performance of Superstreet

In addition to exploring the superior operational properties, some researchers have devoted extensive efforts to justify the safety benefits of Superstreets. For example, Hummer et al. (2012, 2008) summarized the safety benefits, based on the historical crash data collected from the Superstreets in Maryland and North Carolina. Thompson et al. (2001) also confirmed the safety benefits of Superstreet design if properly designed and planned. Lu (2004) found that a signalized Superstreet generates 26 percent fewer conflicts than those intersections allowing direct left-turns.

Impressed by the promising practices in the United States, some researchers from other countries also conducted rigorous investigations on the safety and operational efficiency of Superstreets. Moon and Kim (2011) evaluated how Superstreets can effectively and safely operate under given traffic conditions, compared with a conventional design. Their results also confirm that a Superstreet has the potential to deliver more safety benefits when compared with conventional intersections under the same volume level.

Recently, a series of reports published by FHWA (2009, 2010, 2012, and 2014) offer a comprehensive review of critical concerns related to Superstreet design, including the geometric layout, traffic signalization, and operational and safety comparisons before-and-after the construction of such a design. Aside from improving the operational performance, various studies from Ott (2012), Thompson

(2001), Moon (2011) and Olarte (2011) also confirmed that Superstreets can help to reduce accident rates and mitigate crash severity.

In brief, despite the increasing popularity of Superstreet design among transportation professionals, some critical issues contributing to its successful implementation remain to be addressed. For example, recognizing such needs, Rafael (2011) has provided the designers with a model to assist them in assessing the applicability of an un-signalized Superstreet under a given traffic volume and also to identify the critical zones that are most likely to become bottlenecks.

Three other studies relevant to the safety aspects of Superstreets were conducted independently by Hochstein (2009), Hugues (2010) and Cluck (1999). They all indicated that there are several critical elements in designinga Superstreet, including the width of the median, the need for adding loons or jug-handles, and the offset or distance between the main intersection and the U-turn. For the first two issues, the AASHTO's Green Book (American Association of State Highway and Transportation Officials, 2001) offers some guidelines. However, no design criteria or guidelines with respect to the offset distance are available in the literature yet.

Moreover, a recent FHWA report (Alternative Intersections/Interchanges: Informational Report (AIIR), 2010) and Liu (2008) have both pointed out that the length from the main intersection to the U-turn crossover is the most critical factor in the design of a signalized Superstreet. Liu et al. (2008) conducted statistical analysis

with crash data collected from 140 street segments in Florida and concluded that the separation distance significantly impacts the safety of the segment between the driveway and the U-turn locations. Without an adequate distance for merging, the minor road vehicles are less likely to complete all required lane changes and may cause serious collisions.

Regarding the operational features of a Superstreet, HCM (2010) offers guidelines on these critical design issues. For example, as mentioned by Olarte (2011), HCM does not provide recommendations for highway segments on which merging, weaving and diverging activities may take place concurrently as on a Superstreet (see, for example, HCM 2010 exhibit 13-21).

More recently, the Federal Highway Administration (FHWA, 2014) has offered a series of guides to help transportation professionals perform the design and evaluation of Superstreets. Based on a state of existing practices and the performance data, the report concludes that the distance from the main intersection to its U-turn crossover should range from 400 feet to a half mile. Yet how to set the exact distance remains to be explored.

2.5 Key Research Issues

Despite the increasing attention by the traffic community to the safety and operational aspects of Superstreets, some critical design issues have not been

adequately addressed yet. For example, although a newly published report (FHWA, 2014) has discussed the desirable range of the distance from the main intersection to crossovers, its information is not sufficient to assess the sufficiency of both geometric safety and operation efficiency. Hence, the purpose of this research is to fill the information gap by offering reliable tools to assist traffic engineers in the design of a Superstreet with or without signal controls and to provide an efficient signal progression to better coordinate traffic flows. To address these issues, the entire research consists of the following tasks:

- Identification of the critical factors that may dominate the safety performance of a Superstreet. Several existing studies have indicated that the distance between the main intersection and the U-turn crossover is the key issue in the resulting performance of a Superstreet;
- Producing an applicable tool to assist traffic professionals in the design of an un-signalized Superstreet. The proposed model is capable of capturing the traffic dynamics on the arterial segment and reflecting the uncertainty of human behavior. The model should also faithfully represent the spatial interactions between the gap acceptance behavior and headway distributions on the target arterial;
- Setting the criteria for assessing the need of installing a signal control in an existing un-signalized Superstreet.

- Evaluating the geometric features of a candidate un-signalized intersection, especially on the link length, the turning bay length, and the ratio between the queue length and the predesigned link length.
- Developing of an efficient signal design methodology to coordinate the traffic flows between vehicles from the side street and the main arterial.

2.6 Principal Research Output

More specifically, the research results of all the aforementioned tasks are organized into the following models and their development procedures are specified in Figure 2-1.

- ***Model 1: Development of a Minimum U-turn Offset Length Model for an Un-signalized Superstreet.*** This model is developed to address the design of the U-turn offset length in an un-signalized Superstreet. Based on the data of arterial traffic headway and critical gap distributions among the target driver population, it is expected that the model can generate a reliable estimation of the required U-turn offset length under the given traffic demand. One can also extend the model's results to set the criteria for determining whether a signal needs to be installed .

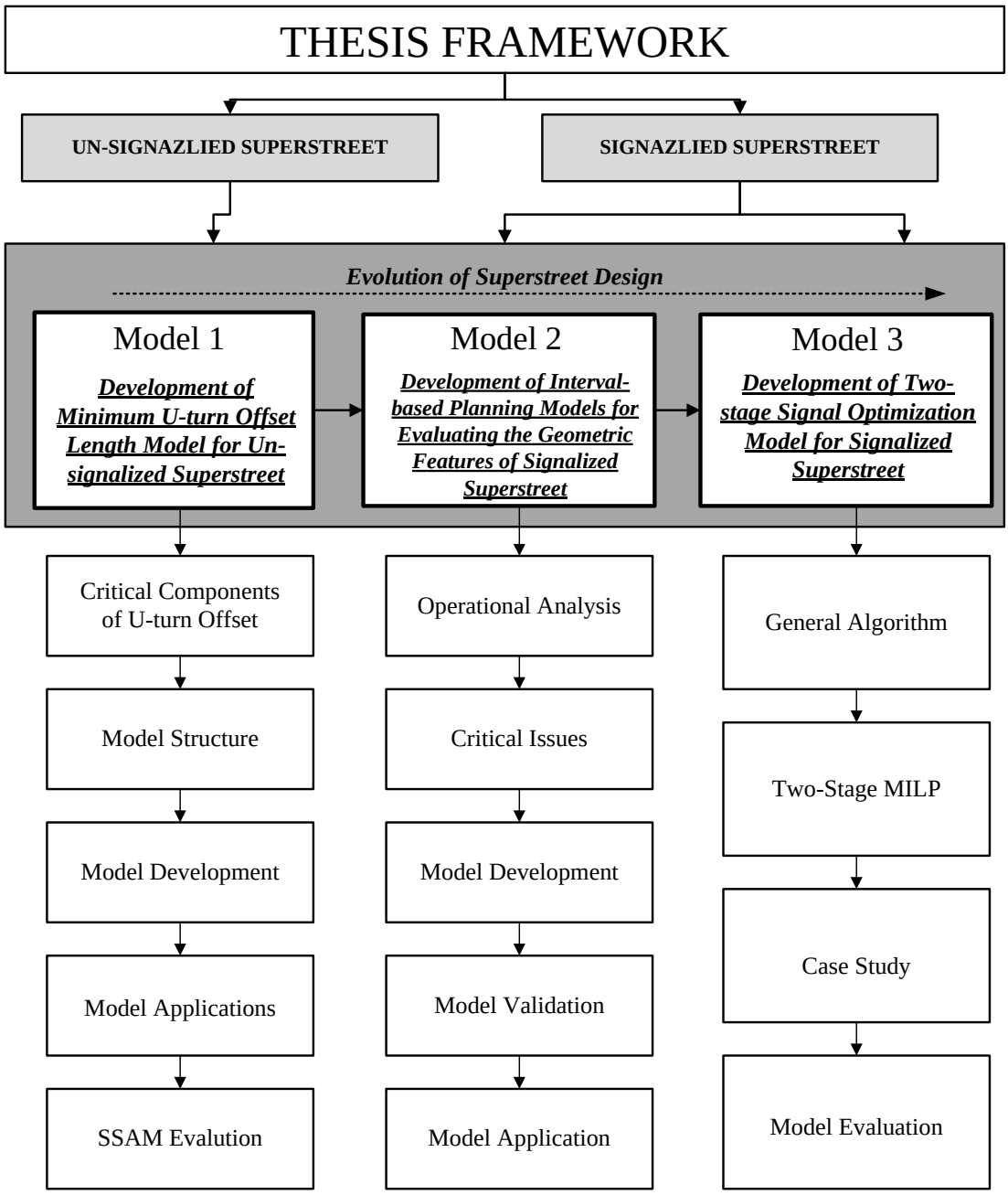

Figure 2-1 Graphical Illustration of the Key Proposed Research Tasks

- ***Model 2: Development of Interval-based Planning/Evaluation Models for Assessing the Geometric Features of a Signalized Superstreet.*** This model aims to assist the users in estimating the range of potential queue variation on each link under a given demand and signal plan. The estimated queue intervals offer the

basis for evaluating whether any critical links in a Superstreet are insufficient to accommodate the potential queues under the given demand level.

- ***Model 3: Development of a Two-Stage Signal Optimization Model for a Signalized Superstreet.*** Since the desirable operational efficiency cannot be achieved without the proper design of signals, this model offers a two-stage solution approach to optimize signals within a Superstreet. At the first stage, a mixed integer programming model with the objective of maximizing traffic throughput is proposed to select the best common cycle length and green splits. To coordinate flows between the main intersection and U-turn crossovers, the second stage offers a multi-objective linear programming formulation for selecting the best offset value for each sub-intersection.

Chapter 3: Minimum U-turn Offset Model for an Un-Signalized Superstreet

3.1 Introduction

This chapter presents a model that is developed to assist traffic engineers in evaluating the offset design for an un-signalized Superstreet. Different from a signalized Superstreet, the minor road drivers at such a Superstreet are often under high risks, especially if the U-turn offset is insufficient to accommodate their needs to change lanes. Some existing studies (AIIR, 2010; Hochstein, 2009; Liu, 2008; Rafael, 2011) concluded that the distance between the main intersection and its U-turn crossover is the critical factor that dominates the effectiveness of an un-signalized Superstreet. Furthermore, some researchers (Hummer, 1998; Bared, 2009; FHWA, 2012) indicate that converting conventional intersections to un-signalized Superstreets has achieved mixed results in terms of reducing the annual crash rate. Zhang (2014) reported that the frequency of injury within the segment from the main intersection to the southern U-turn crossover increased significantly at several field implementations.

Focusing on the same safety issues associated with the Superstreet design, the Maryland State Highway Administration has complied the crash data of such intersections over five years. Table 3-1 shows its before-and-after crash rate comparisons for each studied segment. The statistical test results reveal that only the main intersection experienced statistically significant reduction in crash frequency, but none of the other segments show an apparent safety improvement.

Table 3-1 Before-After Crash Rate Comparisons for Un-signalized Superstreets in a five-year period (2009-2013) in Maryland

Intersection		location																	
		Southern U-turn				Southern offset				Main intersection				Northern Offset				Northern U-turn			
		Before	After	Change (%)	T-test	Before	After	Change (%)	T-test	Before	After	Change (%)	T-test	Before	After	Change (%)	T-test	Before	After	Change (%)	T-test
US 15 @ Hayward Rd	Inter	0.00	0.00	0%		0.67	0.00	-100%		4.00	2.33	-42%		0.00	0.00	0%		0.00	0.00	0%	
	Non-inter	0.00	0.00	0%		2.33	1.00	-57%		0.33	1.00	**203%**		1.67	1.00	-40%		0.00	0.00	0%	
US 15 & Willow Rd	Inter	0.00	0.00	0%		0.00	0.33	**33%**		1.67	0.33	-80%		0.00	0.00	0%		4.33	1.33	-69%	
	Non-inter	0.00	0.00	0%		1.33	4.00	**201%**		0.00	0.00	0%		1.67	3.00	**80%**		0.00	0.00	0%	
US 15 & Biggs Ford Rd	Inter	1.67	0.33	-80%		0.00	0.00	0%		4.33	1.33	-69%		0.00	0.33	n/a		0.33	1.33	**303%**	
	Non-inter	0.00	0.00	0%		1.67	3.00	**80%**		0.00	0.00	0%		1.00	1.67	**67%**		0.00	0.00	0%	
US 15 & Sundays Ln	Inter	4.33	1.33	-69%		0.00	0.33	**n/a**		0.33	1.33	**303%**		0.00	0.33	n/a		0.33	1.00	**203%**	
	Non-inter	0.00	0.00	0%	0.38 [0.71]	1.00	1.67	**67%**	-1.59 [0.13]	0.00	0.00	0%	**2.74[a] [0.01]**	2.00	1.33	-34%	-0.25 [0.81]	0.00	0.00	0%	1.23 [0.24]
US 15 & College Ln	Inter	0.00	0.00	0%		0.00	0.00	0%		3.67	0.33	-91%		0.33	0.33	0%		0.00	0.00	0%	
	Non-inter	0.00	0.00	0%		0.33	0.33	0%		0.00	0.00	0%		0.67	0.33	-51%		0.00	0.00	0%	
US 301 & Main St	Inter	n/a	n/a	n/a		0.33	0.00	-100%		2.67	0.67	-75%		0.00	0.33	-94%		5.33	0.33	-94%	
	Non-inter	n/a	n/a	n/a		0.33	0.67	**10%**		0.67	0.67	0%		1.33	1.67	**26%**		1.67	0.67	-60%	
US 301 & Del Rhodes Ave	Inter	2.67	0.67	-75%		0.00	0.33	**n/a**		5.33	0.33	-94%		0.00	0.00	0%		0.00	0.00	0%	
	Non-inter	0.67	0.67	0%		1.33	1.67	**26%**		1.67	0.67	-60%		0.33	2.33	**606%**		0.00	0.00	0%	
US 301 & Galena Rd	Inter	0.00	0.00	0%		0.00	0.00	0%		5.00	0.67	-87%		0.00	0.00	0%		0.00	0.00	0%	
	Non-inter	0.00	0.00	0%		0.33	0.67	**103%**		0.00	0.00	0%		3.00	0.33	-89%		0.00	0.00	0%	

*1. Numbers in parentheses denote the P-value;

*2. Numbers highlighted in red represent the increased crash rate;

*3. [a] denotes the significant change in before-and-after crash rates at 0.01 significance level.

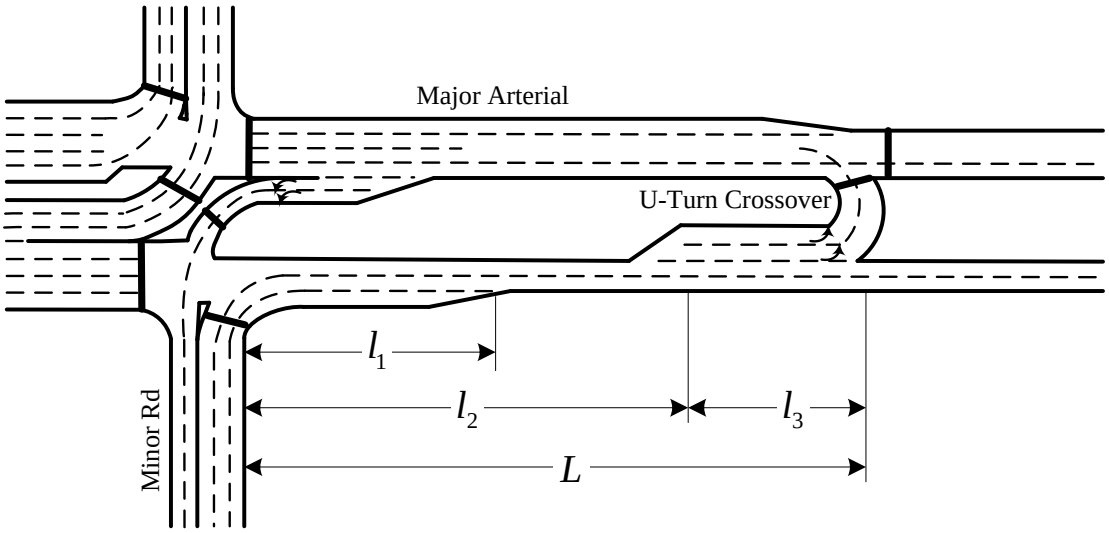

Note: l_1 = Acceleration and merging length;
l_2 = Lane-Changing length;
l_3 = Deceleration and initial-queue length;
L = Minimum U-turn offset length.

Figure 3-1 Illustration of critical components of the U-turn offset length

Figure 3-1 shows the critical components of the entire U-turn offset, where its first segment, denoted as l_1, is the length needed for the minor road drivers to accelerate from a full stop and merge into the mainline traffic; l_2 represents the minimal length for the minor road drivers to successfully conduct k-th lane changes before merging onto the most inner lane. Last, l_3 is the minimal length for vehicles to decelerate and queue at the U-turn bay to wait for acceptable gaps in the opposing arterial traffic. The minimal U-turn offset should equal the sum of l_2 (l_1 is part of l_2) and l_3.

3.2 Model Development

The proposed model for offset estimation consists of three key components, which are: 1) acceleration and merging length; 2) lane-changing length, and 3) deceleration and initial queue length. The required inputs and outputs for each component are shown in Figure 3-2. The notations for all key parameters and variables are described in Table 3-3.

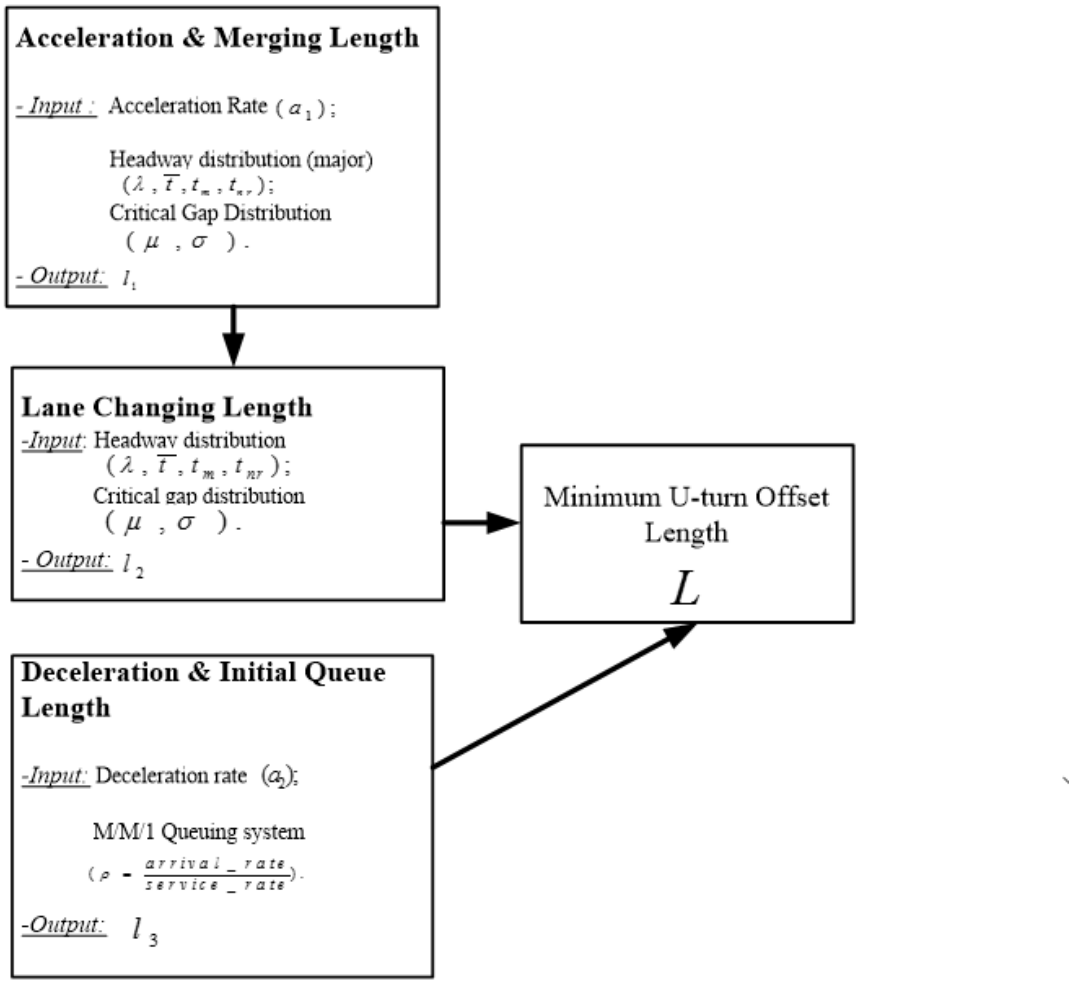

Figure 3-2. Key Components of a Minimum U-turn Offset Model

Table 3-2. Key Notations for Parameters /Variables

Notation	Description
a_1	AASHTO recommended acceleration rate
λ	Parameter for major road headway distribution which is shifted negative exponential distribution
$\bar{t}$	Average gap in second from major traffic
t_m	The minimum headway from major traffic
t_{nr}	The maximum headway from major traffic
μ	Mean of critical gap distribution
σ	Deviation of critical gap distribution
a_2	AASHTO recommended deceleration rate
ρ	Parameter for M/M/1 system, equals arrival rate/ service rate.
l_1	Acceleration & merging length
l_2	K-th lane changing length
l_3	Deceleration & initial queue length
L	Minimum U-turn offset length

Merging Scenarios

As reported in the literature (e.g., Hidas, 2005), one can classify most drivers' merging maneuvers into three distinct types, based on the interactions between the subject and the following vehicles.

- **Free merging:** As shown in Figure 3-3. (a), if there is no noticeable change in the relative gap between the leader and follower during the entire process, it indicates no interaction between them.

- **Forced merging**: Under this type of lane-changing scenario (see Figure 3-3. (b)), the gap between the leading and the following vehicles was unchanged before reaching the entry point. If such a gap is increased to

accommodate the subject vehicle, it indicates that the subject vehicle has "forced" the follower to slow down.

- **Cooperative merging:** This is the most desirable scenario, as shown in Figure 3-3. (c), where the gap between the leading and the following vehicles is increasing and then decreasing afterwards before reaching the entry point. This indicates that the follower chooses to slow down to accommodate the merging vehicle.

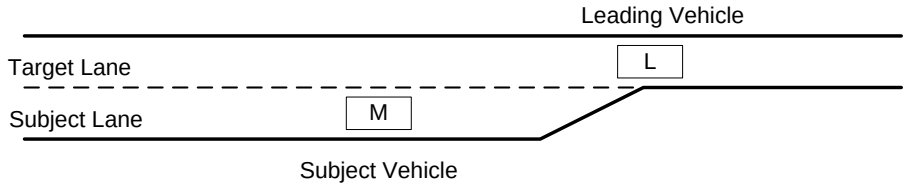

(a) free merging scenario

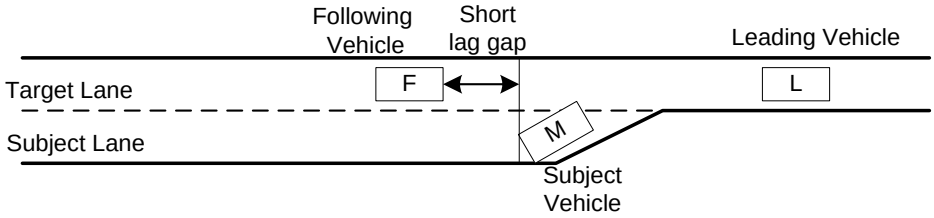

(b) forced merging scenario

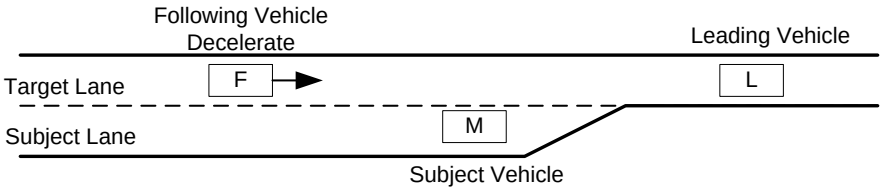

(c) cooperative merging scenario

Figure 3-3. Three Types of Merging Maneuvers

Since the leading vehicle is usually a passive player in the lane-changing process, one needs not to consider its role in defining the merging scenarios. The

main differences among these three types lie in the nature of interactions between the subject and the following vehicles. In a forced lane change, the interaction is such that the subject vehicle plays the active role by initiating the interaction and the follower reacts by slowing down. But in a cooperative lane change, the follower has to cooperatively slow down to enlarge the existing gap so that the subject vehicle can execute a successful merging.

Note that the distinction between the forced and cooperative lane changes is that the former can sometimes yield extremely dangerous situations. As described in Figure 3-3 (b), the time headway between the two active players in a merging scenario cannot be less than the duration needed for the following vehicle to decelerate to the same speed as the merging vehicle. Equation (3-1) show such a relation,

$$(h - t_r) \cdot v_1 - l_v = \frac{(v_1 - v_0)^2}{2a_2} \tag{3-1}$$

Where v_1 is the speed of the following vehicle; v_0 is the speed of the subject vehicle; t_r is the driver reaction time, which is usually set as 1.0 second (AASHTO, 2001); h is the time headway distribution; l_v is the length of the subject vehicle; and a_2 is the deceleration rate, which equals 11.2ft/s^2 (AASHTO, 2001).

For a randomly selected subject vehicle, the acceptable gap should be no less than the minimum headway, $t*$, as shown below:

$$t* \geq \frac{(v_1 - v_0)^2}{2a_2 v_1} + \frac{l_v}{v_1} + t_r \tag{3-2}$$

Acceleration and Merging length

Note that vehicles from the minor road need to first make a full stop, and then accelerate and merge into the major road traffic. Due to the safety concerns, the merging length should be sufficiently long to accommodate the process of acceleration and merging experienced by the minor road vehicles. Let the distance for acceleration be shown as follows:

$$l_a = \frac{v_1^{\,2}}{2a_1} \tag{3-3}$$

Where l_a denotes the acceleration length; v_1 is the subject vehicle's traveling speed; and a_1 is the AASHTO recommended acceleration rate.

Let $P(t)$ denotes the merging probability for a subject vehicle at any time point t during the merging process. The probability for any random vehicle to accept a given gap at time point t can be expressed as follows:

$$F_{tc}(t) = P\{h \geq t_c(t)\} \tag{3-4}$$

where t_c denotes the critical gap for a driver at time point t. Thus, $P\{h \geq t_c(t)\}$ stands for the probability that the headway at the target lane will be larger than or equal to the critical headway.

Assuming that at time point $t + \Delta t$, a driver has successfully merged into the major road traffic, one can then have the following expression:

$$p(t+\Delta t) = p(t) + (1 - p(t))\Delta t(F_{tc}(t)) \tag{3-5}$$

Since Δt is a very small time interval, the changes in the critical gap t_c can be ignored in this case, and one can have the Eq. (3-6).

$$t_c(t+\Delta t) = t_c(t) \tag{3-6}$$

Combining the previous two equations, one can have the following transformations, expressed in Eqs. (3-7)-(3-8).

$$\frac{p(t+\Delta t) - p(t)}{\Delta t} = [1 - p(t)] \cdot F(t_c(t)) \tag{3-7}$$

$$p'(t) = [1 - p(t)] \cdot F(t_c(t)) \tag{3-8}$$

By replacing $F(t_c(t))$ with $F(t)$ in Eq.(3-8), the partial derivative of $p(t)$ can be further expressed with Eq.(3-9) as follows:

$$dP = [1 - p(t)] \cdot F(t) \cdot dt \tag{3-9}$$

$$\int_0^{+\infty} dP = \int_0^{+\infty} [1 - p(t)] \cdot F(t) \cdot dt \tag{3-10}$$

$$-In[1 - p(t)]dP = \int_0^{+\infty} F(t) \cdot dt \tag{3-11}$$

Note that $F(t)$ represents the probability for a random driver to merge into the arterial traffic at any time point t. Unfortunately, one cannot get a closed-form of $P(t)$ since $F(t)$ is not a constant but a function of time and human characteristics (i.e., $t_c(t)$ is the critical gap function).

If $t_c(t)$, as assumed previously, follows a normal distribution, then the probability of a driver with a critical gap equals t_c* at time point t can be shown as follows:

$$f(t_c^*)dt = \left[\frac{1}{\sigma\sqrt{2\pi}} \exp \frac{-(t_c^* - \mu)}{2\sigma^2} \right] dt \tag{3-12}$$

where μ is the mean and σ denotes the standard deviation. As for most related studies, one can assume that the headways of arterial vehicles follow a negative exponential distribution as below:

$$\Pr(h \geq t_c) = \begin{cases} e^{-\lambda(t_c - t_m)}, & for \quad t_c \geq t_m \\ 0, & for \quad t_c < t_m \end{cases} \tag{3-13}$$

where λ is the parameter for shifted negative exponential distribution, $\lambda = 1/(\bar{t} - t_m)$ while $\bar{t}$ is the average gap (s) and t_m is the minimum headway(s).

At time point t, the probability for a driver to have a critical gap equal to t_c* in successful lane merge can be expressed as follows:

$$\Pr(h \geq t_c^*) \bullet f(t_c^*)dt \tag{3-14}$$

In brief, for any random vehicle to conduct successful merging maneuvers can be the integration of Eq. (3-14) from critical gap equals 0 to infinity as follows:

$$\int_{t_c=0}^{\infty} \Pr(h \geq t_c) f(t_c)dt \tag{3-15}$$

By further taking the realistic upper and lower bounds for drivers' critical gaps (Pollatschek and Polus, 2002), one can approximate the successful merging probability with Eq.(3-16), where $t_{sa,}t_{nr}$ represent the practical upper and lower bounds, respectively:

$$\begin{aligned} &\int_{t_c=0}^{\infty} \Pr(h \geq t_c) f(t_c)dt \\ &= \int_{t_c=0}^{\max(t_m,t*)} \Pr(h \geq t_c) f(t_c)dt + \int_{t_c=\max(t_m,t*)}^{t_{nr}} \Pr(h \geq t_c) f(t_c)dt + \int_{t_c=t_{nr}}^{\infty} \Pr(h \geq t_c) f(t_c)dt \end{aligned} \tag{3-16}$$

Note that when $0 \leq t_c \leq \max(t_m, t*)$, it implies that the successful merging probability can be negligible, as shown in Eq. (3-17).

$$\int_{t_c=0}^{\max(t_m,t*)} \Pr(h \geq t_c) f(t_c) dt = \int_{t_c=0}^{\max(t_m,t*)} 0 * f(t_c) dt = 0 \tag{3-17}$$

Also, when $t_{nr} \leq t_c < \infty$, the corresponding merging probability is marginal, as denoted below:

$$\int_{t_c=t_{nr}}^{\infty} \Pr(h \geq t_c) f(t_c) dt = \int_{t_c=t_{nr}}^{\infty} \Pr(h \geq t_c) * 0 dt \approx 0 \tag{3-18}$$

Based on Eqs. (3-16)-(3-18), one can summarize the overall merging probability as shown in Eq. (3-19).

$$\int_{t_c=0}^{\infty} \Pr(h \geq t_c) f(t_c) dt = \int_{t_c=\max(t_m,t*)}^{t_{nr}} \Pr(h \geq t_c) f(t_c) dt \tag{3-19}$$

Combined with the pre-specified model inputs, one can further convert the Eq. (3-19) into a normal distribution form to generate the graphical pattern of the overall merging probability with respect to time. The expression is shown in Eq. (3-20).

$$\int_{t_c=\max(t_m,t*)}^{t_{nr}} \Pr(h \geq t_c) f(t_c) dt = e^{\lambda t_m + \frac{-2\mu\lambda\sigma^2 + \lambda^2\sigma^4}{2\sigma^2}} \int_{\max(t_m,t*)}^{t_{nr}} \frac{1}{\sigma\sqrt{2\pi}} \exp \frac{-\left[t_c - (\mu - \lambda\sigma^2)\right]^2}{2\sigma^2} dt \tag{3-20}$$

Note that the $\int_{\max(t_m,t*)}^{t_{nr}} \frac{1}{\sigma\sqrt{2\pi}} \exp \frac{-\left[t_c - (\mu - \lambda\sigma^2)\right]^2}{2\sigma^2} dt$ follows a normal distribution with the mean of $\mu - \lambda\sigma^2$ and variance of σ^2.

Lane changing length

As showing in Figure 3-4, the k^{th} lane changing length is defined as the distance for vehicles to conduct k^{th} lane change maneuvers. Note that the lane changing length l_2 under this definition is overlapped with the acceleration and merging length (denoted as l_1).

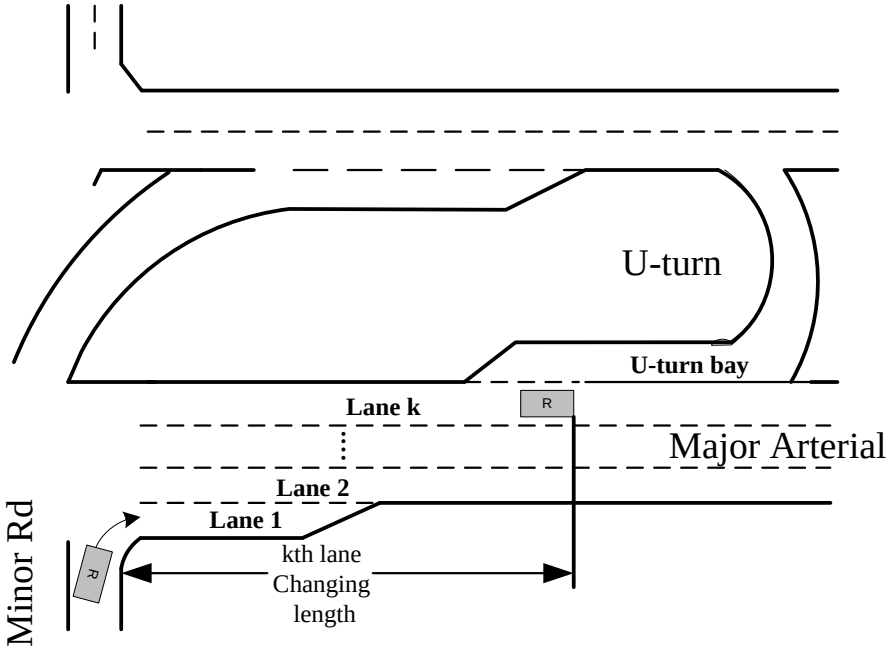

Figure 3-4. Illustration of k^{th} Lane Changing Length

Let $p_k(t)$ denotes the probability that the vehicle is in kth lane at time point t. Following the methodology used to derive merging probability (shown in Eq. (3-5)), one can show the first lane-changing probability as follows:

$$p_1(t+\Delta t) = p_1(t) + (1 - p_1(t))\Delta t F(t) \tag{3-21}$$

Then,

$$p_1'(t) = F(t) \cdot [1 - P(t)] \tag{3-22}$$

For the k-th lane change, one can compute the partial derivative as follows:

$$p_k(t + \Delta t) = p_k(t) + [1 - p_k(t)] \cdot p_{k-1}(t) \cdot \Delta t \cdot F(t) \tag{3-23}$$

$$p_k'(t) = [1 - P_k(t)] \cdot p_{k-1}(t) \cdot F(t) \tag{3-24}$$

Because both F(t) and p(t) are not a constant but vary with time, one cannot have the closed form of $P_k(t)$. Note that the k-th lane-changing probability depends on the success of the previous (k-1) lane changes (denoted as $p_{k-1}(t)$).

Deceleration and Initial Queue length

For a driver to wait at the U-turn location until finding an acceptable gap from the opposing traffic, the U-turn bay has to be sufficiently long for storing those queuing vehicles. Since the U-turn crossover for Un-signalized Superstreets has only one lane, one can formulate the queuing pattern as *M/M/1* system, where,

$$\begin{aligned} E(car \text{ in } queue) &= \frac{\rho}{(1-\rho)} \\ \rho &= \frac{\lambda}{\mu} \end{aligned} \tag{3-25}$$

where $\lambda =$ car arrival rate and $\mu =$ service rate. The headway distribution follows a shifted a negative exponential distribution, as shown below:

$$\Pr(h \geq t_c) = \begin{cases} e^{-\lambda(t_c - t_m)}, & for \quad t_c \geq t_m \\ 0, & for \quad t_c < t_m \end{cases} \tag{3-26}$$

where λ is the parameter for the shifted negative exponential distribution, $\lambda = 1/(\bar{t} - t_m)$ and $\bar{t}$ is the average gap(s); and t_m is the minimum headway(s). Assuming that vehicles decelerate from their traveling speeds to wait at the U-turn location, the length required for their deceleration can be expressed as follows:

$$l_d = \frac{v_3^{\,2}}{2a_2} \tag{3-27}$$

where l_d represents the deceleration length; v_3 is the initial deceleration speed; and a_2 denotes the AASHTO recommended deceleration rate.

$$l_3 = l_q + l_d \tag{3-28}$$

So the sum of the initial queue length and the deceleration length is the minimum value of l_3.

3.3 Numerical Example

A Un-signalized Superstreet intersection, US 301 at Ruthsburg Road in Maryland, is used as a candidate site for numerical analyses, where its southern U-turn crossover locates at 500 feet away from the main intersection.

Some field data in the literature are used in the analysis and are summarized in Tables 3-3* and Table 3-4*, where the former summarizes the lags between vehicles just merged from the minor road into the major through traffic and the latter reports

the gaps observed from three different un-signalized Superstreets in North Carolina (Inman, 2012 and FHWA, 2009).

Table 3-3* Lags between Right-turning Vehicles and the Arrival of the Next Through Vehicles (seconds)

Merge Location	Mean	Count	Minimum	Standard Deviation
Cross gore	4.4	7	2.3	2.0
End of gore line	5.7	58	0.9	2.7
Midway	5.5	27	1.1	2.1
End of merge area	5.3	23	0.0	3.5

*Ref: Hummer, J. E., Haley, R. L., Ott, S. E., Foyle, R. S., & Cunningham, C. M. (2010). Superstreet Benefits and Capacities.

Table 3-4*. Summary for Field Observations of Front and Rear Gaps (in Seconds)

SITE	RTOR		U-turn (flashing yellow)		Major left (flashing yellow)	
	Front gap (sec)	Rear gap (sec)	Front gap (sec)	Rear gap (sec)	Front gap (sec)	Rear gap (sec)
Chapel Hill	2.0	3.6	N/A	N/A	N/A	N/A
Wilmington	2.0	3.6	3.0	7.1	2.0	5.5
US-17	2.5	3.6	N/A	N/A	N/A	N/A

* Ref: Inman, V. W., & Haas, R. P. (2012). Field Evaluation of a Restricted Crossing U-turn Intersection.

As reported in the literature (Fitzpatrick, 2003 and Tian, 1999), the posted speed limit for a Superstreet is generally set below the operating speed by as much as 8 to 12 mph. Hence, one should propose a reasonable U-turn length based on the operating speed. All key input parameters used in numerical analyses are summarized in Table 3-5.

Table 3-5. Summary of the Critical Inputs

PARAMETERS	VALUES
t_{nr}	11 seconds
t_m / t_{sa}	2 seconds
$\overline{t}$	5.6 seconds
$\overline{\lambda}$	0.28
$\overline{\mu}$	0.67
a_1	4.0~4.5 ft/s2
a_2	11.2 ft/s2
v_1	63~67 mph

In practice, most vehicles from the minor approach have to excise two successive lane changes. Figure 3-5 illustrates the relationships between the first lane-changing and the second lane-changing length and their respective probability of success. Each graph presents such interactions under different mainline speeds and acceleration rates, as denoted in the sub-title.

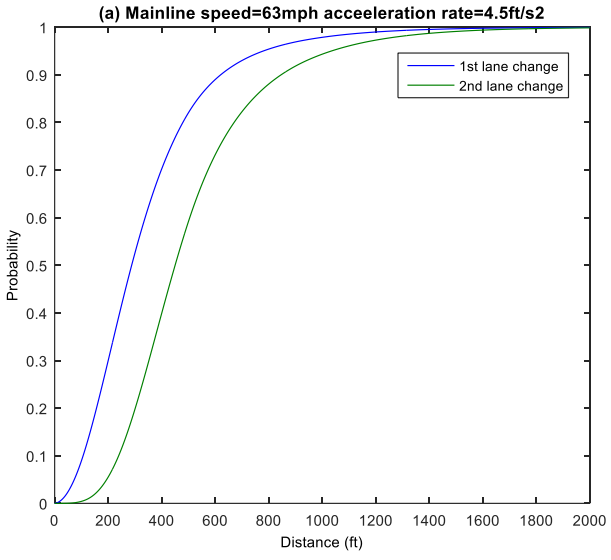

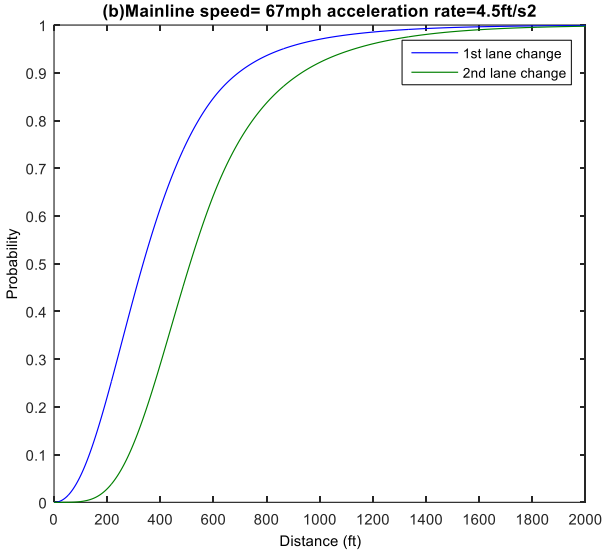

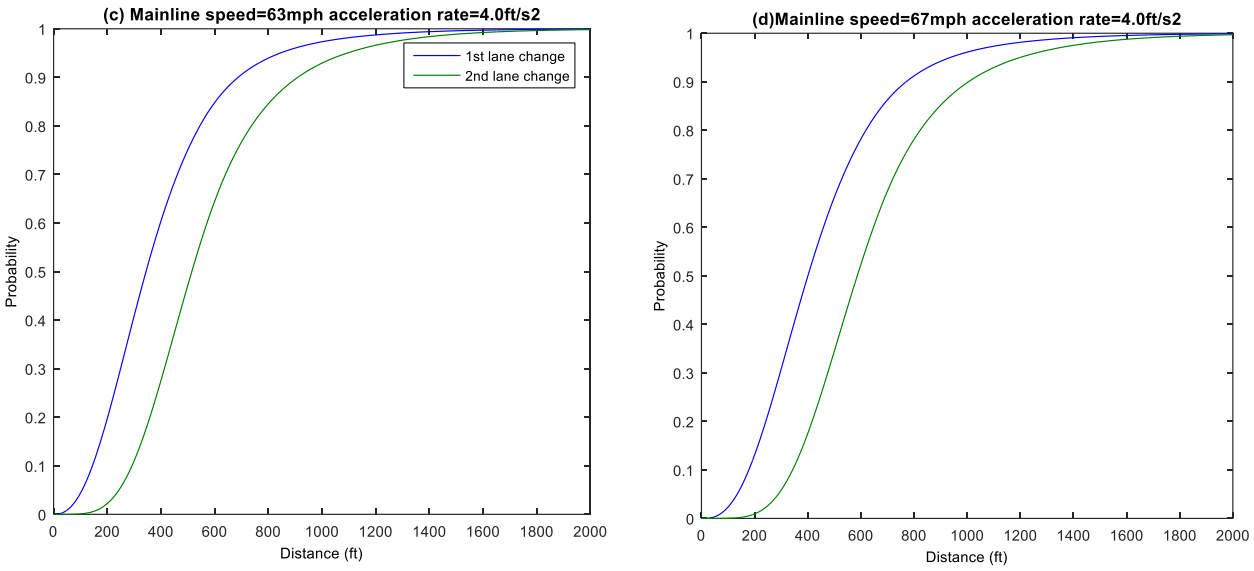

Figure 3-5. Numerical Results for l_1 (Acceleration and Merging length) and l_2 (Lane-Changing Length)

Aside from the trajectory of l_1 and l_2 (as shown in Figure 3-5), the deceleration and initial queue storage length is computed to be 300 feet for this intersection. The minimal U-turn offset length is far shorter than the field measurements of 1500 feet. The generated output indicates a possible over-design in practice. To identify potential excessive design, this study further takes the surrogate safety assessment model as an unbiased tool to evaluate the reliability of the proposed model.

3.4 SSAM Evaluation

To assess the reliability of the proposed model, three simulation experiments, including scenarios with different offset lengths, are conducted for safety comparisons. The first scenario is to replicate the traffic conditions under the existing

geometry features. The second scenario uses the mean of the offset obtained by the model's output as the southern U-turn offset. The third scenario applies a shortened U-turn offset as 700 feet to be the comparison group. As observed from the model's output, the merging probability exhibits a sudden drop around 700 feet. Note that the simulation environment is calibrated with the field collected traffic data to ensure comparability.

- **Scenario 1:** 1500 feet southern U-turn offset (*Field implementation)*
- **Scenario 2:** 1100 feet southern U-turn offset (*Mean of model output*)
- **Scenario 3:** 700 feet southern U-turn offset (*Shortened U-turn offset*)

Note that the only difference among these three scenarios is the length of southern U-turn offset. All geometric features are measured from the field and constructed accordingly in these simulation analyses. After running 30 replications over 3600 seconds per case in VISSIM, the simulated vehicles' trajectory data has been analyzed with the SSAM software, which uses the following measurements to evaluate the severity of the possible conflicts or collisions:

- The minimum time to collision (TTC);
- The minimum post-encroachment time (PET);
- The initial deceleration rate (DR);
- The maximum speed (MaxS);
- The maximum relative speed difference (DeltaS);
- The maximum deceleration rate (MaxD); and

- The maximum "post-collision" relative speed difference (MaxDeltaS).

The first two MOEs measure the severity of potential conflicting events while the rest five assess the severity of possible collisions. SSAM generated the comparison tables with all listed MOEs, and t-tests were performed to check whether the difference is statistically significant at the 95% confidence level.

Table 3-6. Summary of Safety Comparisons between Scenario 1 and 2

	1100 ft	**1500 ft**	**t-test**		
Measures	Mean (variance)	Mean (variance)	t value	Sig	Mean Difference
SSAM Measures					
TTC	0.217 (0.184)	0.217 (0.144)	-0.002	NO	0
PET	0.08 (0.026)	0.083 (0.02)	-0.018	NO	-0.003
MaxS	22.441 (8.983)	22.97 (11.465)	-0.868	NO	-0.529
DeltaS	8.678 (9.953)	9.942 (27.489)	-1.263	NO	-1.265
DR	-1.004 (5.08)	-1.203 (5.582)	0.443	NO	0.2
MaxD	-2.482 (9.743)	-2.838 (10.67)	0.587	NO	0.355
MaxDeltaV	4.485 (2.711)	5.113 (7.253)	-1.214	NO	-0.628
Conflict Types					
Crossing	0 (0)	0 (0)	0	NO	0
Rear-end	5 (22)	7.2 (21.7)	-0.744	NO	-2.2
Lane-changing	1 (2)	1 (0.5)	0	NO	0
Total	6 (36)	8.2 (22.7)	-0.642	NO	-2.2

Table 3-6 summarizes the safety performance comparison between Scenario 1 and Scenario 2 of the studied segment. As shown in the above two tables, no statistically significant difference was observed between the two testing scenarios at the target segment in terms of all possible conflict types and SSAM measures, indicating that safety performance for U-turn segments would be reduced if the U-turn offset is decreased from 1500 feet to 1100 feet.

Table 3-7. Summary of Safety Comparisons between Scenario 1 and 3

	700 ft	**1500 ft**	**t-test**		
Measures	Mean (variance)	Mean (variance)	t value	Sig	Mean Difference
SSAM Measures					
TTC	0.19 (0.187)	0.217 (0.144)	-0.159	NO	0
PET	0.078 (0.028)	0.083 (0.02)	-0.031	NO	-0.003
MaxS	22.952 (8.076)	22.97 (11.465)	-0.036	NO	-0.529
DeltaS	13.111 (37.605)	9.942 (27.489)	3.502	YES	3.168
DR	-0.57 (2.399)	-1.203 (5.582)	1.816	YES	0.633
MaxD	-2.907 (10.679)	-2.838 (10.67)	-0.13	NO	0.355
MaxDeltaV	6.791 (10.316)	5.113 (7.253)	3.434	YES	1.678
Conflict Types					
Crossing	0 (0)	0 (0)	0	NO	0
Rear-end	5.4 (6.3)	7.2 (21.7)	-0.761	NO	-1.8
Lane-changing	2.8 (0.7)	1 (0.5)	3.674	YES	1.8
Total	8.2 (7.2)	8.2 (22.7)	0	NO	0

Note: Cell highlighted represent the significant difference at 95% confidence level.

Table 3-7 summarized the safety comparison between Scenario 1 and Scenario 3 of the studied segment. As shown from the above tables, there are statistically significant differences between the two testing scenarios for the studied segment in terms of possible lane changing conflicts and several SSAM measures, such as DeltaS, DR, and MaxDelatS, indicating more severe collisions under Scenario 3. From these results, one can conclude that the safety performance of the studied U-turn segment is significantly reduced by shortening its length from 1500 feet to 700 feet.

Table 3-8. Summary of Safety Comparisons between Scenario 2 and 3

	700 ft	**1500 ft**	**t-test**		
Measures	Mean (variance)	Mean (variance)	t value	Sig	Mean Difference
SSAM Measures					
TTC	0.19 (0.187)	0.217 (0.184)	-0.136	NO	-0.026
PET	0.078 (0.028)	0.08 (0.026)	-0.01	NO	-0.002
MaxS	22.952 (8.076)	22.441 (8.983)	1.044	NO	0.511
DeltaS	13.111 (37.605)	8.678 (9.953)	3.966	YES	4.433
DR	-0.57 (2.399)	-1.004 (5.08)	0.909	NO	0.434
MaxD	-2.907 (10.679)	-2.482 (9.743)	-0.797	NO	-0.425
MaxDeltaV	6.791 (10.316)	4.485 (2.711)	3.943	YES	2.306
Conflict Types					
Crossing	0 (0)	0 (0)	0	NO	0
Rear-end	5.4 (6.3)	5 (22)	0.168	NO	0.4
Lane-changing	2.8 (0.7)	1 (2)	2.449	YES	1.8
Total	8.2 (7.2)	6 (36)	0.748	NO	2.2

Note: Cell highlighted represent the significant difference at 95% confidence level.

Similar to the previous comparison, Table 3-8 summarized the safety performance comparison between Scenario 2 and Scenario 3 of the studied segment. Analysis results indicate that both the possible number of lane changing collisions and the crash severity measures (DeltaS and MaxDeltaV) are significantly increased in the 700 feet case than under the 1500 feet case. Hence, one can conclude that the safety performance of the studied U-turn segment is compromised by shortening its length from 1100 feet to 700 feet.

From these comparison results, one can see that the safety performance for the case less than 1100 feet shows no difference with the scenario of 1500 feet. However the scenario of 700 feet significantly increases the potential lane-changing conflicts and the severity of collisions compared with the other two cases. Hence, the proposed model is evident to generate the reasonably shortened U-turn offset length without sacrificing the expected safety performance.

3.5 Extended Applications

Another possible application of this model could be for setting a threshold for the increased traffic demand, and allowing the engineers to decide when to convert to a Signalized Superstreet. By applying the same methodology, Figure 3-6 shows the results of a numerical example of the previously studied intersection, where its southern U-turn offset is 1500 feet. Based on the results in Figure 3-6, one can observe a sharp decrease on the overall merging probability when the traffic volume

rises from 2500 to 3000 Veh/h. Once the traffic volume increases over a threshold level, the Un-signalized design may fail to provide sufficient merging opportunities for the minor road driver to conduct safe lane changes. Thus, the traffic professionals may consider placing a signal control under such a demand level.

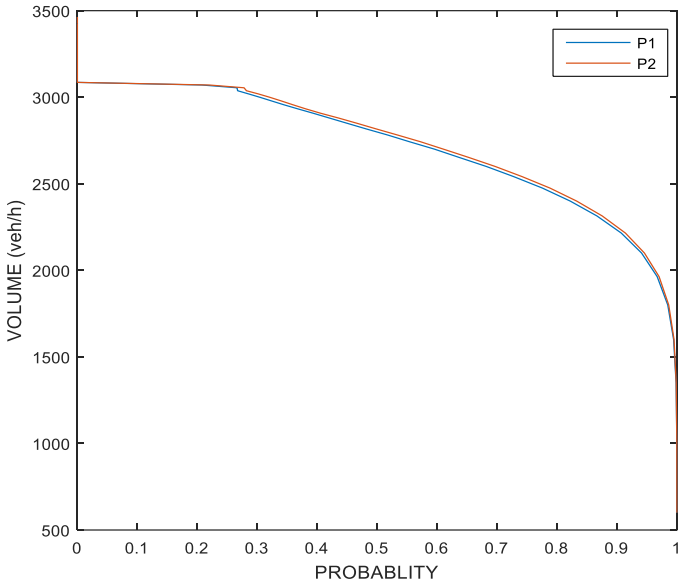

Figure 3-6. The Relationship between Traffic Demand and the Probability of Conducting Twice Lane-Changes

Table 3-9 summarizes the safety performance comparisons under different demand levels for the southern U-turn segment. As shown from the above tables, there are statistically significant differences between the two testing scenarios for the U-turn segment in terms of the possible number of lane-changing conflicts, rear-end conflicts, and the total number of conflicts. Meanwhile, several SSAM measures such as TTC and PET are significantly increased under high demand, indicating more severe possible collisions. Hence, one can conclude that the increased demand level significantly compromises the safety performance of the target U-turn segment.

Driving under such traffic conditions would cause a higher risk of encountering rear-end collisions and lane-changing conflicts. Hence, applying a signal control to such an intersection is the viable alternative.

Table 3-9. Safety Comparisons between Current Demand and High Demand Scenarios (U-turn Segment Only)

	High-volume	**Current-volume**	**t-test**		
Measures	Mean (variance)	Mean (variance)	t value	Sig	Mean Difference
SSAM Measures					
TTC	0.34 (0.322)	0.217 (0.144)	1.962	YES	0.123
PET	0.337 (0.606)	0.083 (0.02)	7.173	YES	0.254
MaxS	19.491 (38.088)	22.97 (11.465)	-6.078	YES	-3.479
DeltaS	7.759 (19.238)	9.942 (27.489)	-2.62	YES	-2.184
DR	-0.881 (2.463)	-1.203 (5.582)	0.864	NO	0.322
MaxD	-2.492 (7.763)	-2.838 (10.67)	0.665	NO	0.346
MaxDeltaV	3.992 (5.118)	5.113 (7.253)	-2.618	YES	-1.121
Conflict Types					
Crossing	0 (0)	0 (0)	0	NO	0
Rear-end	139.8 (137.2)	7.2 (21.7)	23.522	YES	132.6
Lane-changing	19 (23)	1 (0.5)	8.303	YES	18
Total	158.8 (151.7)	8.2 (22.7)	25.5	YES	150.6

Note: Cell highlighted represent the significant difference at 95% confidence level.

Table 3-10 summarizes the safety performance comparison for the overall intersection under two different demand levels. The increased input traffic volume affects not only the target segment but also the overall intersection safety

performance. More specifically, the analysis results indicate an increase in the number of lane-changing, rear-end, and total collisions. The crash severity measures, including TTC and PET, are also significantly increased under the high demand level. As shown in simulation experiments, the incoming traffic also puts the left-turning vehicles from the main intersection at risk due to the queue spillbacks and partial blocks of the main intersection. To prevent such conditions, applying a signal control to the target intersection would be essential to ensure the proper operations of the target intersection.

Table 3-10. Safety Comparisons between Current Demand and High Demand Scenarios (Overall intersection)

	High-volume	**Current-volume**	**t-test**		
Measures	Mean (variance)	Mean (variance)	t value	Sig	Mean Difference
SSAM Measures					
TTC	0.327 (0.299)	0.263 (0.229)	2.39	YES	0.065
PET	0.266 (0.438)	0.163 (0.196)	3.78	YES	0.103
MaxS	20.896 (28.359)	22.902 (16.047)	-8.498	YES	-2.006
DeltaS	11.138 (48.764)	14.73 (68.774)	-8.159	YES	-3.592
DR	-0.945 (2.937)	-1.056 (4.054)	1.042	NO	0.112
MaxD	-2.824 (8.388)	-2.916 (9.504)	0.549	NO	0.092
MaxDeltaV	5.732 (12.867)	7.56 (18.062)	-8.099	YES	-1.828
Conflict Types					
Crossing	6.8 (8.7)	4.2 (7.2)	1.458	NO	2.6
Rear-end	217.8 (374.2)	44 (86)	18.116	YES	173.8
Lane-changing	99.4 (276.3)	35.8 (10.7)	8.395	YES	63.6
Total	324 (1030)	84 (150)	15.623	YES	240

Note: Cell highlighted represent the significant difference at 95% confidence level.

Chapter 4: Interval-Based Bay Length Evaluation Models for a Signalized Superstreet

4.1 Introduction

If any link length in a Superstreet design is not sufficient to accommodate the resulting queueing vehicles, the potential spillover may cause blockages at the intersection and consequently reduce its overall capacity. Figure 1-3 shows the following three possible blockage scenarios in a typical Superstreet: 1) the left-turn bay is insufficient to accommodate the intended left-turn volumes, and thus the vehicles spill back to cause a partial blockage to the through traffic; 2) the overflowed queues from the through lane groups block the entry of the left-turn bay, and thus completely block the left-turn movement; and 3) the queuing vehicles reach the downstream link and block the upstream traffic. Hence, an effective method for evaluating the geometric features of a Superstreet design emerges as an essential task.

Recognizing the aforementioned blockages in a Superstreet implementation, this study aims to propose a planning model to address the following critical issues: 1) How to effectively identify the potential queue spillback locations when a Superstreet needs to accommodate heavy volumes; 2) How to identify those critical links that may be the primary contributors to the overall intersection delay; 3) How to account for the potential variation of flow patterns when evaluating the geometric

design of a Superstreet; and 4) How to perform the preliminary analysis from the planning aspect to offer valuable information for the signal design.

4.2 Operational Analysis

To explore the interrelation between each bay length among a Superstreet and its impact on the resulting queue pattern, this study has first developed a Superstreet simulator for extensive simulation analyses. The developed simulator is based on the field data collected at the intersection of Maryland3 and Waugh Chapel Road and calibrated with the objective of minimizing the differences between the simulated and field flow data. The demand patterns used for simulation experiments range from 4000 to 14000 vehicles/hour and are randomly generated with VISSIM. Also, to eliminate the output variation due to the stochastic nature of microscopic traffic simulation, this study has simulated each demand pattern with five replications using different random seeds.

Figure 4-1 presents the classification of all possible queue types, based on the geometric features of a typical Superstreet:

1) *Type-1 Queue(Q7, Q8, Q9, Q10): External through queues on major and minor roads*
2) *Type-2 Queue(Q3, Q6): U-turn queues at the two crossover intersections*
3) *Type-3 Queue(Q1, Q4): Left-turn queues at the main intersection*

4) Type-4 Queue(Q2, Q5): Internal through queues at the main intersection

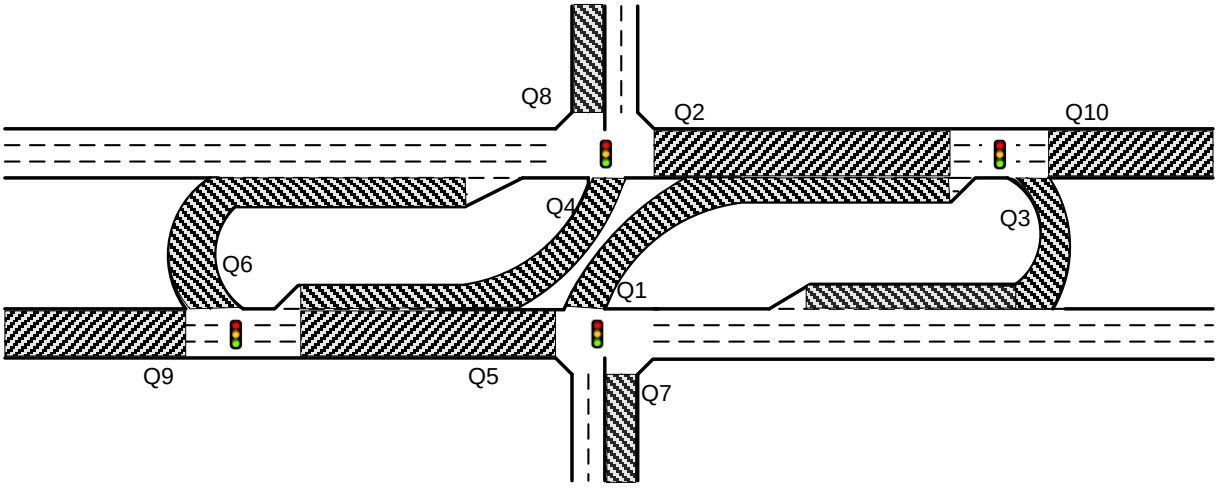

Figure 4-1. Spatial Distributions of all Potential Queues at Superstreet

By defining the QL as the ratio of the maximum queue length over the available bay (or link) length, Figure 4-2 shows the relationship between the average intersection delay and the queuing size within the Superstreet. Note that the average QL ratio is defined as the arithmetic mean of all QL ratios for the ten critical links shown in Figure 4-2. Based on the simulation results, one can observe that the intersection's average delay increases significantly when the QL ratio is close to 1.

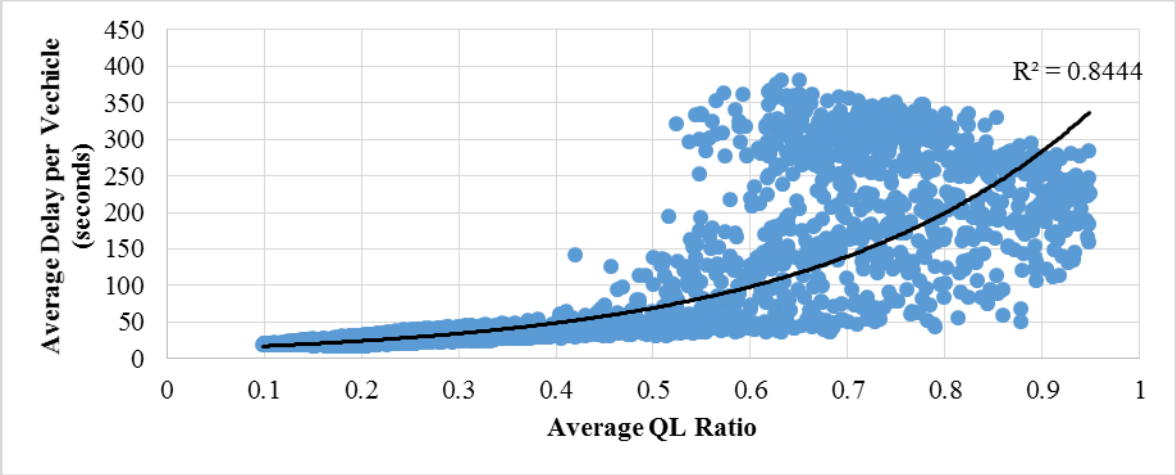

Figure 4-2. Scatter Plot of Average Delay vs. Average QL Ratio

Note that given the general patterns in Figure 4-2, there are queues at some links that may serve as the primary contributors to the total intersection delay. Thus, to rank these queues with respect to their impacts on the intersection's operational efficiency, this study has conducted a correlation analysis between the intersection's average delay and four types of QL ratios. As shown in Table 4-1, the correlation parameters for all types of QL ratios are statistically significant.

Table 4-1. The Correlation Test between QL Ratios and the Overall Intersection Delay

	Parameter Estimate	t-Value	P-Value
Type 1 QL Ratio(Q7,Q8,Q9,Q10)	1.613	35.03	<.0001
Type 2 QL Ratio(Q3,Q6)	0.415	31.72	<.0001
Type 3 QL Ratio(Q1,Q4)	0.064	3.95	<.0001
Type 4 QL Ratio(Q2,Q5)	0.338	11.91	<.0001

4.3 Critical Issues

In view of the high correlation between QL ratios and average intersection delay, this study has further developed a set of queue estimation models, which can collectively serve as a tool for preliminary estimation of potential queue size in each link, and for engineers to assess whether those links are sufficient to store potential traffic queues without using time-consuming and complex simulation tools.

Since the entire Superstreet consists of four sub-intersections, the proposed model should be capable of reflecting the interdependent relations among them under the given range of demand variation. These four types of critical queues can be categorized into two groups, based on the nature of their formations: 1) external through queues (Type-1) on both the major and minor roads, which can only be affected by the demand flow variation; and 2) internal queues (Type-2,3,4) which could be impacted by both the demand variation and the signal coordination plan.

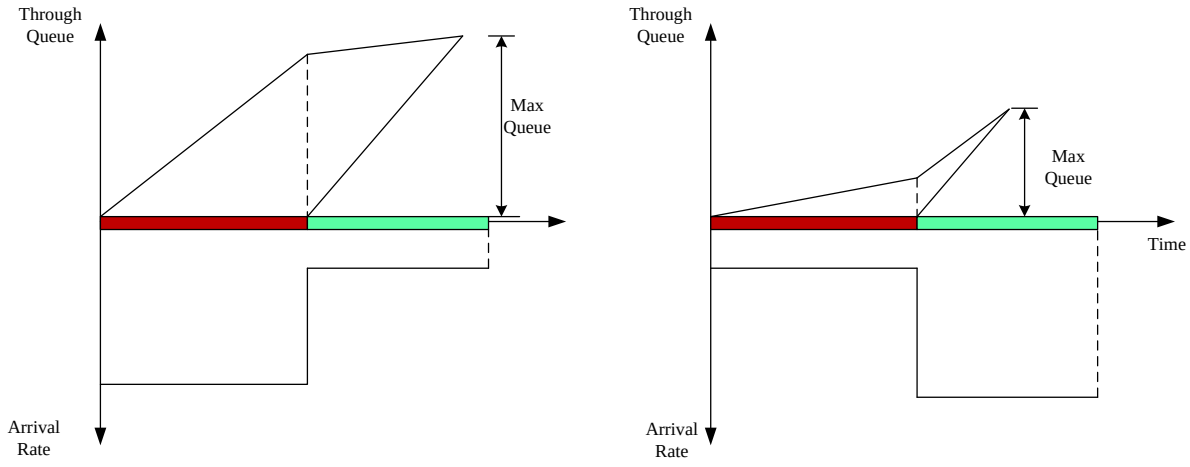

a) Worst Signal Coordination Plan b) Best Signal Coordination Plan

Figure 4-3. Two Signal Coordination Plans for Q5

To analyze the relations between the internal queue and the signal coordination plan, Figure 4-3 shows the discrepancy in the queue patterns between two scenarios, when both have the same flow rate to the intersection but under different signal control plans. Figure 4-3 (a) illustrates the queue formation patterns when most queuing vehicles are from the uncoordinated flows (e.g., the turning flows). In contrast, Figure 4-3 (b) shows the resulting queue patterns when most of those vehicles are from the well-coordinated flows (e.g., through flows). Hence, depending on the implemented signal coordination plan, the resulting queue pattern in a Superstreet may differ significantly even at the same volume level.

4.4 Model Development

To account for the queue variation due to the arriving flow fluctuation under different signal coordination plans, this study has developed a set of interval-based queue estimation models for the design of the link length on a Superstreet.

Type-1 Queue Model (Q7, Q8, Q9, Q10)

These type of queues can be affected only by one traffic signal, and its queue formation process is illustrated in Figure 4-4. Notably, the maximal physical queue length, which equals the distance from the stop-line to the end of the queue, is obtained at the queue vanishing point.

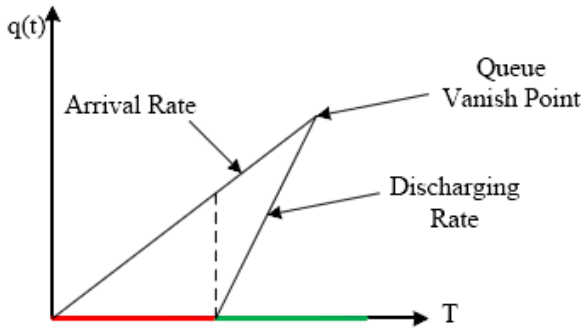

Figure 4-4. The Queuing Process on the Target Link

Let *A(t)* denote the time-dependent arrival rate on the target link and one can obtain the queue clearance time, *t**, by solving the following equation:

$$\int_0^R A(t)dt = \int_R^{t^*} (s - A(t))dt \tag{4-1}$$

where *R* denotes the red duration of the target link; s is the saturation flow rate.

Then, the maximal queue length, *Q*, on the target link, could be estimated with the following equation:

$$Q = \int_0^R A(t)dt + \int_R^{t^*} A(t)dt \tag{4-2}$$

Note that Eq. (4-2) can faithfully reflect the flow uncertainty by adjusting the value of *A(t)*. Hence, assuming that the arrival rate may lie within the interval $[\underline{A}, \overline{A}]$, one can then estimate the resulting queue length interval, $[\underline{Q}, \overline{Q}]$, with the following equations:

$$\underline{Q} = \int_0^R \underline{A} dt + \int_R^{t^*} \underline{A} dt \tag{4-3}$$

$$\overline{Q} = \int_0^R \overline{A} dt + \int_R^{t^*} \overline{A} dt \tag{4-4}$$

Type-2 Queue Model (Q3, Q6)

Since both the through and left-turn flows from the minor streets have to exercise a U-turn in a Superstreet, the formation of Type-2 queues is due mostly to these two streams of flows. Different from the Type-1 queues, the signal coordination plans between the crossovers and the primary intersection could have a significant effect on the formation of such queues.

Let $A_{TL}(t)$ denote the total arrival rate of the through and left-turn flows on the minor street, and one can then estimate the corresponded discharge rate, $D_{TL}(t)$, as follows:

$$D_{TL}(t) = \begin{cases} \min(s, A_{TL}(t) + q_{TL}(t)); & t \in [R_{up}, C] \\ 0; & o.w. \end{cases} \tag{4-5}$$

where C denotes the signal cycle length; R_{up} is the red time of the upstream signal; and $q_{TL}(t)$ is the number of through and left-turn queuing vehicles on the minor street.

Let σ denote the average travel time from the upstream signal to the end of queue, and the arrival rate on the target link could be estimated with the following expression:

$$A(t) = D_{TL}(t - \sigma) \tag{4-6}$$

Since Type-2 queues are affected by two traffic signals, key contributing factors (including the arrival rate, signal green splits, offset, and average travel time) will collectively determine the maximal queue length on the target link. Hence, when the upstream green time is greater than the downstream red time, the queue clearance time, *t**, under the worst case can be estimated with the following equations:

$$\int_0^{t^*} A(t)dt = \int_{R_{up}}^{R_{up}+t^*} D_{TL}(t)dt \tag{4-7}$$

$$\int_0^{R} A(t)dt = \int_{R}^{t^*} (s - A(t))dt \tag{4-8}$$

Then, the maximal queue length under such conditions could be estimated with Eq. (4-9):

$$Q = \int_0^{t^*} A(t) = \int_{R_{up}}^{R_{up}+t^*} D_{TL}(t)dt \quad if \;\; C - R_{up} > R \tag{4-9}$$

Similar to Type-1 queues, the upperbound of the maximal queue length considering the uncertainty of the incoming flows could be estimated as follows:

$$Q = \int_{R_{up}}^{C} D_{TL}(t)dt \quad if \;\; C - R_{up} \le R \tag{4-10}$$

Similar to Type-1 queues, the upperbound of the maximal queue length considering the uncertainty of the incoming flows could be estimated as follows:

$$\overline{Q} = \begin{cases} \int_{R_{up}}^{R_{up}+t^*} \overline{D}_{TL}(t)dt; & if \quad C - R_{up} > R \\ \int_{R_{up}}^{C} \overline{D}_{TL}(t)dt; & if \quad C - R_{up} \le R \end{cases} \tag{4-11}$$

With the best signal coordination plan, most approaching vehicles will arrive at the target link during its green phase. Thus, the lowerbound of the maximal queue length under such conditions can be approximated as follows:

$$\underline{Q} = \begin{cases} \int_{C-(R-R_{up})}^{C} \underline{D}_{TL}(t)dt; & if \quad C - R_{up} > C - R \\ 0; & if \quad C - R_{up} \le C - R \end{cases} \tag{4-12}$$

Where, ($R - R_{up}$), represents the green time difference between the two traffic signals.

Type-3 Queue Model (Q1, Q4)

Note that Type-3 queues come from only one primary source, i.e., the left-turn volume departing from its upstream link (i.e., Q9 & Q10 in Figure 4-1). Let $A_L(t)$ denote the arrival rate of the left-turn flows on the upstream link, and the corresponding discharge rate, $D_L(t)$, could be estimated as follows:

$$D_L(t) = \begin{cases} \min(s, A_L(t) + q_L(t)); & t \in [R_{up}, C] \\ 0; & o.w. \end{cases} \quad (4\text{-}13)$$

Then, by replacing $D_{TL}(t)$ with $D_L(t)$, one can directly implement Eqs.(4-11)-(4-12) to estimate the variation range of Type-3 queues.

Type-4 Queue Model (Q2, Q5)

Different from the other types of queues, both the major through and U-turn flows from the crossovers may contribute to the formation of Type-4 queues. Hence, the arrival rate on the target link depends actually on the following departure rates:

$$D_T(t) = \begin{cases} \min(s, A_T(t) + q_T(t)); & t \in [R_{up}, C] \\ 0; & o.w. \end{cases} \quad (4\text{-}14)$$

$$D_U(t) = \begin{cases} \min(s, A_U(t) + q_U(t)); & t \in [0, R_{up}] \\ 0; & o.w. \end{cases} \quad (4\text{-}15)$$

where $D_T(t)$, $A_T(t)$, and $q_T(t)$ denote the departure rate, arrival rate, and number of queuing vehicles, respectively, at time t from the upstream through link (i.e., Q9 & Q10 in Figure 4-1); $D_U(t)$, $A_U(t)$, and $q_U(t)$ are the departure rate, arrival rate, and the number of queuing vehicles, respectively, at time t from the upstream U-turn link (i.e., Q3 & Q6 in Figure 4-1); R_{up} is the red time for the upstream through traffic.

Also, it is noticeable that $D_T(t)$ will be much larger than $D_U(t)$ since the major approach flows can usually dominate the minor street flows on a typical Superstreet. Hence, when the green time for the upstream through traffic is greater than the red time of the target link, the queue clearance time, t^*, under the worst case can be approximated with the following equations:

$$\int_0^{t^*} A(t)dt = \int_{R_{up}}^{R_{up}+t^*} D_T(t)dt + \int_0^{\max(t^*-R_{up},0)} D_U(t)dt \tag{4-16}$$

$$\int_0^{t^*} A(t)dt = \int_R^{t^*} sdt \tag{4-17}$$

Then, the upper-bound of the maximal queue length under such signal coordination plan could be estimated with Eq. (4-18):

$$\overline{Q} = \int_{R_{up}}^{R_{up}+t^*} \overline{D}_T(t)dt + \int_0^{\max(t^*-R_{up},0)} \overline{D}_U(t)dt \quad if \quad C - R_{up} > R \tag{4-18}$$

If the green time of the upstream through traffic is less than the red time of the target link, the upperbound of the maximal queue length can be computed with the following expression:

$$\overline{Q} = \int_{R_{up}}^{C} D_T(t)dt + \int_0^{R-(C-R_{up})} D_U(t)dt \quad if \quad C - R_{up} \le R \tag{4-19}$$

With the best signal coordination plan, most upstream through traffic will arrive at the target link during its green phase. Approximated with the following

expression, the lower-bound of the maximal queue length under such a condition can be expressed as follows:

$$\underline{Q} = \begin{cases} \int_0^{R_{up}} \underline{D}_U(t)dt + \int_{C-(R-R_{up})}^{C} \underline{D}_T(t)dt; & if \quad C - R_{up} > C - R \\ \int_{R_{up}-R}^{R_{up}} \underline{D}_U(t)dt; & if \quad C - R_{up} \le C - R \end{cases} \tag{4-20}$$

4.5 Simulation Assessment

To illustrate the model's potential for applications and its effectiveness, this study has further taken the Superstreet design for the intersection of Maryland 3 and Waugh Chapel Road in Maryland for experimental analyses. The geometric layout of this field site is shown in Figure 4-5.

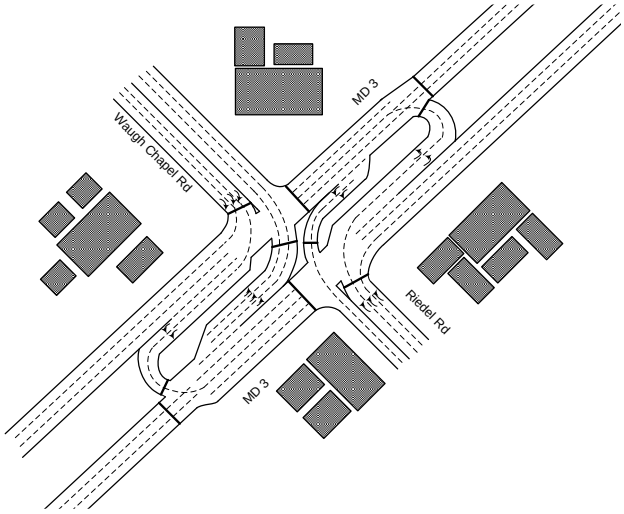

Figure 4-5. The Geometric Layout of the Target Superstreet in Maryland

Based on the collected field data during PM peak hours, Figure 4-6 presents the observed upperbound and lowerbound of each stream of turning flows on the

Superstreet. Notably, the flow rate from the major approach (i.e., East-Westbound) clearly dominates the ones from the minor streets.

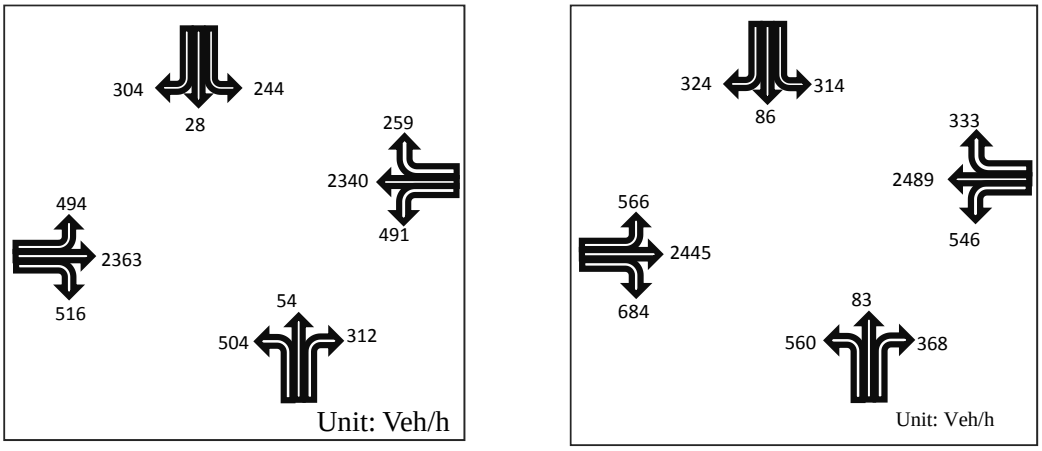

a) Minimum traffic inputs

b) Maximum traffic inputs

Figure 4-6. Intervals for Demand Pattern

To facilitate the estimation of the queue variation interval, this study has also collected the current cycle length and signal timings from the field site. Due to the high traffic volumes, the cycle length is set as 180 seconds, and the green time of each phase is presented in Figure 4-7.

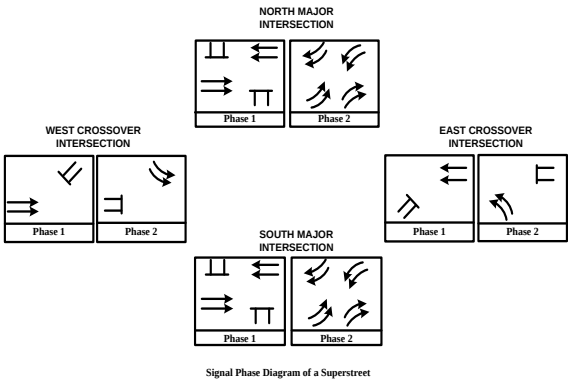

	Phase 1	Phase 2
NORTHERN INTERSECTION	149	31
SORTHERN INTERSECTION	140	40
WESTERN INTERSECTION	157	23
EASTERN INTERSECTION	143	37

Figure 4-7. Green Splits for each Sub-intersection

With the above information, Table 4-2 presents the estimated queues on each critical link (see Figure 4-1) with the proposed models.

Table 4-2. Summary of The Estimated Queue Intervals (Unit: feet)

	Q1	Q2	Q3	Q4	Q5	Q6	Q7	Q8	Q9	Q10
Queue Lower-bound	212	421	261	133	549	173	261	170	655	815
Queue Upper-bound	292	747	422	174	660	217	316	220	1858	1315
Measured Link Length	412	720	752	466	**500**	485	**267**	794	2500	1400

To test the reliability of the proposed queue models, this study has further calibrated a Superstreet simulator to estimate the resulting queues in each link under 30 different demand levels. The simulated maximal queue length on each critical link along with the estimated queue intervals with the proposed models are shown in Figure 4-8. It is noticeable that most simulated queues fall within the estimated intervals.

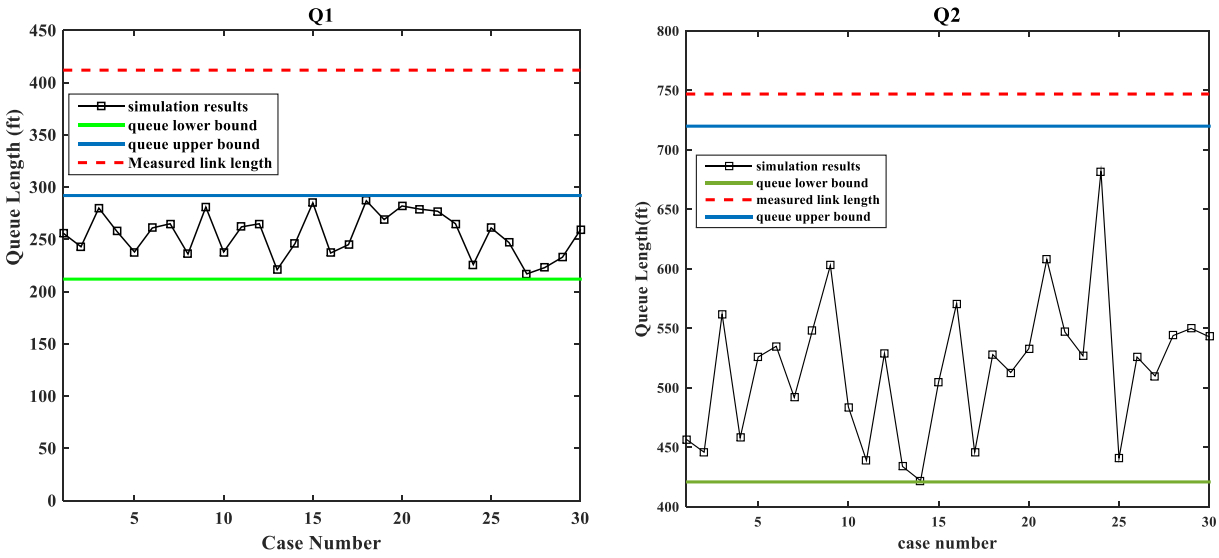

(A)

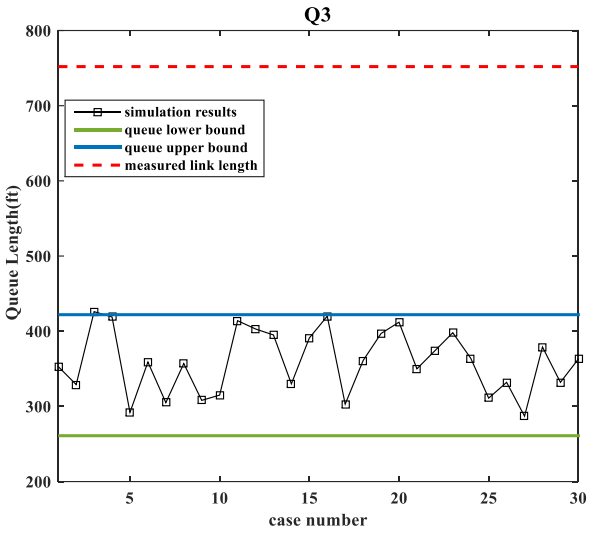
Q3
Queue Length(ft)
case number
simulation results
queue lower bound
queue upper bound
measured link length

(B)

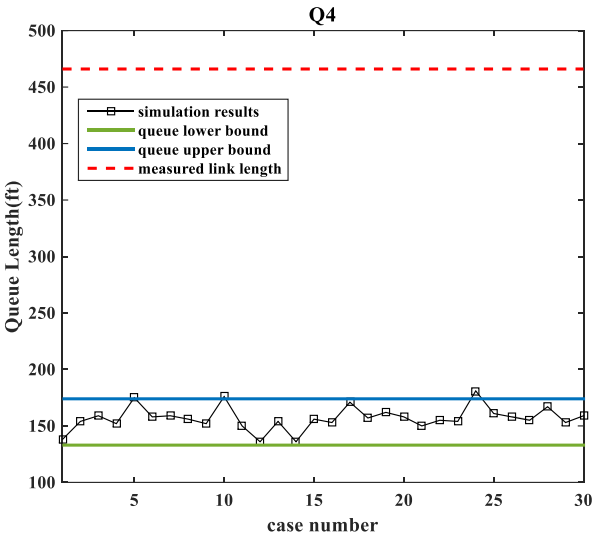
Q4
Queue Length(ft)
case number
simulation results
queue lower bound
queue upper bound
measured link length

(C)

(D)

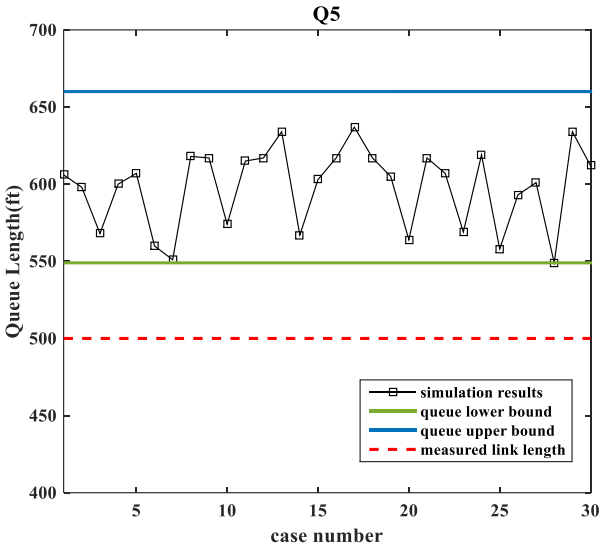
Q5
Queue Length(ft)
case number
simulation results
queue lower bound
queue upper bound
measured link length

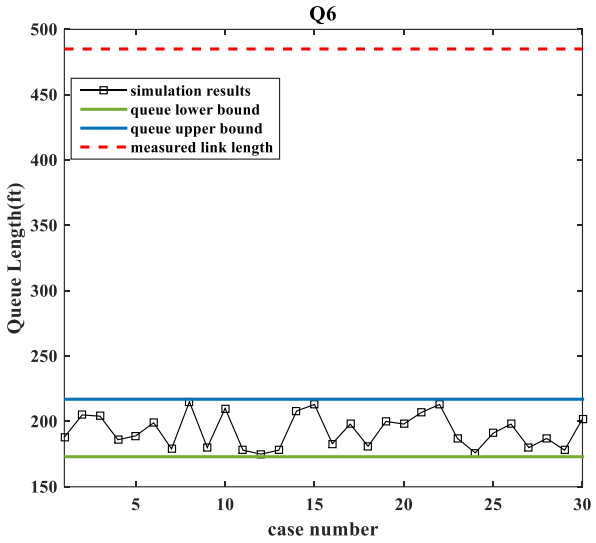
Q6
Queue Length(ft)
case number
simulation results
queue lower bound
queue upper bound
measured link length

(E)

(F)

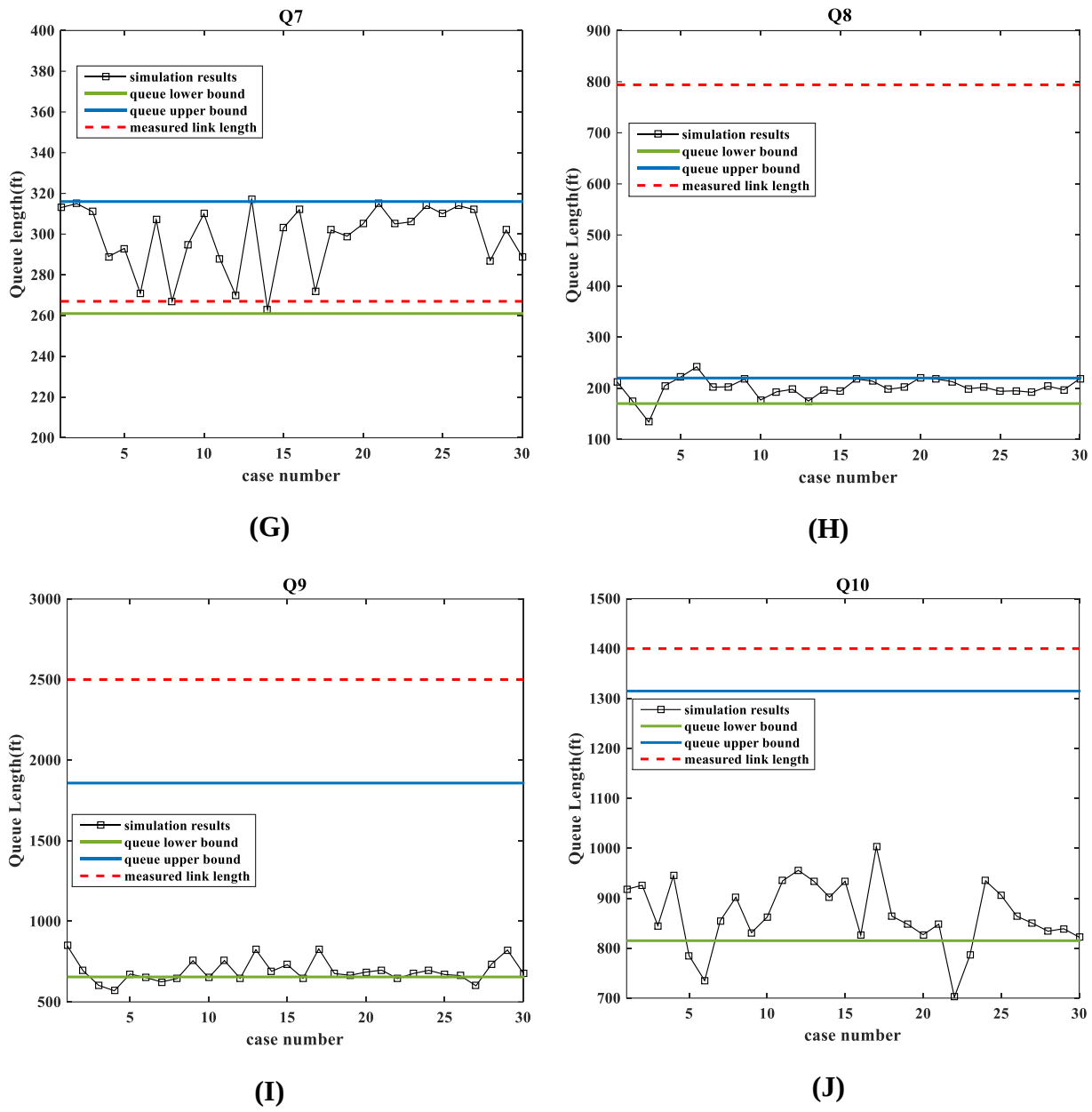

Figure 4-8. The Distribution of Simulated Maximal Queue Length on Each Critical Link

By comparing the queue intervals with the actual link length, one can note that queue spillovers may occur on links Q5 and Q7. For the case of Q7, since its lower-bound queue is less than the link length, a signal progression priority may help to reduce the queue and consequently prevent the occurrence of queue spillover.

However, the estimated lowerbound of the queue is greater than the link length on link Q5, indicating the high likelihood of having the queue spillover. Also, such queue spillovers can cause the complete blockage (Scenario 3 in Figure 1-3(C)), and consequently affect the upstream flows on both Q6 and Q9. To overcome the potential queue spillover, one should consider adopting a shorter cycle length such as reducing the cycle length to 135 seconds. Table 4-3 presents the resulting queues with the proposed models, and the simulation evaluations are shown in Figure 4-9.

Table 4-3. Summary of Model Outputs (Unit: feet)

	Q1	Q2	Q3	Q4	Q5	Q6	Q7	Q8	Q9	Q10
Queue Lower-bound	159	316	196	100	404	130	196	128	466	611
Queue Upper-bound	219	560	317	130	493	201	237	165	1373	955
Measured Link Length	412	720	752	466	500	485	267	794	2500	1400

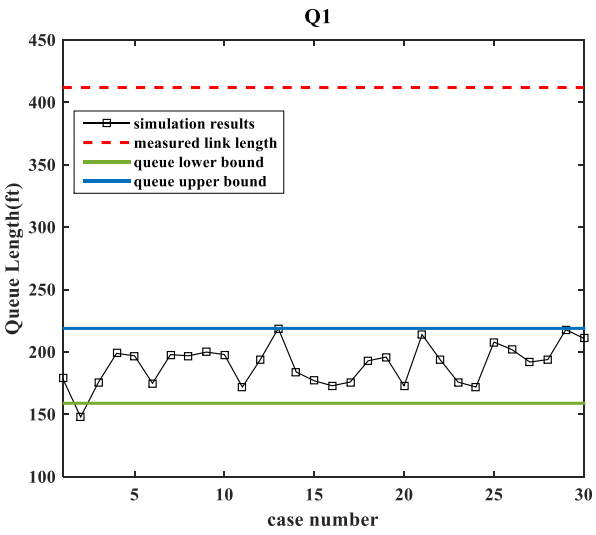

(A)

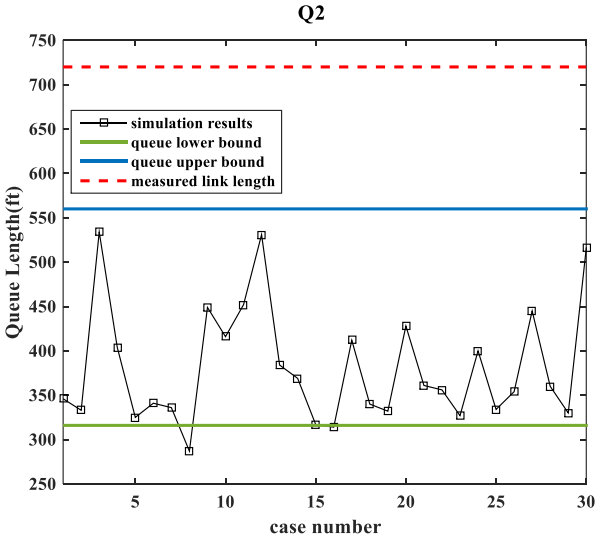

(B)

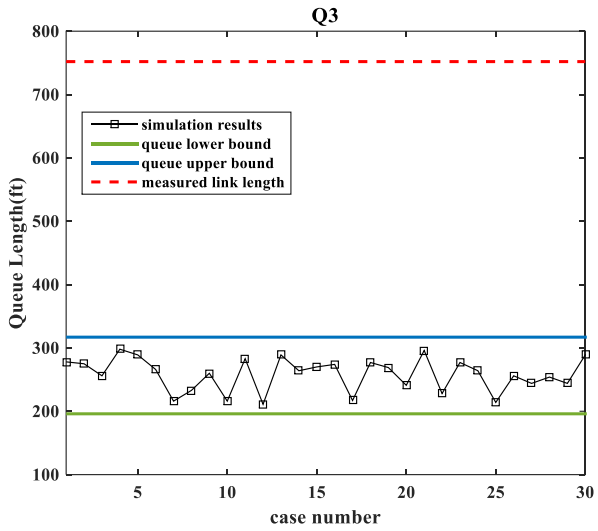
Q3
simulation results
queue lower bound
queue upper bound
measured link length
Queue Length(ft)
case number

(C)

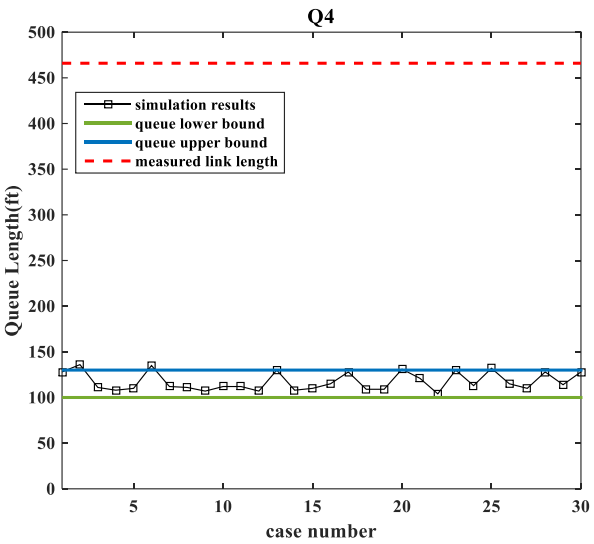
Q4
simulation results
queue lower bound
queue upper bound
measured link length
Queue Length(ft)
case number

(D)

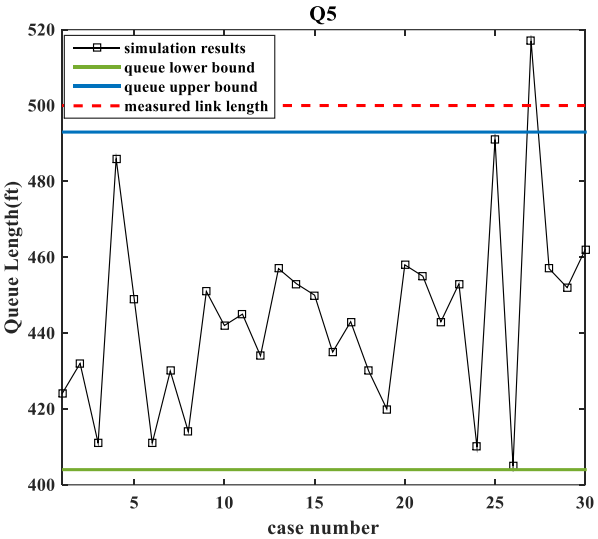
Q5
simulation results
queue lower bound
queue upper bound
measured link length
Queue Length(ft)
case number

(E)

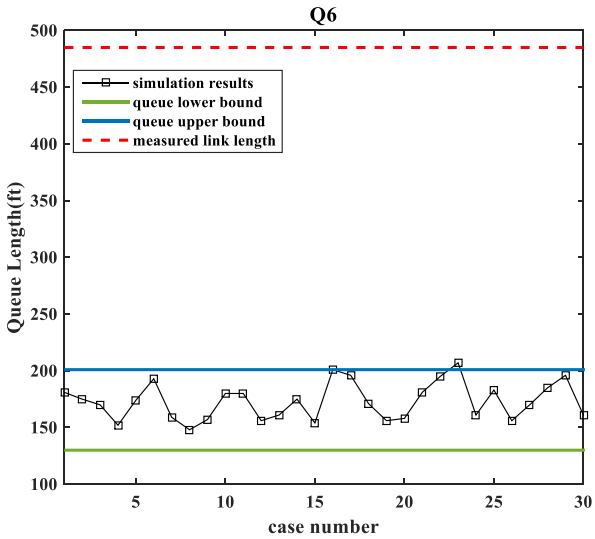
Q6
simulation results
queue lower bound
queue upper bound
measured link length
Queue Length(ft)
case number

(F)

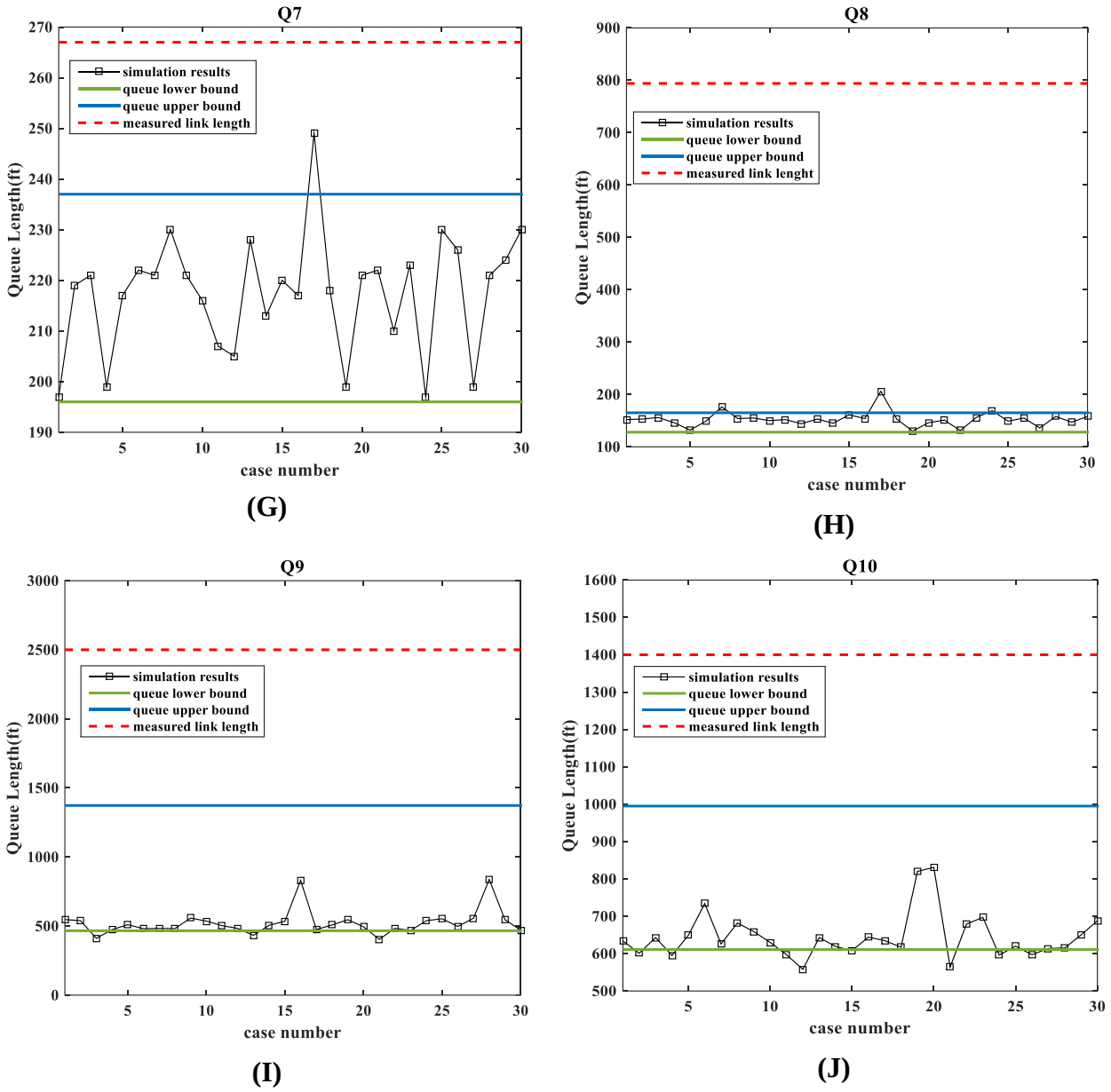

Figure 4-9. The Distribution of Simulated Maximal Queue Length on Each Critical Link

Using the 30 demand patterns generated for the above simulation analyses, the resulting average traffic delays over the entire Superstreet under two different signal cycle lengths are presented in Figure 4-10. It is evident that the case with a shorter cycle length (135s) can clearly produce a much lower delay than with the other one.

The simulation results also show that the queue spillover on some critical links (e.g., Q5, and Q7) indeed occurs on the Superstreet designed with the longer cycle length (180s). Such queue spillovers can result in the mutual blockage between flows on the left-turn bay and through lanes and consequently increase the average delay over the entire intersection.

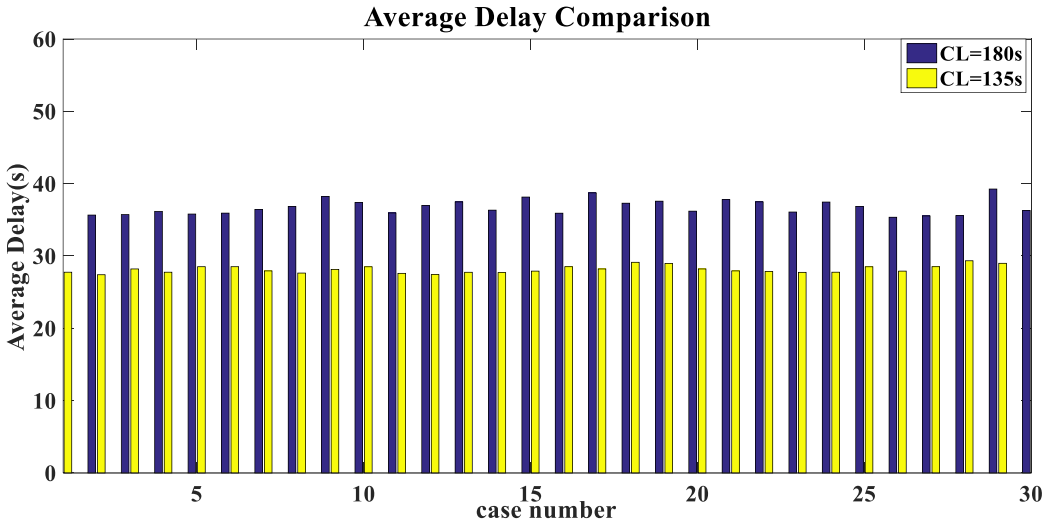

Figure 4-10. Comparison of Superstreet Average Delay with Two Different Signal Designs

4.6 Model Application and Summary

This chapter has proposed a set of models for assessing a Superstreet geometric design. Due to the interdependent nature of traffic queues among the closely-spaced sub-intersections in a Superstreet, the proposed model employs the QL ratios on those critical links as the key evaluation indicators and allows the users to estimate the range of potential queue variation on each link under a given demand and signal plan. The estimated queue intervals offer a basis for evaluating whether any critical links in a Superstreet are insufficient to accommodate the potential queues

under the given demand level. Design engineers can then use the comparison results between the estimated queue and link length to conduct the revision by either changing the geometric parameters or the signal timing plan. To assess the applicability of these proposed models, this study has further conducted a case study using the field data from a Superstreet in Maryland. The results of extensive experiments confirm the effectiveness and reliability of the proposed models.

Using the proposed model to evaluate the geometric features of a Superstreet design, one may encounter the following conditions when comparing the link length with the estimated queue intervals:

- If the upperbound of the estimated queues is less than the link length, then the target link is sufficient to store the queueing vehicles;

- If the lowerbound of the estimated queues is greater than the link length that indicates the likelihood of having queue spillbacks, then one should either increase the link length, the number of lanes, or adopt a smaller signal cycle length;

- The upperbound of the queue is longer than the link length, but its lowerbound is less than the link length. If revising the geometric design is allowed, then one should increase the link length or the number of lanes. Otherwise, providing signal progression to this link may help to prevent the queue spillover.

Chapter 5: Two-stage Signal Optimization Model for a Signalized Superstreet

5.1 Introduction

By eliminating the conflicts between the through or left-turn volumes from the minor roads and the main arterial traffic, a Superstreet enables the use of a simple two-phase signal control to guide its complex traffic movements. The reduced number of signal phases can significantly reduce the total lost time and increase the effective green time. Yet such a desirable operational efficiency cannot be achieved without an efficient signal design. This chapter presents a two-stage signal optimization method for a Superstreet, where its first stage is to maximize the total traffic throughput. To coordinate the flows between the main intersection and the U-turn crossovers, the second stage offers a multi-objective signal plan that can concurrently maximize the progression bandwidth and minimize vehicle delays.

5.2 Literature Review

Aiming to maximize the green bandwidth and intersection throughput (Silcock, 1997; Wong et al, 2003; Yang et al., 2014), or to minimize the total delay (Webster, 1956), traffic researchers have developed various models to address those issues, including the design of the optimal cycle length and green splits. (Miller, 1963; Allsop, 1971, 1972, 1976; Tully, 1976; Burrow,1987). For example, to tackle

the impacts of over-saturated conditions on signal design, Gazis (1964) proposed a signal optimization strategy to cope with residual queues under over-saturated traffic conditions. Based on his model, Michalopoulos and Stephanoloplos (1977a, 1977b) proposed a "Bang-Bang" approach to determine the optimal switch point for Gazis's strategy; Chang and Lin (2000) further advanced this model with discrete formulations.

Simulation-based approaches have also been widely adopted by the researchers to investigate the complex interactions between traffic flows and key signal control parameters. Among all existing traffic models for signal optimization, Transyt (Robertson, 1969) and Transyt-7F (Wallace et al., 1988) are perhaps the most widely used programs among the delay-based signal designs.

Focusing on the operational efficiency of the entire arterial, another group of studies in signal design focused on optimizing the signal progression band. Little (1966) first presented a mixed-integer linear program model to optimize the offsets between intersections along an arterial to achieve maximized progression bands under the given cycle length. Based on this model, Little (1981) further developed a model, called 'MAXBAND,' to generate the optimal offsets for the maximal weighted bandwidth. Along the same line, Chang (1988) presented MAXBND-86 to address the design of a left-turn phase sequence in optimizing the arterial signal progression.

Based on the core logic of MAXBAND, Gartner et al. (1991) presented an optimization approach (called "MULTIBAND") for arterial progression that could generate an optimally weighted bandwidth for the roadway segment in each direction under different traffic volumes. Based on this approach, Stamatiadis and Gartne (1996) further developed a new model, called "MULTIBAND-96," which could optimize the signal control variables in a network. During the same period, the Texas Transportation Institute developed "PASSER IV" (1996), a personal computer-based program for optimizing signal timings for arterials and multi-arterial closed-loop networks. Tian and Urbanik (2007) developed a partition technique to facilitate the progression in the more important direction; Li (2014) presented a robust signal optimization method to account for uncertainty in progression time.

Over the past decades, many researchers continued to study this topic with different mathematical algorithms. To find the optimal solution for coordinated traffic signal timing plans along the arterial, Hadi (1993) and Park (1991) applied a genetic algorithm while Lo (1999, 2001) employed a cell-transmission model to investigate queue dissipation and kinematic waves at signalized intersections.

Despite the promising development in signal control for conventional intersections, those methodologies may not be applicable to a typical Superstreet design due to its unique geometric characteristics. Major concerns involved in the design of a Superstreet signal are: 1) how to achieve an efficient signal coordination among the closely-spaced sub intersections to accommodate heavy arterial flows (as

shown in Figure 5-1); 2) how to avoid the potential queue spillbacks for critical links; and 3) how to limit the delays experienced by drivers from the minor approach to go through a series of sub-intersections (see in Figure 5-2).

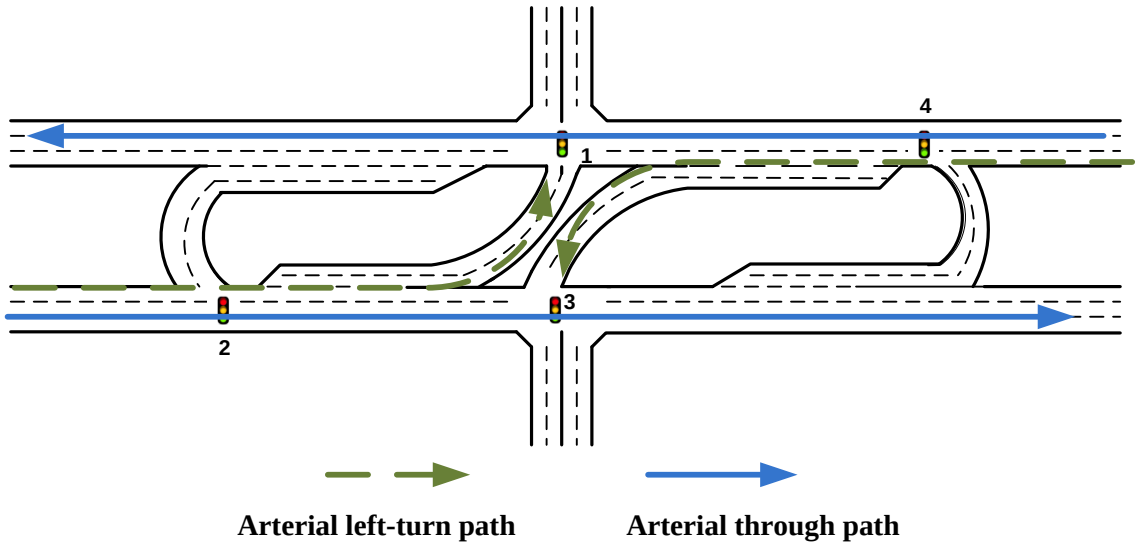

Figure 5-1 Two Types of Critical Paths for a Superstreet as a Corridor Segment

Note that a Superstreet can operate as an isolated intersection or as a segment on the local arterial. The main advantage of implementing such a design is to provide ideal signal progression for heavy arterial traffic. Hence, intuitively, 1) without a proper signal progression, those flows may encounter a red phase at the downstream sub-intersection and consequently cause long queues within the segment between the main intersection and its U-turn crossovers, 2) the arterial flows usually dominate those from the minor approach, so a reduction in arterial delays can directly improve the operational efficiency for the entire Superstreet, and 3) prevention of potential queue spillback occurrence is also an essential step to enhance the operational efficiency.

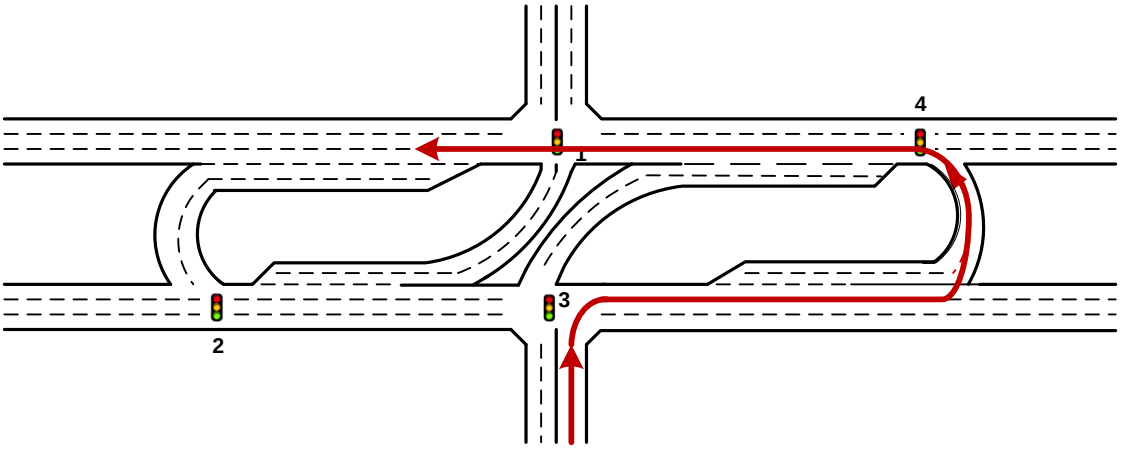

Figure 5-2. The Particular Path for Minor Road Through and Left-turn Movements

As indicated in Figure 5-2, to pursue their original direction, the minor road drivers have to pass through three sub-intersections successively. If the signals are not properly coordinated, they may experience excessive delay and consequently impair the intersection's overall performance.

5.3 Signal Control Algorithm

This study proposes a two-stage signal optimization problem that intends to address the aforementioned key issues at the same time. The index of a sub-intersection is denoted in Figure 5-2. The phase sequences for each sub-intersection are further indicated in Figure 5-3.

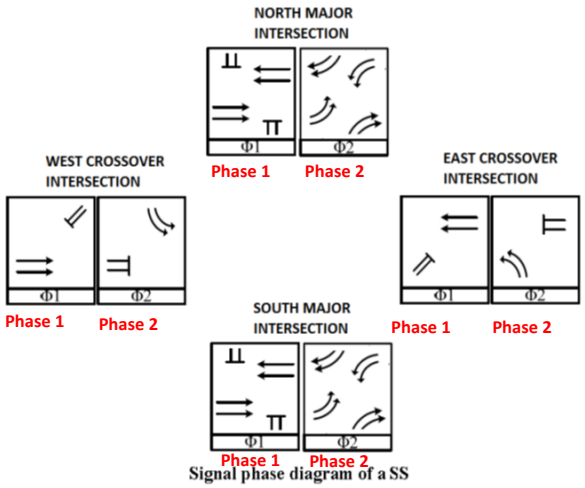

Figure 5-3. Signal Plan for Superstreet

Recognizing that both the cycle length and the offsets can impact an intersection's overall performance, the proposed solution algorithm for a Superstreet signal design comprises two stages, where Stage 1 selects the best common cycle length for all sub intersections and Stage 2 generates the offsets to achieve the signal progression and also to minimize the waiting time of drivers from the minor road. Figure 5-4 shows the iterative procedures between Stage 1 and Stage 2, where the process will be terminated if the change in the cycle length between two successive iterations is less than one second.

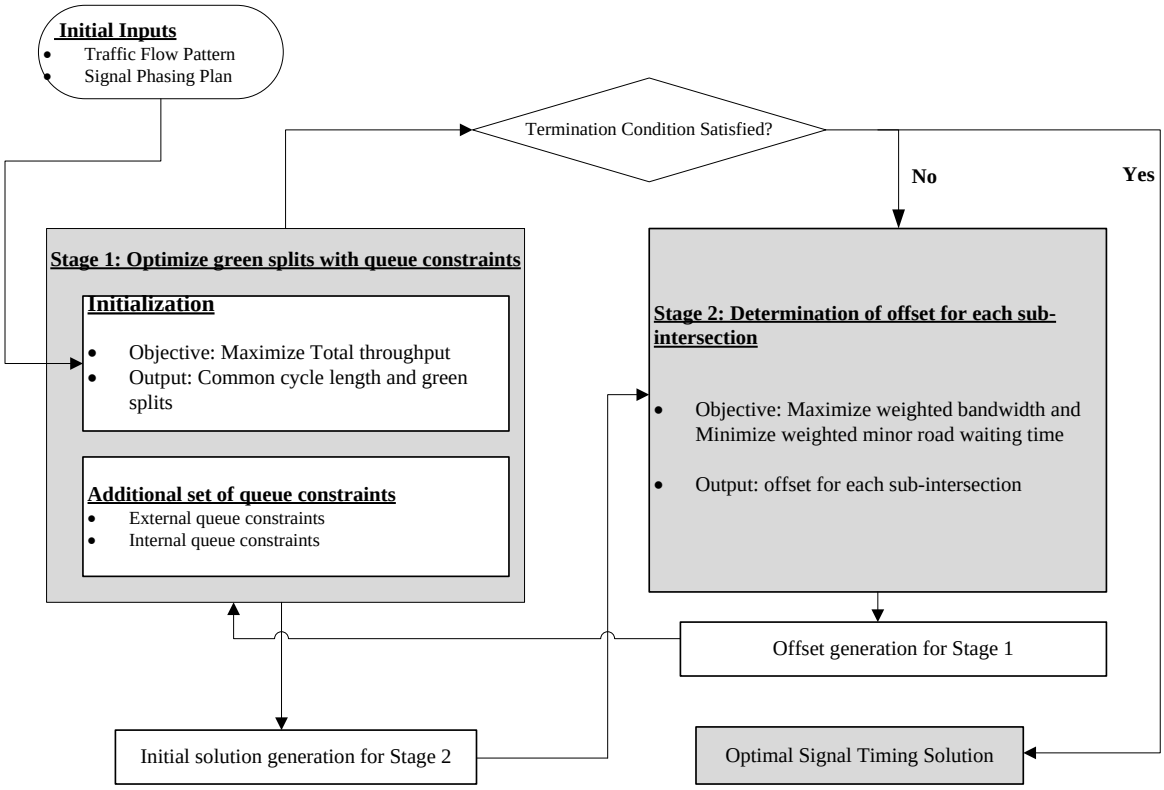

Figure 5-4. General Algorithm of the Proposed Two-stage Signal Optimization

Also for convenience of discussion, Table 5-1 summarizes the key notations for variables used thereafter.

Table 5-1. Notation for Key Variables / Parameters

Notation	Description
Sets:	
I={1,2,3,4}	Set of sub-intersections. 1 denotes the northern sub-intersection; 2 denotes the western one; 3 denotes the southern while 4 denotes the eastern one.
P={1,2,3,4,5,6}	Set of paths
J={1,2,…,10}	Signal controlled movements group among entire superstreet, illustrated in Figure 6-5, where (2,3) and (7,8) belong to the same group.
K={1,4}	Set of paths from minor roads
Variables:	
μ_i	Multiplier to traffic volume at intersection i , representing ratio between actual capacity and the volume
C	Common cycle length for all sub-intersections
ϕ_{ij}	Duration of green time for movement j at intersection i (proportional to cycle length)
θ_i	Offset of intersection i
w_{ip}	Time between the start of a cycle and the start of the band for path p at intersection i
b_p	Bandwidth for path p
n_{ip}	Integer indicator for cycle length; 0,1,2...n
x_1, x_2, x_3	Binary variables indicating green phase when = 1; o.w. indicating red phase
ξ	The reciprocal of cycle length
T_{ik}	The (waiting time/ cycle length) ratio for path k vehicle at intersection i
Parameters:	
σ_p	Set of intersections passed by path-flow p
s	Saturation flow rate (per lane)
t_l	Lost time for each movement in seconds
η_p	Weighting factor for path p
$C_{\min}$	Minimum cycle length in real application
$C_{\max}$	Maximum cycle length in real application
$g_{\min}$	Minimum green time for one movement
$g_{\max}$	Maximum green time for one movement
$t_{i,i+1}$	Travel time from sub-intersection i to i+1.
q_{ij}	Traffic arrival rate for movement j at intersection i (per lane)
L_j	Maximum queue length for external movements (in this case, j=2,5,7,10)
α_{ij}	Lane use factor for movement j at intersection i
λ	Multiplier to total travel time for paths from minor road

Initialization

The initialization is to generate the initial solution that includes the common cycle length and the green splits for each sub intersection. The index for all traffic movements is denoted in Figure 5-5.

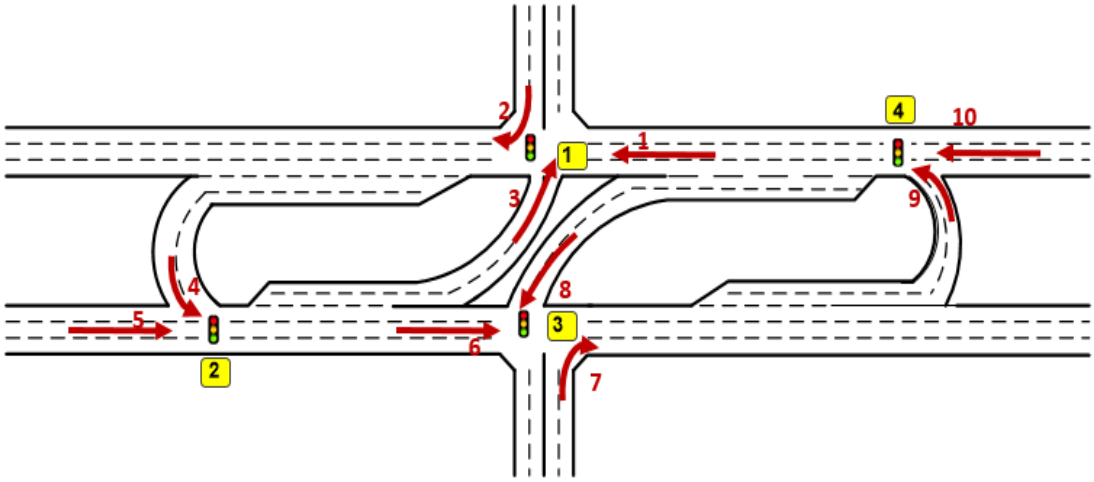

Figure 5-5. Illustration of Index for Each Movement among a Typical Superstreet

As reported in the literatures (Yagar, 1975; Xuan et al., 2011), a well-designed signal needs to achieve the capacity maximization under the given intersection geometry. Based on the assumption that the traffic demand matrix can be multiplied with a common multiplier μ to represent the maximum amount of the increased volume that would still allow the intersection to perform reasonably well (Wong, 2003), the objective function for the initialization stage is to search for the maximal multiplier and be expressed as follows:

$$Max(\sum_{i \in I} \mu_i) \tag{5-1}$$

Where $i \in I$ denotes the set of sub-intersections among the entire Superstreet, μ_i is the traffic flow multiplier assigned to sub-intersection i. By maximizing the summation of μ_i for all sub-intersections, the overall intersection throughput can be reasonably optimized. Note that the entire intersection is under an over-saturated traffic condition if the generated $\mu_{\max}$ is more than 1.

Given the traffic demand pattern at each intersection, the following constraint should be satisfied to ensure that the degree of saturation at each movement is below the acceptable limit:

$$\mu_i \alpha_j q_{ij} \le s(\phi_{ij} - \xi \times t_l) \ \forall i, j \tag{5-2}$$

Where s denotes the saturation flow rate (unit: veh/hour/lane); q_{ij} denotes the traffic demand for movement j at sub intersection i; α_j is the lane use factor for the lane group of movement j; ϕ_{ij} is the assigned g/c ratio (includes lost time) for movement j at sub intersection i; ξ is the reciprocal of cycle length and t_l stands for the lost time due to the transition between consecutive signal phases. The movement index J is denoted in Figure 5-5.

For any selected common cycle length, it should fall within the range of acceptable limits:

$$\frac{1}{C_{\max}} \le \xi \le \frac{1}{C_{\min}} \tag{5-3}$$

Where, $C_{\max}$ is the upper bound of a feasible cycle length and $C_{\min}$ stands for its lower bound.

The green ratio for each movement group should also be subjected to the following constraint:

$$\xi \times g_{\min} \le \phi_{ij} \le g_{\max} \times \xi \tag{5-4}$$

Where $g_{\max}$ and $g_{\min}$ stands for its upper limit and lower limit, respectively. Since each sub-intersection has one signal controller, its sum of all g/c ratios should be equal to 1:

$$\phi_{ij_1} + \phi_{ij_2} = 1 \quad j_1, j_2 \in J \text{ and } j_1 \neq j_2 \tag{5-5}$$

Where $j_1, j_2 \in J$ stands for all movements included sub intersection i.

Initialization Summary

Objective function:	$Max(\sum_{i \in I} \mu_i)$
Subject to:	Eqs. (5-2)-(5-5)

Stage 2- DETERMINE THE OFFSETS FOR EACH SUB INTERSECTION

Stage 2 proposes a multi-objective mixed integer linear programming model, which aims to address the issues of maximizing the weighted bandwidth and

concurrently minimizing the delay experienced by the minor road drivers. Figure 5-6 shows the critical paths among a signalized Superstreet, where paths 1, 4 denote the through and left-turn movements from the minor roads; paths 2, 5 are the arterials' through and right-turn movements and paths 3, 6 represent the arterials' left-turning flows.

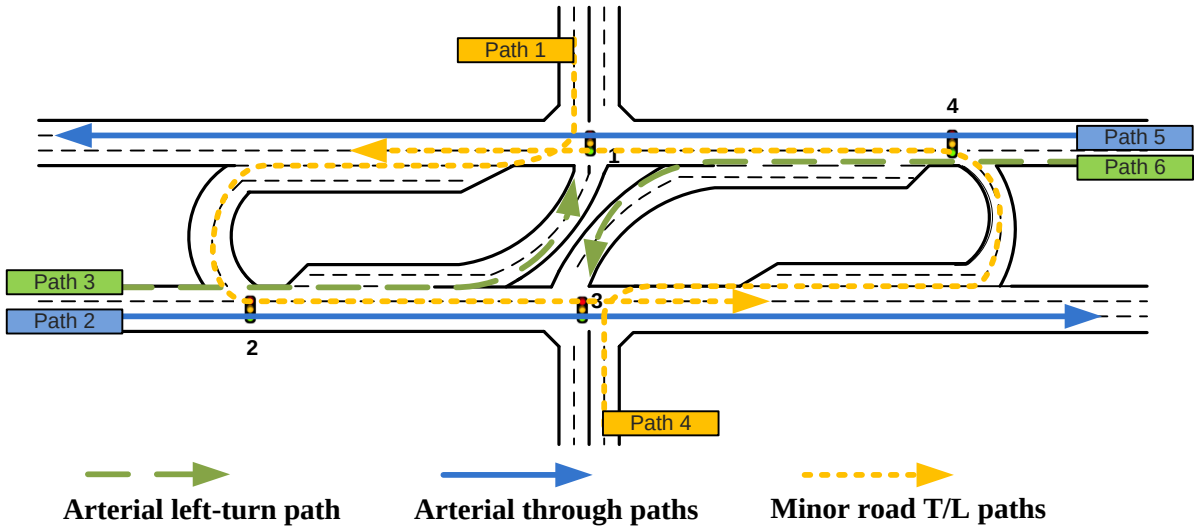

Figure 5-6. Critical Paths within a Superstreet

In order to achieve the signal progression and minimal waiting time for minor road drivers, one should formulate the control objective as follows:

$$Max(\sum_{p\in P}\eta_p b_p - f_k \sum_{k\in K} T_{ik}) \tag{5-6}$$

Where η_p is the weighting factor for path $p \in P$ while P stands for the set of critical paths. And b_p is the bandwidth of path p; f_k is a positive weight factor for the waiting time of path $k \in K$ in the minor approach while K stands for the set of paths

from the minor road, and T_{ik} is the waiting time caused by the signal at sub intersection i for path k. By adjusting η_p and f_k, one can set one of these two goals to a higher priority. In this case, the bandwidth maximization is set as the first priority since the main benefit of such a design is to provide uninterrupted arterial flows.

As there are only two phases for each sub-intersection, the impact of the phase sequence on the entire Superstreet's operational performance is negligible. In addition, the constraints (as shown in Eqs. (5-7)-(5-10)) should be satisfied for the weighted bandwidth maximization. Figure 5-7 presented the graphical illustration of each term.

For each direction, as θ_i denotes the offset at sub-intersection i, its interference constraints are listed below:

$$0 \le w_{ip} + b_p \le g_{ip} \tag{5-7}$$

$$w_{ip}, b_p \ge 0 \tag{5-8}$$

Where w_{ip} is the time from the right side of the signal phase to the boundary of the green band for path p at sub-intersection i; g_{ip} is the received green time at intersection i for path p. As illustrated in Figure 5-7, the sum of the bandwidths and w_{ip} should not exceed the total green time.

As in most progression formulations, the loop integer constraint for each path can be expressed as follows:

$$\theta_i + r_{ip} + w_{ip} + t_{i,i+1} + n_{ip}C \geq \theta_{i+1} + r_{i+1,p} + w_{i+1p} + n_{i+1p}C \quad \forall p \in P; \forall i \in \sigma_p \qquad (5\text{-}9)$$

$$\theta_i + r_{ip} + w_{ip} + t_{i,i+1} + n_{ip}C \leq \theta_{i+1} + r_{i+1p} + w_{i+1p} + n_{i+1p}C \quad \forall p \in P; \forall i \in \sigma_p \qquad (5\text{-}10)$$

Where $t_{i,i+1}$ is the travel time from sub-intersections i to i+1; n_{ip} is an integer variable and C is the total cycle length.

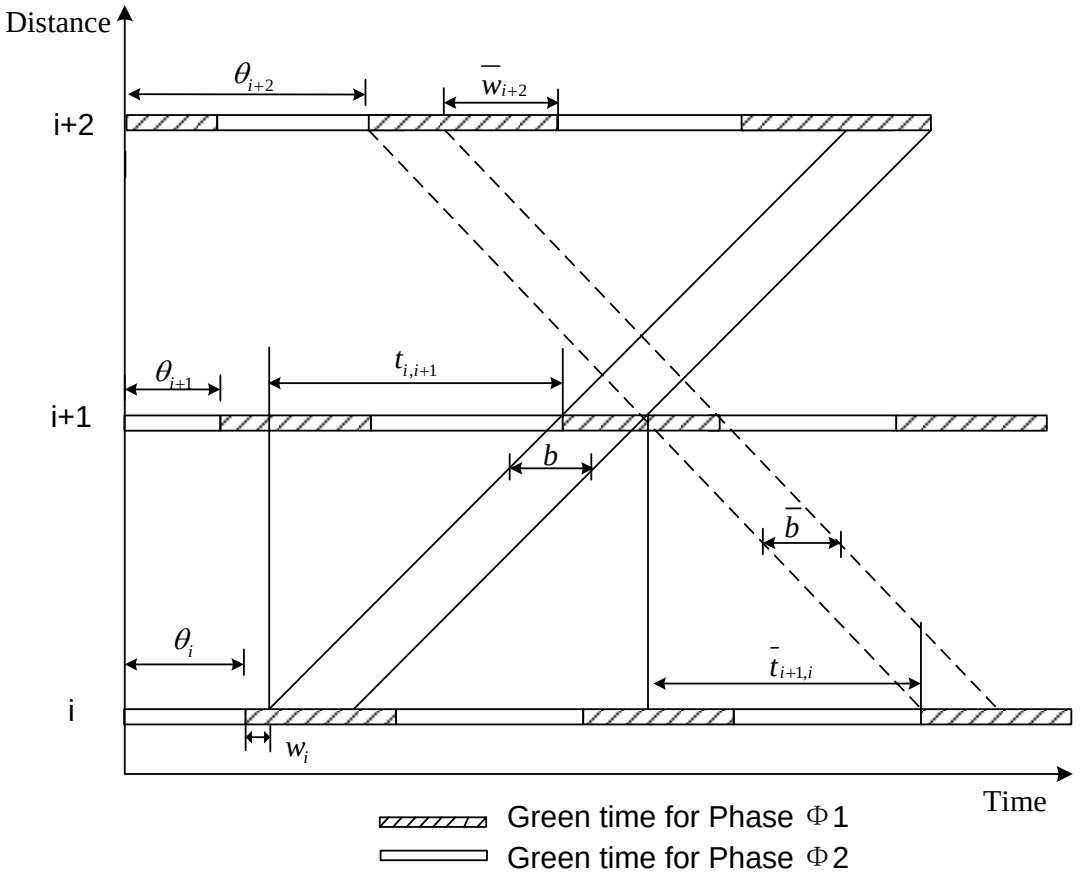

Figure 5-7. Time-Space Diagram for MAXBAND

The constraints presented above are based on the logic of the MAXBAND algorithm (Little, 1981), which is used to provide the progression band for all critical paths within a Superstreet. Furthermore, the minor road waiting time constraints are

specified to avoid the excessive waiting time experienced by the minor road drivers due to the signal control. Taking path 1 as an example, the minor road drivers in this path have to pass three successive sub-intersections, including sub-intersections 1, 2 and 3. Note that it is not desirable for a vehicle to wait at every red phases at all the sub-intersections. The proposed waiting time constraints are formulated to describe the total waiting time of a vehicle that stops over an entire red phase at the first sub intersection because the red time ratio at sub-intersection 1 usually dominates the other phase within one cycle and it also takes the major part over the sum of waiting time among all sub-intersections. The waiting time ratio (denoted as T_{11}) for such the vehicle at sub-intersection 1 can be expressed as follows:

$$T_{11} \geq \phi_{11} \tag{5-11}$$

Where ϕ_{11} denotes the ratio of the red phase over the cycle length at sub-1, which is also the green time for movement 1. After passing sub-intersection 1, whether the vehicle will hit the red phase at sub-intersection 2 can be indicated by a binary variable x_{11}, where M is a larger enough positive number.

$$x_{11} \geq \frac{\theta_2 + \phi_{25} - \theta_1 - \phi_{11} - t_{12} * \xi}{M} \tag{5-12}$$

$$x_{11} \leq \frac{\theta_2 + \phi_{25} - \theta_1 - \phi_{11} - t_{12} * \xi}{M} + 1 \tag{5-13}$$

Note that since t_{12} is the travel time (in seconds) from sub-intersections 1 to 2, it has to be converted into a time ratio by multiplying ξ.

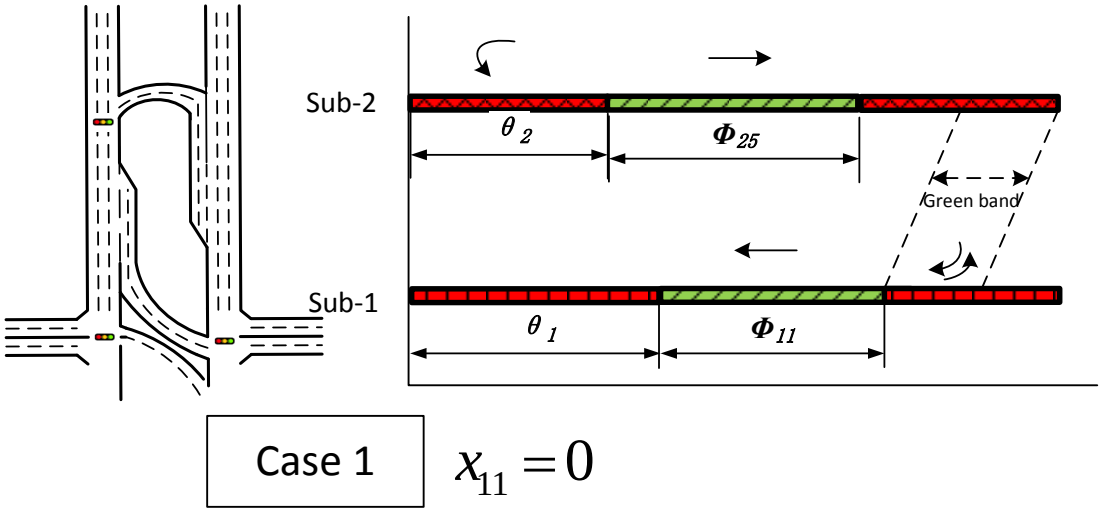

(a) Time-space diagram for $x_{11}=0$

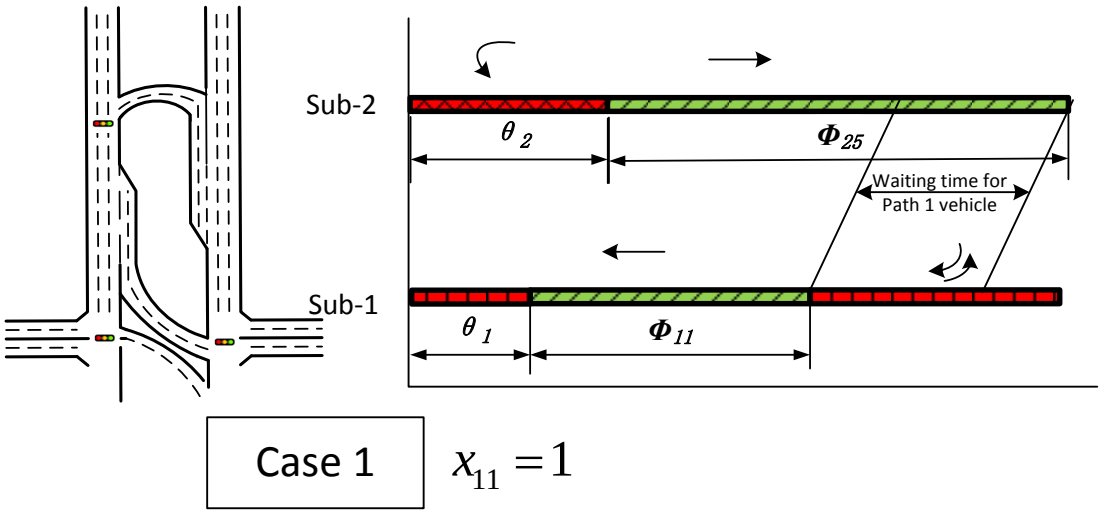

(b) Time-space diagram for $x_{11}=1$

Figure 5-8. Graphical Illustration of Binary Variable x_{11}

As presented in Figure 5-8 (b), if the signal plans for sub-intersections 1 and 2 follow the graphical presentation, then the leading vehicle departing right after the end of ϕ_{11} will hit the red phase at the downstream sub-intersection 2 (the green phase for vehicles in movement 5, denoted as ϕ_{25}). On the other hand, if the incoming

vehicle from sub-intersection 1 encounters the green phase at sub-intersection 2, as shown in Figure 5-8 (a), then x_{11} will be set to 0.

As shown in Eq. (5-14), if the incoming vehicle in path 1 hit the green phase at the downstream signal, where $x_{11} = 1$, then the following relaxation will exist.

$$\theta_2 + \phi_{25} - \theta_1 - \phi_{11} - t_{12} * \xi \geq 0; \tag{5-14}$$

If x_{11} equals to 1, the waiting time ratio (the waiting time/cycle length) for path 1 vehicle at sub-intersection 2 (represented as T_{21}), which are denoted in Figure 5-8 (b), can be expressed as follows:

$$T_{21} \geq (\theta_2 + \phi_5 - \theta_1 - \phi_1 - t_{12} * \xi) - (1 - x_{11})M; T_{21} \geq 0 \tag{5-15}$$

In the other case, if $x_{11} = 0,$ this constraint will be relaxed since T_{21} is strictly non-negative.

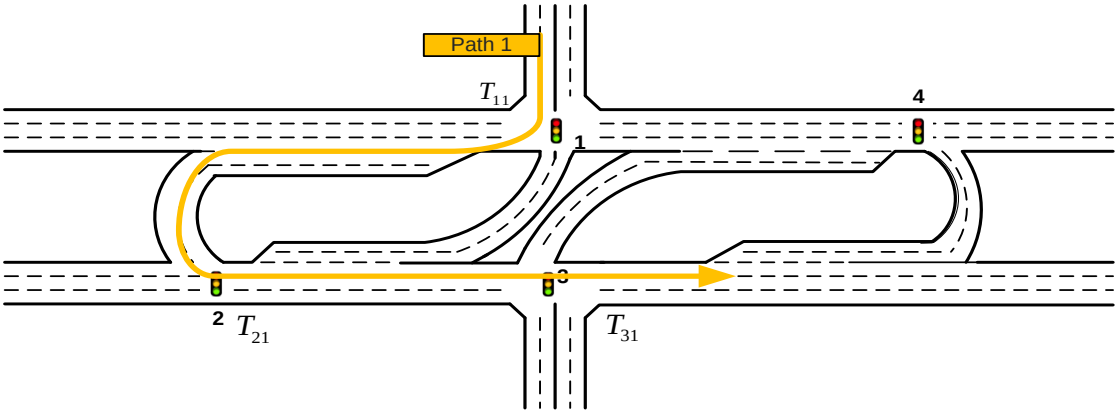

Figure 5-9. Route for Vehicles from Path-1

Following the same methodology, the maximum waiting time experienced by the vehicle in path 1 due to a signal control can be denoted as the sum of T_{11}, T_{21}, T_{31}. Following the same logic, one can express T_{21}, T_{11} *and* T_{31} with Eqs. (5-16)-(5-19):

$$x_{21} \geq \frac{\theta_2 + \phi_{25} + t_{23} * \xi - \theta_3 - \phi_{36}}{M} \tag{5-16}$$

$$x_{21} \leq \frac{\theta_2 + \phi_{25} + t_{23} * \xi - \theta_3 - \phi_{36}}{M} + 1 \tag{5-17}$$

$$T_{31} \geq (1 - \theta_2 - \phi_{25} - t_{23} * \xi + \theta_3) - (1 - x_{11})M - (1 - x_{21})M \tag{5-18}$$

$$T_{31} \geq (1 - \theta_1 - \phi_{11} - t_{12} * \xi - t_{23} * \xi + \theta_3) - x_{11}M - (1 - x_{21})M; T_{11}, T_{21}, T_{31} \geq 0 \tag{5-19}$$

The sum of the waiting time ratios at all sub-intersections should be less than the preset threshold:

$$T_{11} + T_{21} + T_{31} \leq \lambda \xi * (t_{12} + t_{23}) \tag{5-20}$$

Where λ is the multiplier for the sum of travel times from intersections 1 to 2 and from 2 to 3. The sum of t_{12}, t_{23} is the travel time from sub-intersections 1 to 3 without a signal control. When multiplied by ξ, it can be further converted into a time ratio, the preset upper bound for the total waiting time ratio experienced by the vehicle in path 1.

Summary of Stage 2 formulation

Objective function:	$Max(\sum_{p \in P} \eta_p b_p - f_k \sum_{k \in K} T_{ik})$
Subject to:	
For all critical paths:	Refer to Eqs (5-7) - (5-10).
For minor road paths:	Refer to Eqs (5-11) - (5-20).

Stage 1- Optimization of green splits with queue constraints

According to the general algorithm summarized in Figure 5-4, one can get a set of offsets for each sub-intersection based on the common cycle length generated in the initialization step. Note that the initialization does not account for the impact of the common cycle length in the formation of queues. Hence, aside from keeping all such constraints and the objective function in the initialization step, Stage 1 adds a set

of queue constraints to prevent the formation of traffic spillback. Figure 5-10 shows the spatial distribution of all potential queues among a Superstreet.

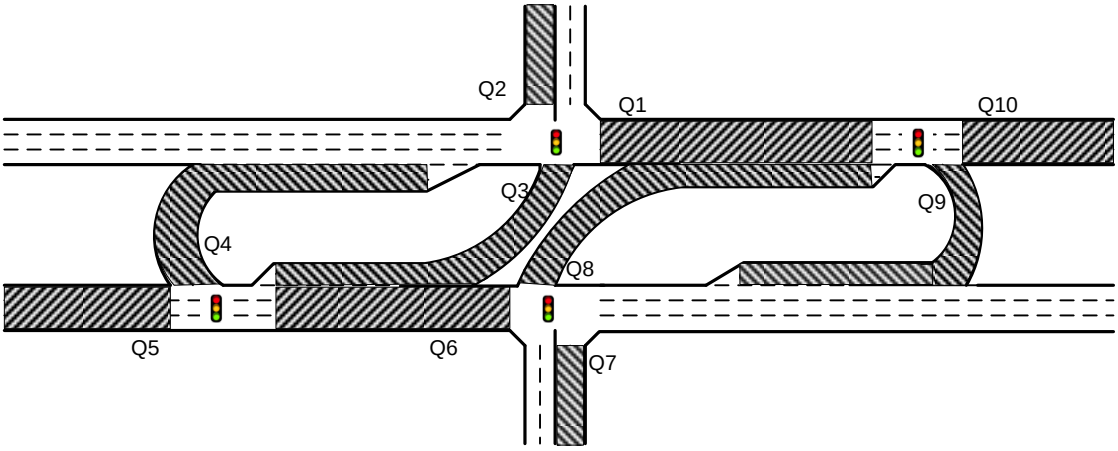

Figure 5-10. Spatial Queue Distribution among a Superstreet

External Queues: Q2, Q5, Q7, Q10

Figure 5-11 illustrates the external queue formation process, which consists of two components: the vehicle accumulated during the red phase and the residual queue during the initial green time. To prevent queue spillback, the maximum allowable queue cannot exceed the link length.

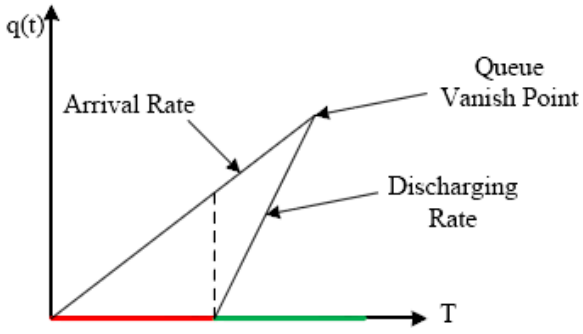

Figure 5-11. Queue formation process

One can then derive the following expression,

$$L_j = \frac{(1-\phi_{ij}+t_l*\xi)*\alpha_{ij}q_{ij}*s}{(s-\alpha_{ij}q_{ij})\xi} \quad (5\text{-}21)$$

Where L_j denotes the link length for queue j, while $j \in J$ the set of all potential queues. The following queue length constraints are specified to prevent external-queue spillback:

$$(1-\phi_{12}+t_l*\xi)\alpha_{12}q_{12}s \le L_2(s-\alpha_{12}q_{12})\xi \quad (5\text{-}22)$$

$$(1-\phi_{25}+t_l*\xi)\alpha_{25}q_{25}s \le L_5(s-\alpha_{25}q_{25})\xi \quad (5\text{-}23)$$

$$(1-\phi_{37}+t_l*\xi)\alpha_{37}q_{37}s \le L_7(s-\alpha_{37}q_{37})\xi \quad (5\text{-}24)$$

$$(1-\phi_{410}+t_l*\xi)\alpha_{410}q_{410}s \le L_{10}(s-\alpha_{410}q_{410})\xi \quad (5\text{-}25)$$

Internal Queues: Q1,Q6,Q3,Q8,Q4,Q9

Note that in Stage 1, there are offsets for all sub-intersections, so the set of binary parameters (f_1, f_3, f_4, f_6, f_8, and f_9) can be determined based on the previously generated offsets. The additional notations for the set of internal queue constraints are shown in Table 5-2.

Table 5-2. Additional Variable Notation for the Set of Queue Constraints

Notation	Description
L_j	Link length for certain movement j
f_1	Binary parameter; (=1, if $\theta_1 \ge \theta_4 + t_{41}*\xi$;o.w =0)
f_3	Binary parameter; (=1, if $\theta_1 \ge \theta_2 + t_{21}*\xi$;o.w =0)

f_4	Binary parameter; (=1, if $\theta_1 \geq \theta_2 - t_{12} * \xi$;o.w =0)
f_6	Binary parameter; (=1, if $\theta_3 \geq \theta_2 + t_{23} * \xi$;o.w =0)
f_8	Binary parameter; (=1, if $\theta_3 \leq \theta_4 + t_{43} * \xi$;o.w =0)
f_9	Binary parameter; (=1, if $\theta_3 \geq \theta_4 - t_{34} * \xi$;o.w =0)
y_4	Binary variable; (=1, if $\theta_1 + \phi_{11} \leq \theta_2 + \phi_{25} - t_{12} * \xi$;o.w =0)
y_9	Binary variable; (=1, if $\theta_3 + \phi_{36} \leq \theta_4 + \phi_{410} - t_{34} * \xi$;o.w =0)
y_6	Binary variable; (=1, if $\theta_3 + \phi_{36} - t_{23} * \xi \leq \theta_2 + \phi_{25}$;o.w =0)
y_1	Binary variable; (=1, if $\theta_1 + \phi_{11} - t_{41} * \xi \leq \theta_4 + \phi_{410}$;o.w =0)
y_3	Binary variable; (=1, if $\theta_2 + \phi_{25} \leq \theta_1 + \phi_{11} - t_{21} * \xi$;o.w =0)
y_8	Binary variable; (=1, if $\theta_4 + \phi_{410} \leq \theta_3 + \phi_{36} - t_{43} * \xi$;o.w =0)
Q_j', Q_j''	Partial internal queues for movement j

The set of internal queues can further be categorized into the following three types:

- Type-1 internal U-turn queue: Q4 and Q9 (U-turn crossover queue);
- Type-2 internal left-turn queue: Q3 and Q8 (main left-turn queue on arterial);
- Type-3 internal through queue: Q1 and Q6 (main through queue on arterial).

Type-1 internal queue: Q4 and Q9 (U-turn crossover queue)

These types of queues are contributed by the left-turn and through vehicles from the minor streets. If those incoming vehicles encounter a red phase at the downstream U-turn crossover, the queue will start to accumulate. To formulate such relations, let the binary variable, y_4, represent the downstream signal phase during the arrival of upstream vehicles. Taking Q4 as an example, it may be formed over two

intervals. The queue lengths accumulated during these two time intervals are denoted as Q_4' and Q_4'', respectively.

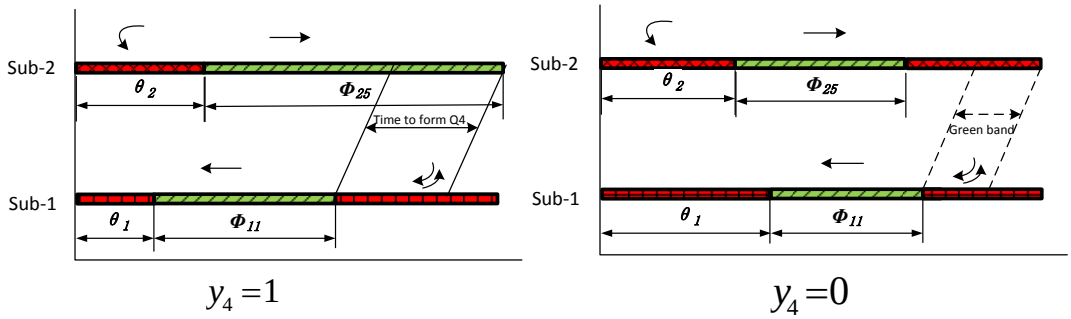

$y_4 = 1$ $y_4 = 0$

Figure 5-12. Graphical Illustration of Binary Variable y_4

As presented in Figure 5-12, the status $y_4 = 1$ indicates that the incoming vehicle hits the red phase at the downstream sub-intersection 2, while $y_4 = 0$ stands for a green phase at sub-intersection 2. The mathematical expression for y_4 can be expressed as follows:

$$y_4 \geq \frac{\theta_2 + \phi_{25} - t_{12} * \xi - \theta_1 - \phi_{11}}{M} \tag{5-26}$$

$$y_4 \leq \frac{\theta_2 + \phi_{25} - t_{12} * \xi - \theta_1 - \phi_{11}}{M} + 1 \tag{5-27}$$

Note that since all these offsets and phase durations are expressed in time ratios, the travel time t_{12} is multiplied by ξ as to be transferred in ratios. Hence, the maximum length of Q_4' during such a time period can be formulated as follows:

$$Q_4' \geq (\theta_2 + \phi_{25} - \theta_1 - \phi_{11} - t_{12} * \xi)\alpha_{24} q_2^{LT} - (1 - y_4)M; Q_4' \geq 0 \tag{5-28}$$

If $y_4 = 0$, this constraint will be relaxed since Q_4' is strictly non-negative. Except for the time to form Q_4', the other possible time duration to form Q_4'' is denoted in Figure 5-13. A binary parameter f_4 is introduced as follows:

$$f_4 = \begin{cases} 1 & \text{if } \theta_2 < \theta_1 + t_{12} * \xi; \\ 0 & o.w \end{cases} \tag{5-29}$$

Note that f_4 is the indicator to indicate whether the incoming flow hits the red phase at sub-2, as shown in Figure 5-13.

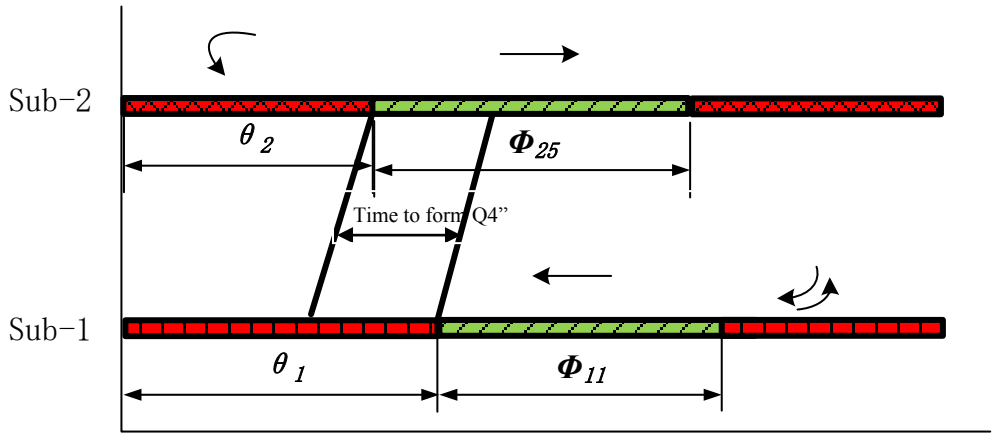

Figure 5-13. Graphical Illustration for Binary Parameter $f_4 = 1$

The queue length, Q_4'', accumulated during such a time period (as denoted in Figure 5-13) can be expressed using Eq. (5-30).

$$Q_4'' = \alpha_4 q_2^{LT} f_4\left(\theta_1 - \theta_2 + t_{12} * \xi\right) \tag{5-30}$$

So the maximum queue length for link 4 during each cycle can be expressed as the sum of the vehicles accumulated during these two time durations.

$$Q_4' + Q_4'' \le \xi L_4 \tag{5-31}$$

Where q_2^{LT} is the demand for left-turn and through vehicles departing from Q2. The maximum length of Q4 cannot exceed the link length, denoted as L_4. The same methodology can be applied to derive a queue constraint for Q9.

Type-2 internal queue: Q3 and Q8 (Main left-turn queue)

Vehicles forming this type of internal queue are the departures from Q5 and Q10. Similar to the methodology to obtain Q4, a set of binary parameters and variables should be defined first to denote the signal phase at the downstream sub-intersection. Likewise, a binary variable y_3 is set to 1 if the departures from Q5 encounter the red phase at sub-intersection 1; otherwise, it will be equal to 0.

$$y_3 \ge \frac{\theta_2 + \phi_{25} + t_{21} * \xi - \theta_1 - \phi_{11}}{M} \tag{5-32}$$

$$y_3 \le \frac{\theta_2 + \phi_{25} + t_{21} * \xi - \theta_1 - \phi_{11}}{M} + 1 \tag{5-33}$$

A graphical illustration for a definition of y_3 is shown in Figure 5-14.

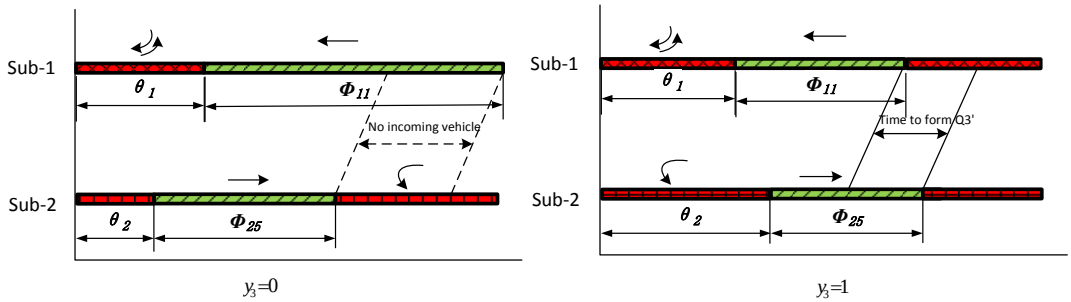

Figure 5-14. Graphical Illustration for Binary Variable y_3

Thus one can formulate a maximum length of Q_3' during this time period as shown below:

$$Q_3' \geq (\theta_2 + \phi_{25} + t_{21} * \xi - \theta_1 - \phi_{11})\alpha_{13} q_5^L - (1 - y_3)M; Q_3' \geq 0 \tag{5-34}$$

If $y_3 = 0$, this constraint (Eq. (5-34)) will be relaxed since Q_3' is strictly non-negative. Except for the time to form Q_3', the other possible time duration is denoted as Q_3'' (as shown in Figure 5-15). A binary parameter f_3 is introduced as follows:

$$f_3 = \begin{cases} 1 & if\ \theta_1 \geq \theta_2 + t_{21} * \xi \\ 0 & o.w \end{cases} \tag{5-35}$$

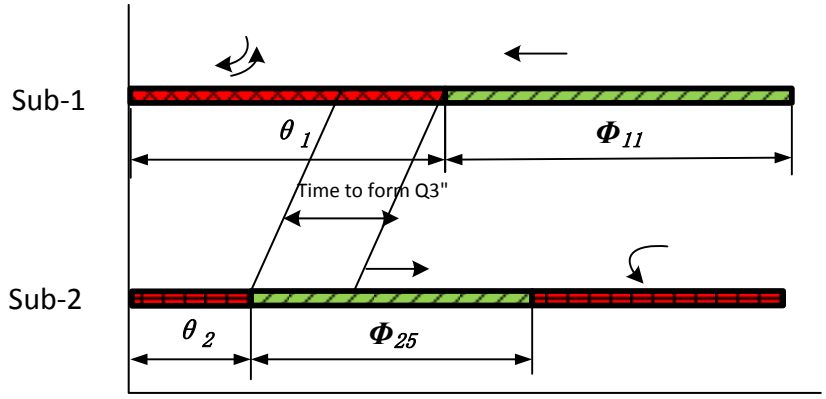

Figure 5-15. Graphical Notation for $f_3 = 1$

The queue accumulated during that time period that $f_3 = 1$ can be

$$Q_3'' = \alpha_3 q_5^L * f_3(\theta_1 - t_{21} * \xi - \theta_2) \tag{5-36}$$

So the maximum queue length in link 3 during each cycle can be expressed as the sum of the vehicle accumulated during these two possible durations (denoted as Q_3' and Q_3'', respectively) as follows:

$$Q_3' + Q_3'' \le \xi L_3 \tag{5-37}$$

Where q_5^L is the flow rate for left-turn vehicles from Q5. The maximum length of Q3 cannot exceed the link length L_3. The same methodology can be applied to derive the queue constraint for link 8.

Type-3 internal queue: Q1 and Q6 (Main Through queue)

Different from the previous two types, there are two possible sources to contribute to this type of queue. Taking Q1 as an instance, both the departures from

Q4 and Q5 can contribute to the formation of Q1. Let Eq. (5-38)-Eq. (5-39) be used to define a binary variable y_1:

$$y_1 \geq \frac{\theta_4 + \phi_{410} + t_{41} * \xi - \theta_1 - \phi_{11}}{M} \tag{5-38}$$

$$y_1 \leq \frac{\theta_4 + \phi_{410} + t_{41} * \xi - \theta_1 - \phi_{11}}{M} + 1 \tag{5-39}$$

Figure 5-16 shows a graphical illustration of y_1 under two different states.

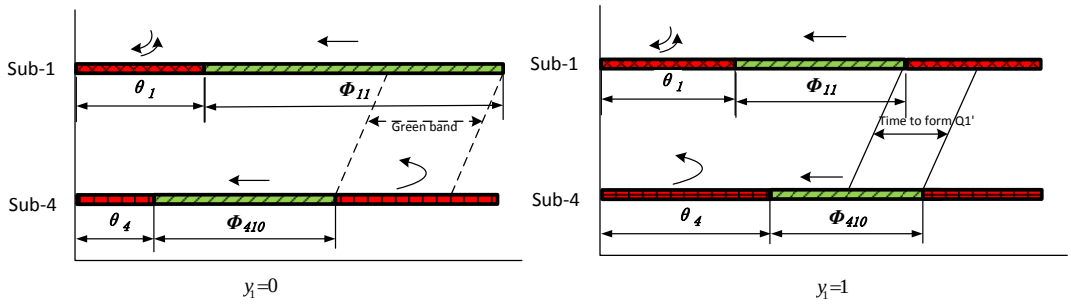

Figure 5-16. Graphical Notation for y_1

So the maximum length of Q_1' and Q_1'' during such time interval can be formulated as follows:

$$Q_1' \geq (\theta_4 + \phi_{410} - \theta_1 - \phi_{11} + t_{41} * \xi)\alpha_{11} q_{10}^T - (1 - y_1)M; Q_1' \geq 0 \tag{5-40}$$

$$Q_1'' \geq (1 - \theta_4 - \phi_{410} - t_{41} * \xi)\alpha_{11} q_9 - (1 - y_1)M; Q_1' \geq 0 \tag{5-41}$$

If $y_1 = 0$, this constraint will be relaxed since Q_1', Q_1'' are strictly non-negative. Note that the Q_1' and Q_1'' denote the partial queues on link 1 formed by two different incoming flows under the scenario that $y_1 = 1$. Except for the time to

form Q_1' and Q_1'', the other possible time durations are denoted in Figure 5-17. A binary parameter f_1 is introduced in the following:

$$f_1 = \begin{cases} 1 & if\ \theta_1 \geq \theta_4 + t_{41} * \xi \\ 0 & o.w \end{cases} \tag{5-42}$$

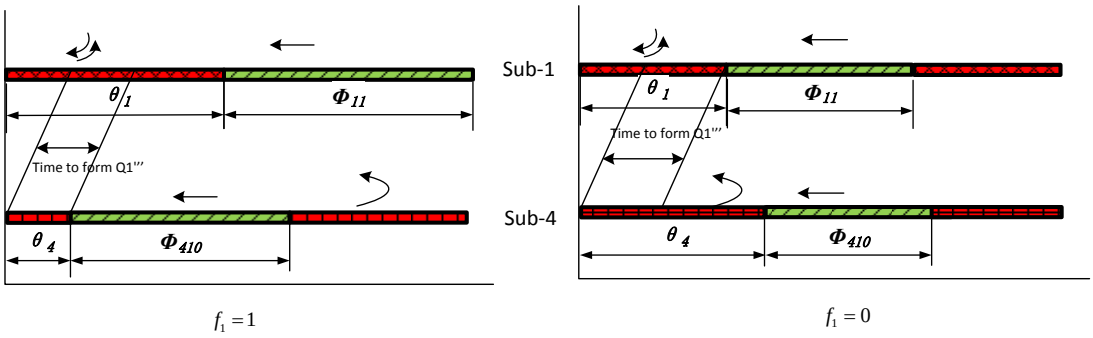

Figure 5-17. Graphical Illustration for Binary Parameter f_1

$$Q_1''' \geq f_1 * \theta_4 \alpha_{11} * q_{10}^T + (1 - f_1) * \alpha_{11} q_9 * \theta_1; Q_1''' \geq 0 \tag{5-43}$$

So the maximum length queue on link 1 during each cycle can be expressed as the sum of the vehicles accumulated during those three possible time durations as follows:

$$Q_1' + Q_1'' + Q_1''' \leq \xi L_1 \tag{5-44}$$

where q_{10}^T is the demand for through vehicles departing from Q10, and q_9 stands for departures from Q9. The maximum length of Q1 cannot exceed the link length L_1. The same methodology can be applied to derive Q6.

Summary of Stage 1 formulation

Objective function:	$Max(\sum_{i \in I} \mu_i)$
Subject to:	
General constraints:	Eqs. (5-2)-(5-5)
For external queue constraints:	Eqs. (5-22)-(5-25)
For internal Queue constraints:	Eqs. (5-26)-(5-44)

Using the "switch" algorithm, after running Stage 1, the new common cycle length will be taken as the input to re-run Stage 2. The results from Stage 2 will be set as a new input in Stage 1, and the iteration will go on until the termination condition is satisfied.

5.4 Numerical Analysis

To assess the effectiveness of the embedded queue constraints and the delays of minor-road vehicles, this study has further proposed a base model to perform a comparison.

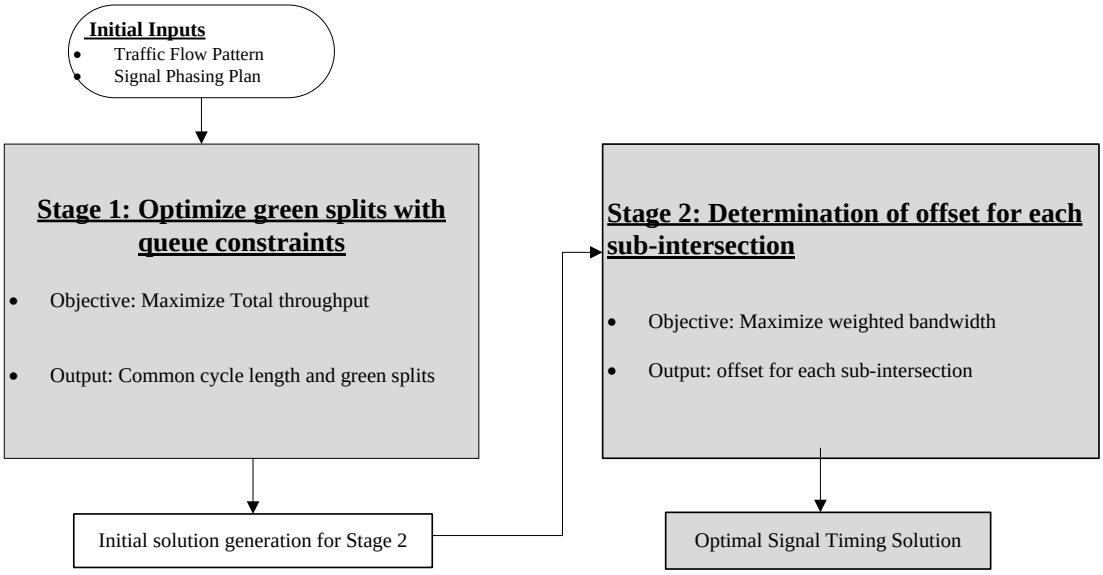

Figure 5-18. General Algorithm of Base Model

As shown in Figure 5-18, the base model also follows a two-stage structure. Different from the proposed model, the base model does not include the set of external and internal queue constraints in Stage 1. The Stage 2 applies the MAXBAND algorithm without the constraints on the waiting time experienced by the minor road drivers.

The numerical example is based on the field data collected from intersection Maryland3 at Waugh Chapel Road, in Maryland. The geometric layout and volume distribution of this intersection are shown in Figure 5-19 (a) and Figure 5-19 (b), respectively.

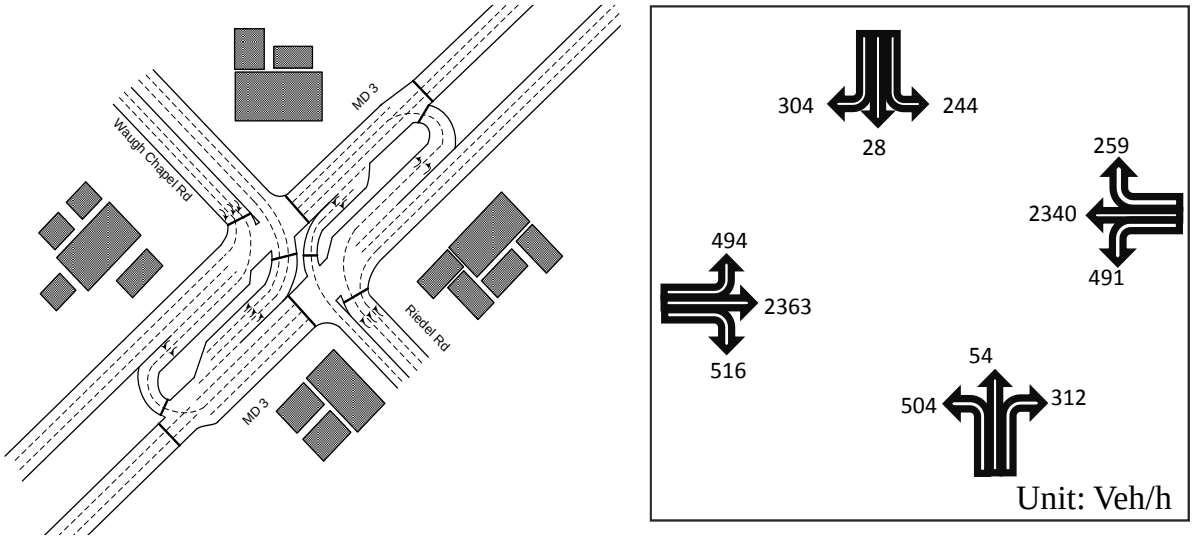

a) MD 3@ Waugh Chapel Rd

b) Input traffic flow rate (unit: veh/h)

Figure 5-19. Target Intersection Geometry and Input Traffic Flow Rate

Figure 5-20 presents the summary of green splits and offsets for each sub-intersection obtained by these two different models with the cycle length of 67 seconds and 170 seconds from the proposed model and the base model, respectively. Note that in the proposed model, the constraint for Q6 has been relaxed as its maximum queue exceeds its designed link length.

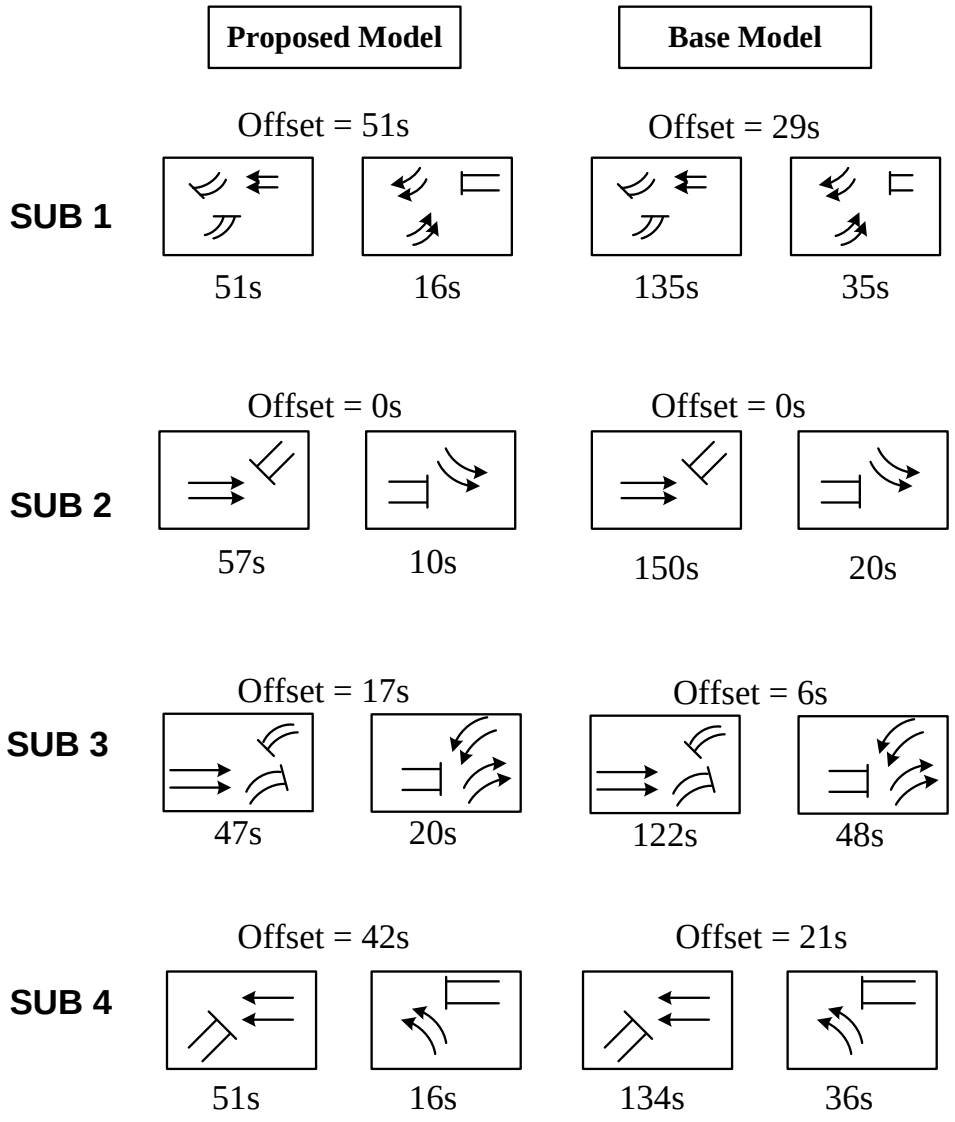

Figure 5-20. Optimal Green Splits and Offsets Produced by Different Models

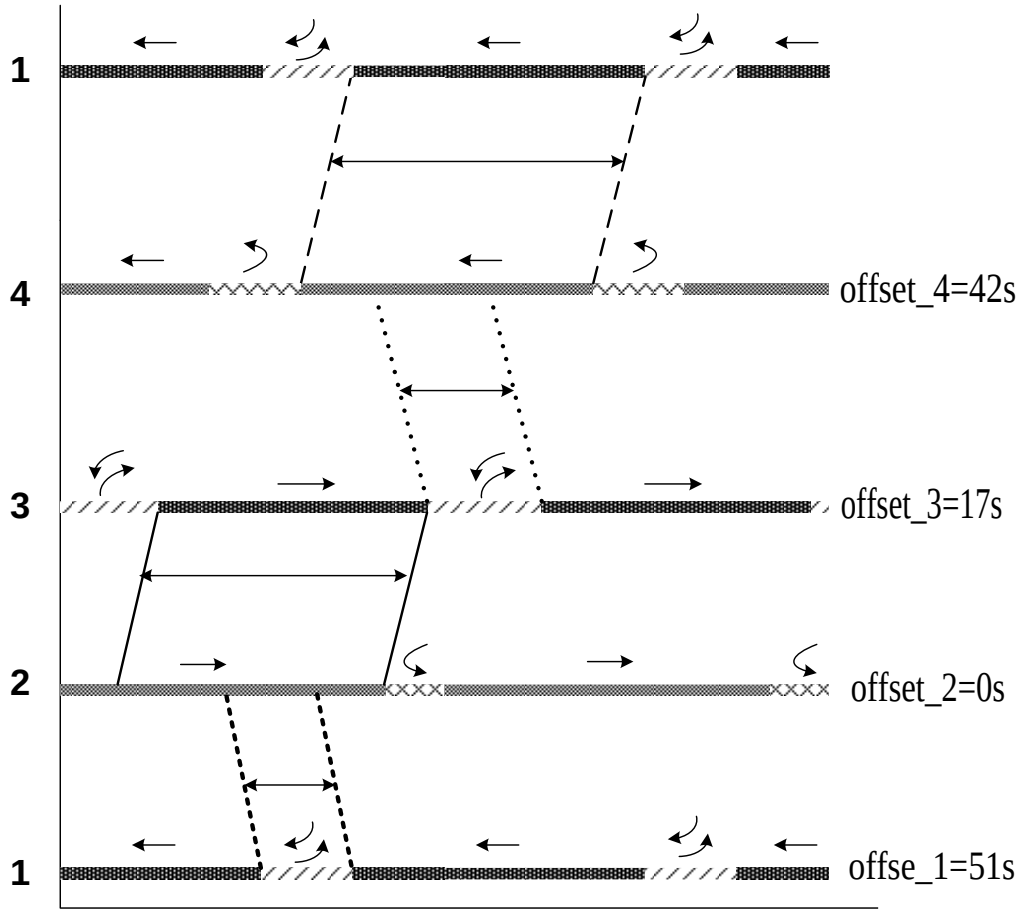

Figure 5-21. The Green Band Solution Obtained by the Proposed Model

A signal progression solution generated by the proposed model is illustrated in Figures 5-20 and 5-21. The offset for each sub-intersection has been listed on the right-hand side in the band diagram. The solution from the base model was summarized in Figures 5-20 and 5-22.

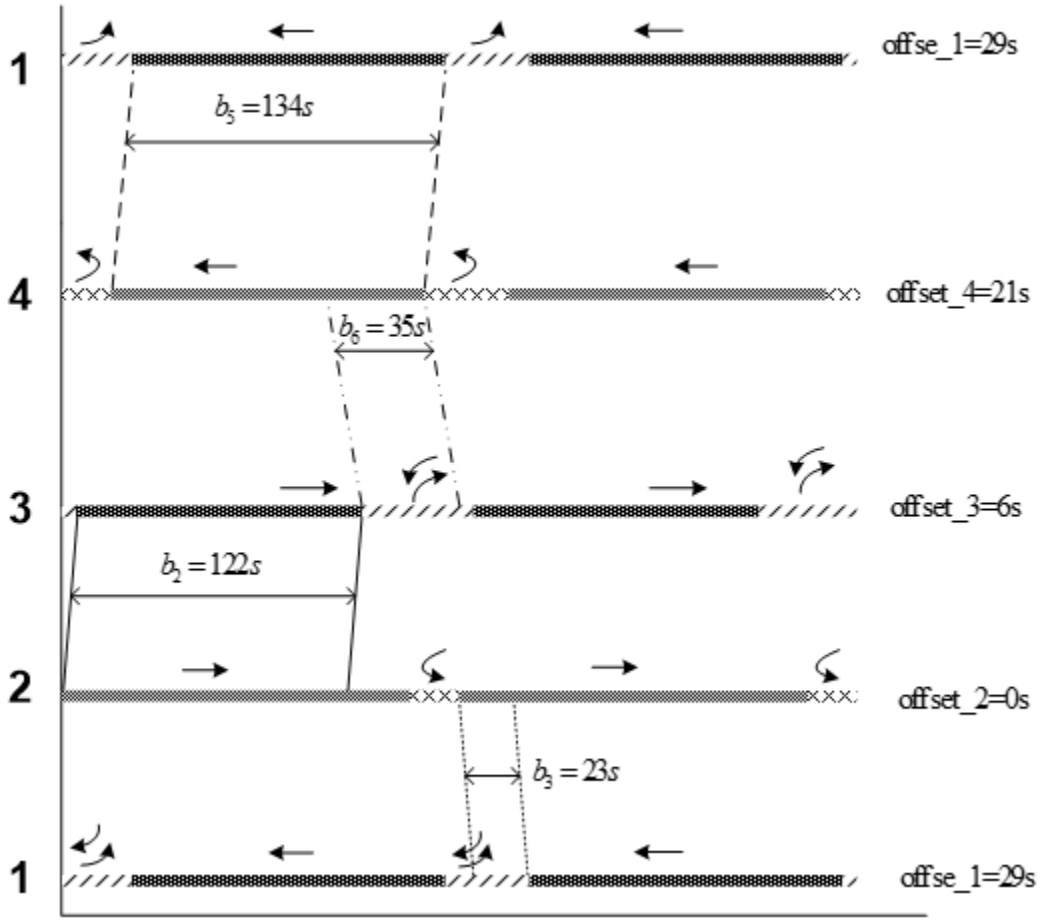

Figure 5-22. The Green Band Solution Obtained by the Base Model

Based on the optimization results, it is noticeable that the proposed model generates a much shorter cycle length (67 seconds) compared with the base model solution (170 seconds). This is due to the set of queue constraints embedded in Stage 1 of the proposed model, which function to prevent link queue spillbacks and yield a shorter common cycle length. To further investigate the progression efficiency of those critical paths among a Superstreet, Figure 5-21 and Figure 5-22 present the generated green bandwidths from the proposed model and the base model, respectively. As shown above, one can observe that only the four paths along the arterial receive green bands while the two minor road paths do not have the

progression. This is consistent with the fact that the arterial's through and left-turn traffic volumes clearly receive a higher priority than those minor street flows.

To assess the reliability of the evaluation results, this study has further calibrated a Superstreet simulator to test whether this model can effectively prevent the formation of the queue spillbacks while achieving the predefined optimal conditions. To capture the flow variations in real-world traffic conditions, the analysis have conducted 30 simulation replications to perform the comparison studies. The simulated maximal queue length on each critical link collected under these two signal plans along with the field measured link length are shown in Figure 5-23. It is noticeable that most simulated queues under the base model are much larger than those under the proposed model. Although most of those critical links are not under the risk of having queue spillback, Q7 under these two models has exhibited quite different patterns. The proposed model effectively limits the maximum queue length without exceeding the designed link length while the base model fails to prevent such blockages. The maximum queue length distribution of Q6 shows that both signal plans fail to prevent the formation of queue spillback.

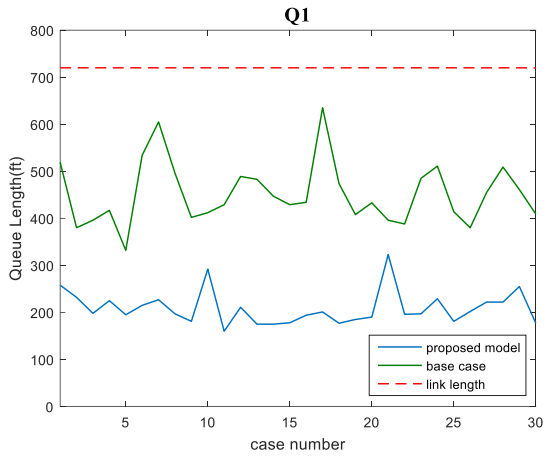
Q1
Queue Length(ft)
case number
proposed model
base case
link length

(A)

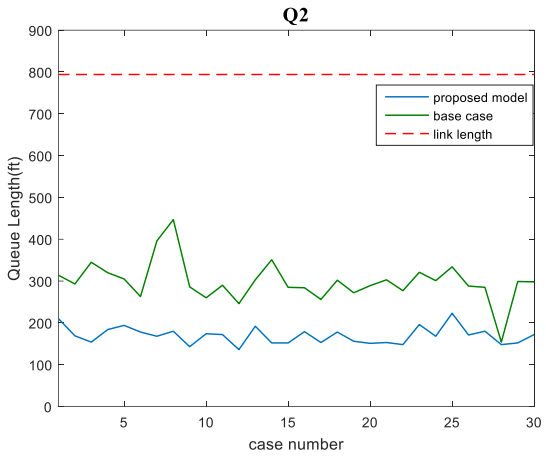
Q2
Queue Length(ft)
case number
proposed model
base case
link length

(B)

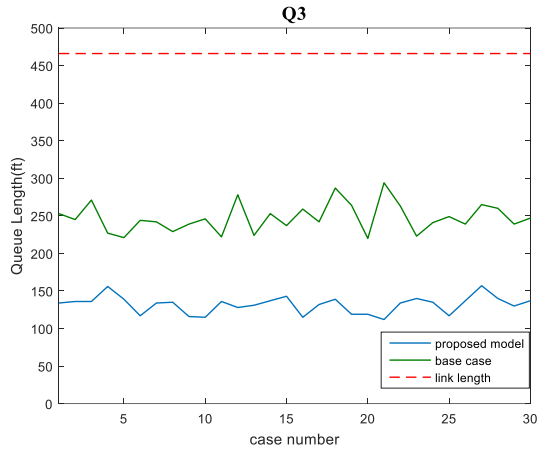
Q3
Queue Length(ft)
case number
proposed model
base case
link length

(C)

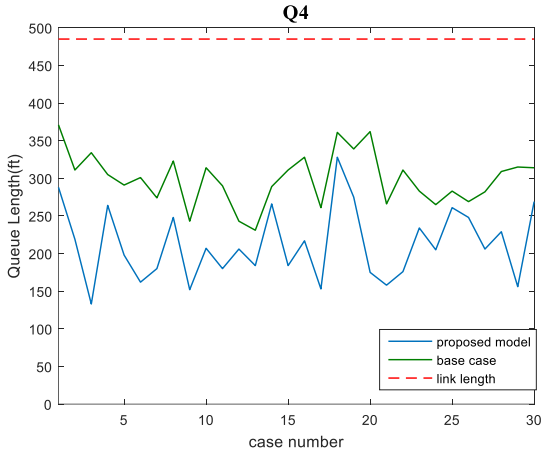
Q4
Queue Length(ft)
case number
proposed model
base case
link length

(D)

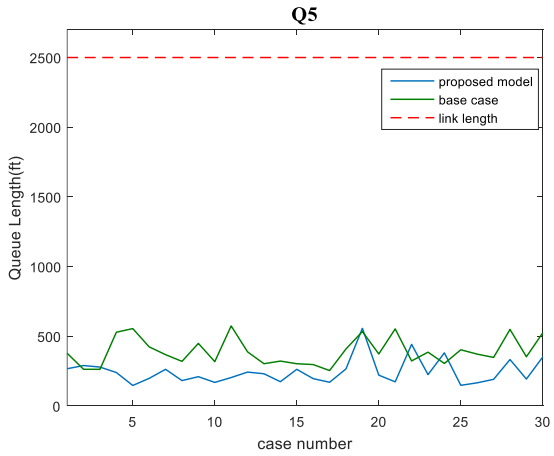
Q5
Queue Length(ft)
case number
proposed model
base case
link length

(E)

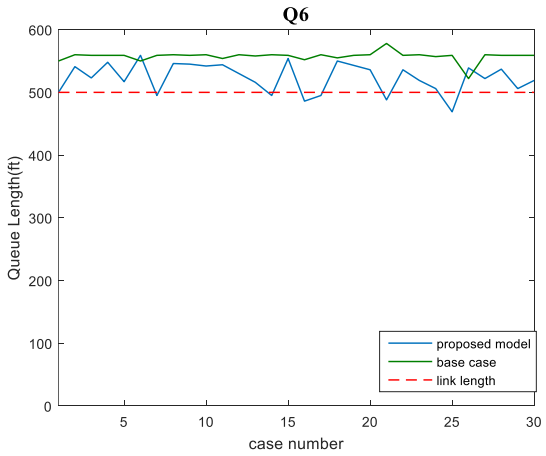
Q6
Queue Length(ft)
case number
proposed model
base case
link length

(F)

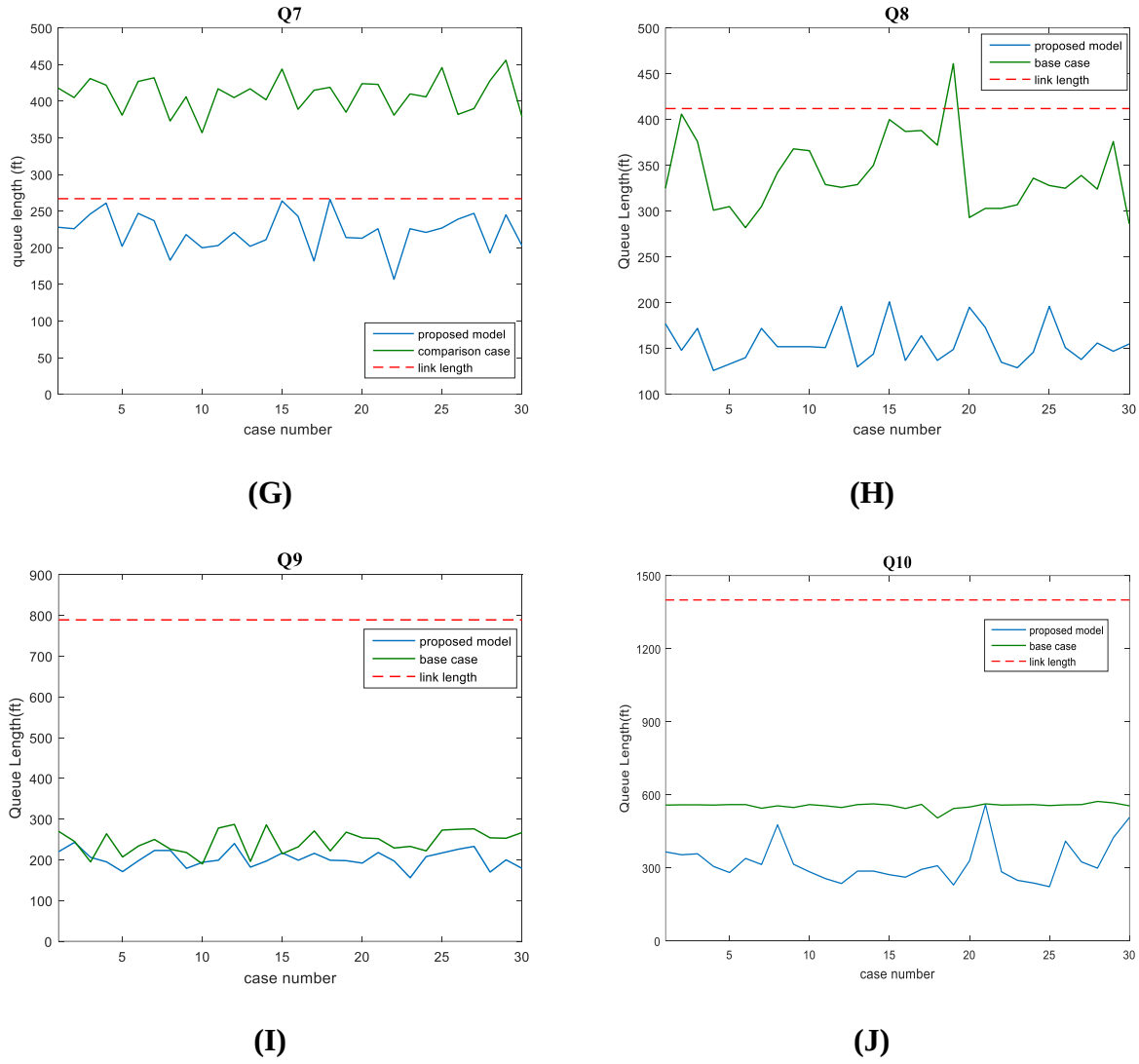

Figure 5-23. The Distribution of all Simulated Maximum Queue Lengths under Two Signal Plans

The simulation results also show that the queue spillover on some critical links (e.g., Q6, and Q7) indeed occurs on the Superstreet designed with the longer cycle length as produced by the base model. Such queue spillovers can result in several blockages on the left-turn bay and through lanes and consequently increase the average delay over the entire intersection. The resulting average traffic delays

over the entire Superstreet under two signal plans are summarized in Figure 5-24. It is clear that the proposed model can produce much lower delays than with the other one.

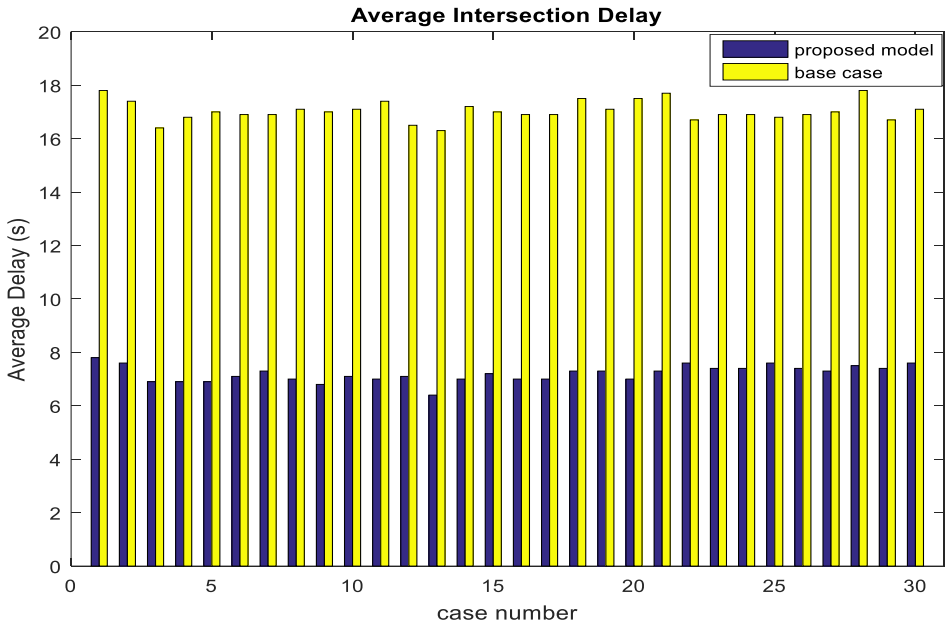

Figure 5-24 Comparison of Superstreet Average Delay with Two Different Signal Designs

To promote the efficiency of a signalized Superstreet, this study has used the Mixed-Integer-Linear-Programming (MILP) technique to generate an optimal signal plan using a two-stage switching algorithm. The results of extensive simulation experiments have confirmed that the proposed model clearly outperforms the conventional signal design method as with the base model. In conclusion, the proposed model can efficiently offer signal progressions while preventing potential queues from spillback and minimizing the extensive delay by those minor road drivers.

Chapter 6: Conclusions and Future Work

6.1 Conclusions

In response to the urgent needs for developing reliable tools to assist traffic professionals in the design and evaluation of both signalized and un-signalized Superstreets, this study has developed a set of models for that purpose . The contributions of this study include: 1) the procedures and formulations to compute the minimum required U-turn offset length for an un-signalized Superstreet; 2) interval-based models for evaluating the bay length design in a signalized Superstreet under the given demand variation; and 3) an efficient two-stage signal optimization model to prevent queue spillback on intersection links and to minimize the delays experienced by minor road drivers.

Recognizing the critical role of the U-turn offset length on the operational efficiency of an Un-signalized Superstreet, the method proposed in Chapter 4 is capable of generating the minimum required offset length that accounts for the safety needs. While capturing the dynamics of traffic flows and discrepancies among drivers' gap acceptance behavior, this model can also be used to generate recommendations for the design of an un-signalized Superstreet or the evaluation of a candidate plan. This model can be used in the future as an evaluation tool to decide whether or not a signal should be placed at a Superstreet.

The second contribution of this study is to produce a set of models described in Chapter 5 for evaluating the design of link length on a Superstreet. Due to the interdependent nature of traffic queues among the closely-spaced sub-intersections in a Superstreet, the proposed model employs the QL ratios on those critical links as the key evaluation indicators and allows the users to estimate the range of potential queue variation on each link under a given demand and signal plan. The estimated queue intervals offer the basis for evaluating whether any critical links in a Superstreet are insufficient to accommodate the potential queues under the given demand level. To assess the applicability of these developed models, extensive simulations were conducted and their results have confirmed the resulting effectiveness as well as the reliability.

The third contribution is to develop a two-stage signal optimization method, described in Chapter 6, which takes into account the unique geometric features of a Superstreet and the conflicts between the major and minor road traffic flows. The first stage is to set the optimal common cycle length for all four closely-spaced sub intersections among the entire intersection. Accounting for queue constraints on all critical links, the cycle length generated in Stage 1 can effectively prohibit the occurrence of potential queue blockages. The focus of the computation at Stage 2 is to employ multi-objective mixed integer linear programming that can concurrently maximize the sum of weighted bandwidths and minimize the signal waiting time experienced by minor road drivers. Using the 'switch' algorithm, the solution generation process can circumvent the complex interference between these two stages

and offer an optimal solution to meet all critical concerns. To further demonstrate the efficiency of the developed two- stage model, extensive simulations were performed to assess the operational performance. The results confirms its effectiveness on preventing queue spillback and reducing average delay for the entire Superstreet.

6.2 Future Work

Despite the contributions of this study, the author fully recognizes that much remains to be done on this subject. Some priority issues along the line for future study include:

- ***Field calibration and evaluation on the minimum U-turn offset length model for an Un-signalized Superstreet.*** Although the proposed model can take into account the traffic dynamics and the intricate nature of human behavior, parameter calibration with field data and more demonstration evaluations are essential for the potential applicability by the traffic community.

- ***Evaluation of the impacts of a Superstreet on its neighboring intersections***. Note that the signalized Superstreet is more likely to be part of a major arterial, and thus evaluation of a Superstreet's impact on its neighboring intersections should be studied in the future. Also, the development of operational tools that allow engineers to analyze the resulting delays, the

required bay length, and the distance between two crossovers is essential to the promotion of Superstreet implementations.

- ***Coordination of a signal plan for a signalized Superstreet with its neighboring intersections on the same corridor.*** Since a Superstreet will be a major intersection in an arterial or local corridor, its signal plan should be properly coordinated with other intersections to ensure that the entire arterial traffic conditions can benefit from its signal, not to yield only a local optimal condition but actually impede the progression of the entire arterial flows. Hence, to develop such a signal plan is an essential task for future work.

Bibliography

1. Kramer, R.P, New Combinations of Old Techniques to Rejuvenate Jammed Suburban Arterials, Strategies to Alleviate Traffic Congestion, Conference Proceedings, Institute of Transportation Engineers, Washington, D.C., 1987, pp. 139-148.
2. Jonathan D. Reid and Joseph E. Hummer, Travel Time Comparisons Between Seven Unconventional Arterial Intersection Designs, Transportation Research Record 1751, No. 01-2957, 2001, pp. 56-66.
3. Haley, Rebecca, Sarah Ott, Joseph Hummer, Robert Foyle, Christopher Cunningham, and Bastian Schroeder. "Operational effects of signalized superstreets in North Carolina." *Transportation Research Record: Journal of the Transportation Research Board* 2223 (2011): 72-79.
4. Taehyeong Kim, Praveen K. Edra, and Joe G. Bared, Operational and Safety Performance of a Non-Traditional Intersection Design: the Superstreet, Transportation Research Board, TRB 2007 Annual Meeting CD-ROM. 2007.
5. Kim, M., Chang, G. L., & Rahwanji, S. (2007). Unconventional arterial intersection designs initiatives. In IEEE Conference on Intelligent Transportation Systems, Seattle.
6. FHWA, US. Department of Transportation, Restricted Crossing U-Turn Intersection, Publication No. FHWA-HRT-09-059, October 2009.
7. FHWA, US. Department of Transportation, Alternative Intersections/ Interchanges: Informational Report (AIIR), Publication No. FHWA-HRT-09-060, April 2010.
8. FHWA, US. Department of Transportation, Restricted Crossing U-turn Informational Guide, Publication No. FHWA-SA-14-070, August 2014.
9. Ott, Sarah E., Rebecca L. Haley, Joseph E. Hummer, Robert S. Foyle, and Christopher M. Cunningham. "Safety effects of un-signalized superstreets in North Carolina." *Accident Analysis & Prevention* 45 (2012): 572-579.
10. Thompson, Cipriana D., and Joseph E. Hummer. *Guidance on the Safe Implementation of Unconventional Arterial Designs*. No. Draft Final Report. 2001.
11. Moon, Jae-Pil, Young-Rok Kim, Do-Gyeong Kim, and Suk-Ki Lee. "The potential to implement a superstreet as an unconventional arterial intersection design in Korea." *KSCE Journal of Civil Engineering* 15, no. 6 (2011): 1109-1114.
12. Olarte, Rafael, Joe G. Bared, Larry F. Sutherland, and Anand Asokan. "Density Models and Safety Analysis for Rural Unsignalised Restricted Crossing U-turn Intersections." *Procedia-Social and Behavioral Sciences* 16 (2011): 718-728.
13. NCHRP Report 650, Median Intersection Design for Rural High-speed divided highways, Transportation Research Board, 2010.
14. Bared, Joe G., and Evangelos I. Kaisar. "Median U-turn design as an alternative treatment for left turns at signalized intersections." *ITE journal* 72, no. 2 (2002): 50-54.
15. Daniel Carter, Joseph E. Hummer, Robert S. Foyle, and Stacie Phillips, Operational safety effects of U-turns at signalized intersections, Transportation

Research Record 1912, 2005, pp. 11-18.
16. Liu, Pan, Jian John Lu, Huaguo Zhou, and Gary Sokolow. "Operational effects of U-turns as alternatives to direct left-turns." *Journal of transportation engineering* 133, no. 5 (2007): 327-334.
17. Jian John Lu, Pan Liu and Lingjun Lu, Understanding factors affecting safety effects of indirect driveway left-turn treatments, Journal of Transportation safety and security, Vol 1, 2009, pp. 61-73.
18. Joseph E. Hummer, Victor J. Blue, Jon Cate, and Rynal Stephenson, Taking Advantage of the Flexibility offered by Unconventional Arterial Designs, ITE Journal, September 2012, pp. 38-43.
19. Manual, Highway Capacity. "HCM2010." *National Academy of Sciences. Yhdysvallat* (2010).
20. America, I. T. S. "American Association of State Highway and Transportation Officials." (2001).
21. Hummer, Joseph E., and Ram Jagannathan. "An update on superstreet implementation and research." In *Eighth National Conference on Access Management, Transportation Research Board, Baltimore, Md*. 2008.
22. Hummer, J. E., Haley, R. L., Ott, S. E., Foyle, R. S., & Cunningham, C. M. (2010). Superstreet Benefits and Capacities (No. FHWA/NC/2009-06).
23. Haley, R., Ott, S., Hummer, J., Foyle, R., Cunningham, C., & Schroeder, B. (2011). Operational effects of signalized superstreets in North Carolina. Transportation Research Record: Journal of the Transportation Research Board, (2223), 72-79.
24. Hochstein, J. L., Maze, T., Welch, T., Preston, H., & Storm, R. (2009) The J-Turn Intersection: Design Guidance and Safety Experience. Presented at 88th Annual Meeting of the Transportation Research Board, Washington, D.C., U.S.A.
25. Gartner, N. H., Little, J. D. C., and Gabbay, H. (1975). "Optimization of traffic signal settings by mixed integer linear programming. Part I: The network coordination problem." Transp. Sci., 9(4), 321–343.
26. Little, J. D. C., Kelson, M. D., and Gartner, N. H. (1981). "MAXBAND: A program for setting signals on arterials and triangular networks." Transportation Research Record 795, Transportation Research Board, Washington, DC.
27. Cohen, S. L., and Liu, C. C. (1986). "The bandwidth-constrained TRANSYT signal optimization program." Transportation Research Record 1057, Transportation Research Board, Washington, DC.
28. Wong, C. K., and Wong, S. C. (2003). "Lane-based optimization of signal timings for isolated junctions." Transp. Res. B Method., 37(1), 63–84.
29. Robertson, D. I. (1969). "TRANSYT: A traffic network study tool." RRL Rep. LR 253, Road Research Laboratory, England.
30. Wallace, C. E., Courage, K. G., Reaves, D. P., Shoene, G.W., Euler, G.W., and Wilbur, A. (1988). "TRANSYT-7F user's manual: Technical report." Univ. of Florida, Gainesville, FL.
31. Little J D C, Martin B V, Morgan J T. The synchronization of traffic signals by mixed-integer linear programming. Operations Research 1966, 14: 568–594.
32. Chang E C P, Cohen S L, Liu C C, et al. MAXBAND-86: program for

optimizing left turn phase sequence in multi-arterial closed networks. Transportation Research Record 1181, 1988, 61–67.
33. Gartner N H, Assmann S F, Lasaga F L, et al. A multi-band approach to arterial traffic signal optimization. Transportation Research B, 1991, 25(1): 55–74.
34. Stamatiadis, C, Gartner, N H. MULTIBAND-96: A program for variable-bandwidth progression optimization of multiarterial traffic networks. Transportation Research Records, 1996, 9–17.
35. Chaudhary N A, Pinnoi A, Messer C J. Proposed Enhancements to MAXBAND-86 Program. Transportation Research Record 1324, 1991, 98–104.
36. Chaudhary N A, Messer C J. PASSER-IV: A program for optimizing signal timing in grid networks. Paper presented at the 72nd Annual Meeting of the Transportation Research Board, Washington, D.C., 1993.
37. Hadi M A, Wallace C E. Hybrid genetic algorithm to optimize signal phasing and timing. Transportation Research Record 1421, 1993, 104–112.
38. Pillaia R S, Rathi A K, Cohen S L. A restricted branch-and-bound approach for generating maximum bandwidth signal timing plans for traffic networks. Transportation Research Part B: 1998, 32(8): 517–529.
39. Gartner N H, Stamatiadis C. Arterial-based control of traffic flow in urban grid networks. Mathematical and Computer Modeling, 2002, 35: 657–671.
40. D'Ans, G. C., and Gazis, D. C. (1976). "Optimal control of oversaturated store-and-forward transportation networks." Transp. Sci., 10(1), 1–19.
41. Papageorgiou, M. (1995). "An integrated control approach for traffic corridors." Transp. Res. Part C, 3(1), 19–30.
42. Kashani, H. R., and Saridis, G. N. (1983). "Intelligent control for urban traffic systems." Automatica, 19(2), 191–197.
43. Wu, J., and Chang, G. L. (1999). "An integrated optimal control and algorithm for commuting corridors." Int. Trans. Oper. Res., 6(1), 39–55.
44. Yang, Xianfeng, Gang-Len Chang, and Saed Rahwanji. "Development of a signal optimization model for diverging diamond interchange." *Journal of Transportation Engineering* (2014).
45. Gipps, Peter G. "A model for the structure of lane-changing decisions." *Transportation Research Part B: Methodological* 20, no. 5 (1986): 403-414.
46. Yang, Qi, and Haris N. Koutsopoulos. "A microscopic traffic simulator for evaluation of dynamic traffic management systems." *Transportation Research Part C: Emerging Technologies* 4, no. 3 (1996): 113-129.
47. CORSIM User Manual, Ver. "1.01." *The Federal Highway Administration, US Dept. of Transportation* (1996).
48. Miller, Alan J. "Nine estimators of gap-acceptance parameters." *Publication of: Traffic Flow and Transportation* (1900).
49. Herman, Robert, and George Weiss. "Comments on the highway-crossing problem." *Operations Research* 9, no. 6 (1961): 828-840.
50. Drew, Donald R. "Gap acceptance characteristics for ramp-freeway surveillance and control and discussion." *Highway Research Record* 157 (1967).
51. Daganzo, Carlos F. "Estimation of gap acceptance parameters within and across the population from direct roadside observation." *Transportation Research Part B: Methodological* 15, no. 1 (1981): 1-15.

52. Kita, Hideyuka. "Effects of merging lane length on the merging behavior at expressway on-ramps." *Transportation and Traffic Theory* (1993).
53. Cluck, J., Levinson, H.S., Stover, V., 1999. Impacts of Access Management Techniques, NCHRP Report 420, National Cooperative Highway Research Program, Transportation Research Board.
54. Hummer, J. E. (1998). Unconventional Left-Turn Alternatives for Urban and Suburban Arterials-Part One. *ITE journal*, *68*, 26-29.
55. Lu, J.J., Pirinccioglu, F., Pernia, J., 2004. Safety Evaluation of Right-Turns followed by U-turns at Signalized Intersection (six or more lanes) as an Alternative to Direct Left Turns: Conflict Data Analysis. Florida Department of Transportation.
56. Inman, V. W., & Haas, R. P. (2012). *Field Evaluation of a Restricted Crossing U-turn Intersection* (No. FHWA-HRT-11-067).
57. Bared, J. (2009). *Restricted Crossing U-Turn Intersection* (No. FHWA-HRT-09-059).
58. Liu, Pan, Jian John Lu, and Hongyun Chen. "Safety effects of the separation distances between driveway exits and downstream U-turn locations." *Accident Analysis & Prevention* 40, no. 2 (2008): 760-767.
59. Superstreet benefits and capacities, Final report, Publication No. FHWA/NC/2009-06, NCDOT.
60. Zhang et al, "crash prediction models for Rural Restricted Crossing U-turn Intersections ", 2014 TRB Alternative Intersections & Interchange Symposium.
61. Hidas, P. (2005). Modelling vehicle interactions in microscopic simulation of merging and weaving. *Transportation Research Part C: Emerging Technologies*, *13*(1), 37-62
62. Pollatschek, M. A., Polus, A., & Livneh, M. (2002). A decision model for gap acceptance and capacity at intersections. *Transportation Research Part B: Methodological*, *36*(7), 649-663.
63. Fitzpatrick, K. (2003). *Design speed, operating speed, and posted speed practices* (No. 504). Transportation Research Board.
64. Fitzpatrick, K., Carlson, P., Brewer, M., & Wooldridge, M. D. (2003, January). Design speed, operating speed, and posted speed limit practices. In *82nd Annual* Meeting of the Transportation Research Board, Washington, DC.
65. Tian, Z., Vandehey, M., Robinson, B. W., Kittelson, W., Kyte, M., Troutbeck, R., & Wu, N. (1999). Implementing the maximum likelihood methodology to measure a driver's critical gap. Transportation Research Part A: Policy and Practice, 33(3), 187-197.
66. Tian, Z. Z., Troutbeck, R., Kyte, M., Brilon, W., Vandehey, M. A. R. K., Kittelson, W., & Robinson, B. (2000, June). A further investigation on critical gap and follow-up time. In Proceedings of the 4th International Symposium on Highway Capacity, Maui/Hawaii, Transportation Research Circular E-C018 (pp. 409-421).
67. Guide, CORSIM User'S. "Version 5.1." ITT Industries, Inc., FHWA Office of Operations Research (2003).
68. Version, PTV VISSIM. "5.2 Manual." Volume 1 (2009): 3.
69. Gettman, Douglas, Lili Pu, Tarek Sayed, and Steven G. Shelby. Surrogate safety

assessment model and validation: Final report. No. FHWA-HRT-08-051. 2008.
70. Ahmed, Kazi Iftekhar. "Modeling drivers' acceleration and lane changing behavior." PhD diss., Massachusetts Institute of Technology, 1999.
71. Bruce W. Robinson, Zongzhong Tian, Wayne Kittelson, Mark Vandehey. et al. (1999)Extensions of theoretical capacity models to account for special conditions. Transportation research-A vol.33, 217-236.
72. Hani Mahmassani, Yosef Sheffi. (1981) Using gap sequences to estimate gap acceptance function, Transportation Research-B vol. 15, 143-148.
73. Troutbeck, R. J. Estimating the critical acceptance gap from traffic movements. Physical Infrastructure Centre, Queensland University of Technology, 1992.
74. Cassidy, Michael J., Samer M. Madanat, M-H. Wang, Fan Yang, and R. Troutbeck. "Unsignalized intersection capacity and level of service: revisiting critical gap. Discussion. Authors' closure." Transportation research record1484 (1995): 16-23.
75. Chaudhary, Nadeem A., and Carroll J. Messer. PASSER IV-96, version 2.1, User/Reference manual. No. FHWA/TX-97/1477-1. 1996.
76. Chaudhary, Nadeem A., and Carroll J. Messer. Passer IV: A program for optimizing signal timing in grid networks (with discussion and closure). No. 1421. 1993.
77. Webster, F. V., (1956), Traffic signal settings, Road Research Technical Paper, No. 39, HMSO.
78. Miller, A.J., (1963), Settings for fixed cycle traffic signals, Operations Research Quarterly, Vol. 14, No. 4, pp. 373-386.
79. Allsop, R.E., (1971), Delay-minimizing settings for fixed-time traffic signals at a single road junction, IMA Journal of Applied Mathematics, 8 (2): 164-185.
80. Allsop, R.E., (1972), Delay at a fixed time traffic signal-I: Theoretical analysis, Transportation Science, 6(3), 260-285.
81. Allsop, R.E., (1976), Sigcap: A computer program for assessing the traffic capacity of signal controlled road junctions, Traffic Engineering and Control, vol. 17, 338-341.
82. Burrow, I. J., (1987), OSCADY: a computer program to model capacities, queues and delays at isolated traffic signal junctions, No. RR 105.
83. Heydecker, B. G. (1996). A decomposition approach for signal optimization in road networks. Transportation Research Part B: Methodological, 30(2), 99-114.
84. Silcock, J. P., (1997), Designing signal-controlled junctions for group-based operation, Transportation Research Part A: Policy and Practice, 31(2), 157-173.
85. Yang, X., Lu, Y. C., and Chang, G. L., (2014), Dynamic Signal Priority Control Strategy to Mitigate the Off-ramp Queue Spillback to the Freeway Mainline Segment, Transportation Research Record: Journal of the Transportation Research Board, vol. 2438, pp 1-11.
86. Wong, C. K., and Wong, S. C., (2003), Lane-based optimization of signal timings for isolated junctions, Transportation Research Part B: Methodological, 37(1), 63- 84.
87. Gazis, D. C., (1964), Optimum control of a system of oversaturated intersections, Operations Research, 12(6), 815-831.
88. Michalopoulos, P. G., and Stephanopoulos, G., (1977a), Oversaturated signal

systems with queue length constraints—I: Single intersection, Transportation Research, 11(6), 413-421.
89. Michalopoulos, P. G., and Stephanopoulos, G., (1977b), Oversaturated signal systems with queue length constraints—II: Systems of intersections, Transportation Research, 11(6), 423-428.
90. Chang, T. H., and Lin, J. T., (2000), Optimal signal timing for an oversaturated intersection, Transportation Research Part B: Methodological, 34(6), 471-491.
91. Gartner, N. H., and Stamatiadis, C., (2002), Arterial-based control of traffic flow in urban grid networks, Mathematical and Computer Modelling, 35(5), pp. 657-671.
92. Gartner, N. H., and Stamatiadis, C., (2004), Progression optimization featuring arterial-and route-based priority signal networks, Journal of Intelligent Transportation Systems, 8(2), pp. 77-86.
93. Tian, Z. and Urbanik, T., (2007), System partition technique to improve signal coordination and traffic progression, Journal of transportation engineering, 133(2), 119-128.
94. Li, J. Q., (2014), Bandwidth Synchronization under Progression Time Uncertainty, IEEE Transactions on ITS, 15(2), 1-11.
95. Hadi, M. A., and Wallace, C. E., (1993), Hybrid genetic algorithm to optimize signal phasing and timing, Transportation Research Record, 1421, 104-112.
96. Park, B., Messer, C.J., and Urbanik, T., (1999), Traffic signal optimization program for oversaturated conditions: genetic algorithm approach. Transportation Research Record, 1683, 133–142.
97. Daganzo, C. F., (1994), The cell transmission model: A dynamic representation of highway traffic consistent with the hydrodynamic theory, Transportation Research Part B: Methodological, 28(4), 269-287.
98. Lo, H., (1999), A novel traffic signal control formulation, Transportation Research, Part A, 44, 436–448.
99. Lo, H., (2001), A cell-based traffic control formulation: strategies and benefits of dynamic timing plan, Transportation Science, 35, 148–164.
100. Lo, H., Chang, E., Chan. Y. C., (2001), Dynamic network traffic control. Transportation Research, Part A, 35, 721–744.